

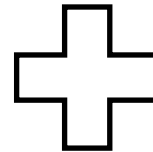
Status and challenges of neutrino-nucleus cross sections

Marco Martini



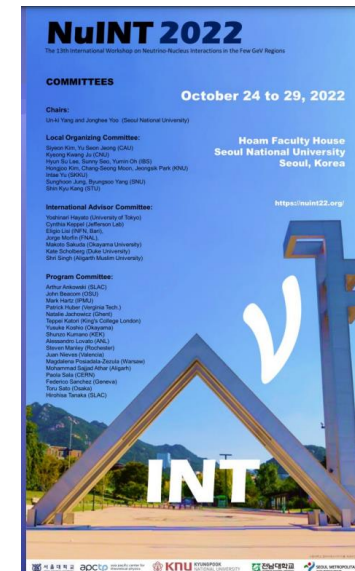
- Summary of my lectures at Ecole de GIF 2022

[Ecole de Gif 2022: La Physique des Neutrinos \(5-9 septembre 2022\): Sections efficaces d'interaction de neutrinos](#)

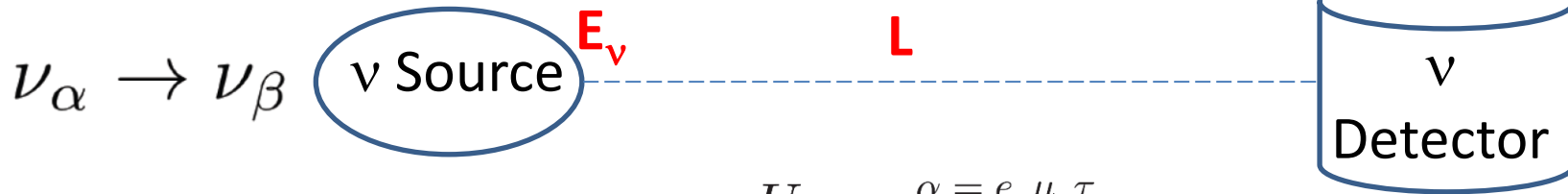


- Latest from NuINT 2022

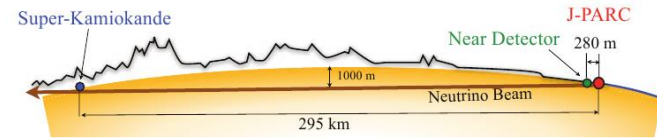
[NuInt 2022 \(24-29 octobre 2022\): Accueil · Indico \(cern.ch\)](#)



Neutrino oscillation experiments



$$\nu_\alpha = U_{\alpha i} \nu_i \quad \begin{matrix} \alpha = e, \mu, \tau \\ i = 1, 2, 3 \end{matrix}$$



$$N_{\nu_\beta}(\overline{E_\nu}) \sim \int \Phi_{\nu_\alpha}(E_\nu) P_{\nu_\alpha \rightarrow \nu_\beta}(E_\nu, L, \{\Theta\}) \sigma_{\nu_\beta}(E_\nu) \epsilon_{\text{det.}} d(E_\nu, \overline{E_\nu}) dE_\nu$$

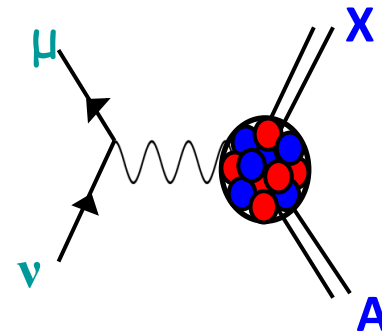
Reconstructed ν energy $\overline{E_\nu}$ (blue box)
 True ν energy E_ν (pink box)

Number of detected events



Modern accelerator-based neutrino oscillation experiments:

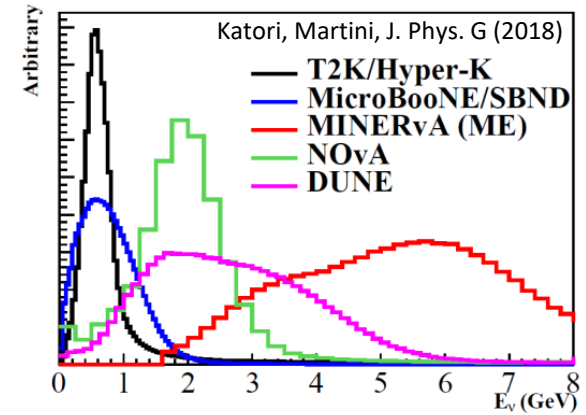
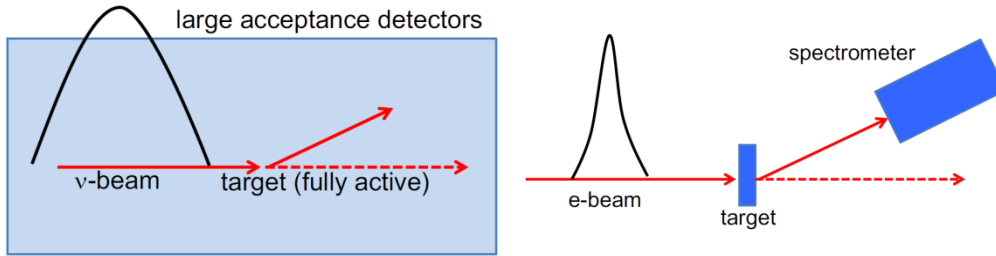
- The neutrino energy is reconstructed from the final states
- Nuclear targets (C, O, Ar, Fe...)



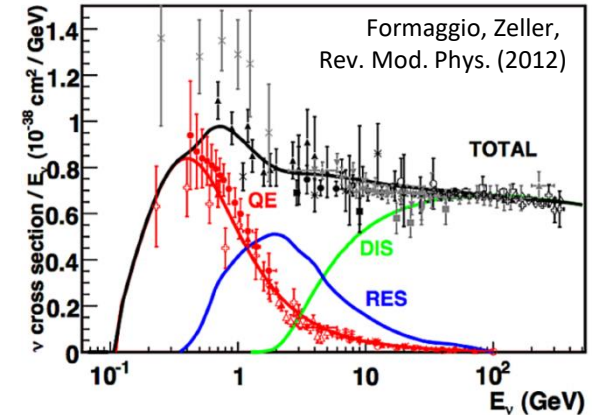
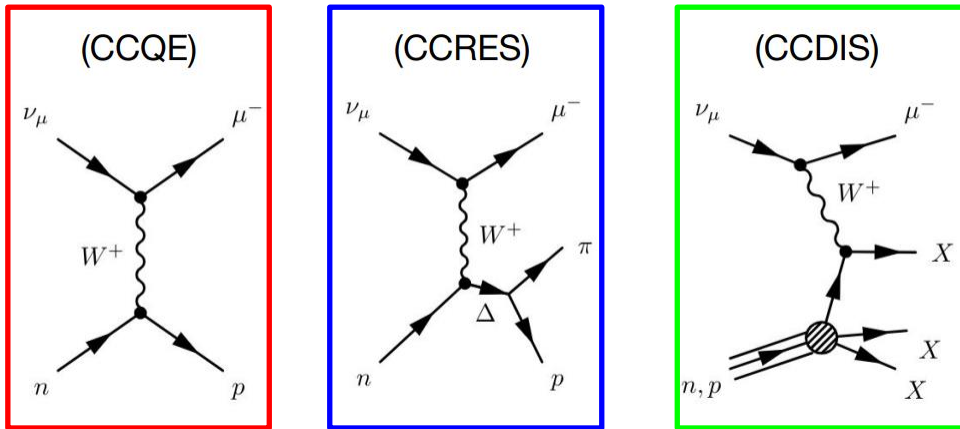
→ the knowledge of the neutrino-nucleus cross section is crucial

Some important points of the accelerator-based ν experiment

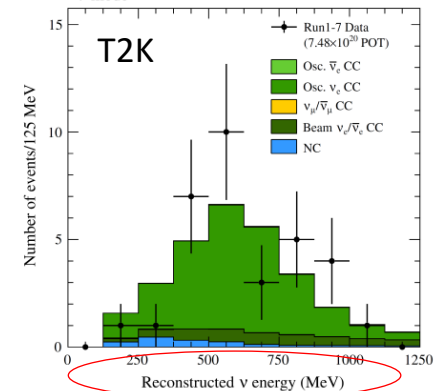
- Neutrino beams are not monochromatic (at difference with respect to electron beams)



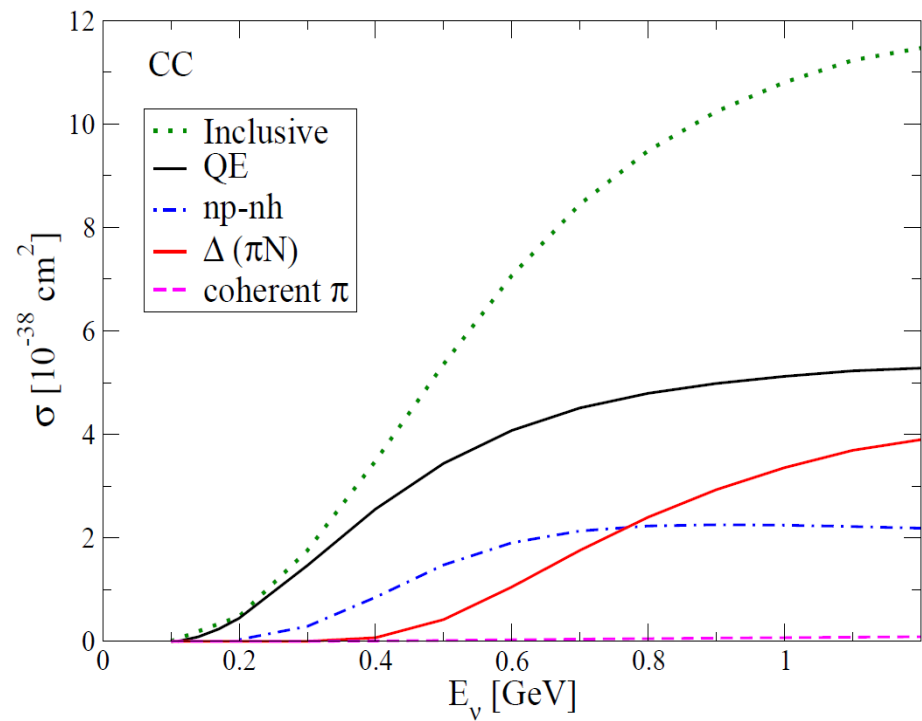
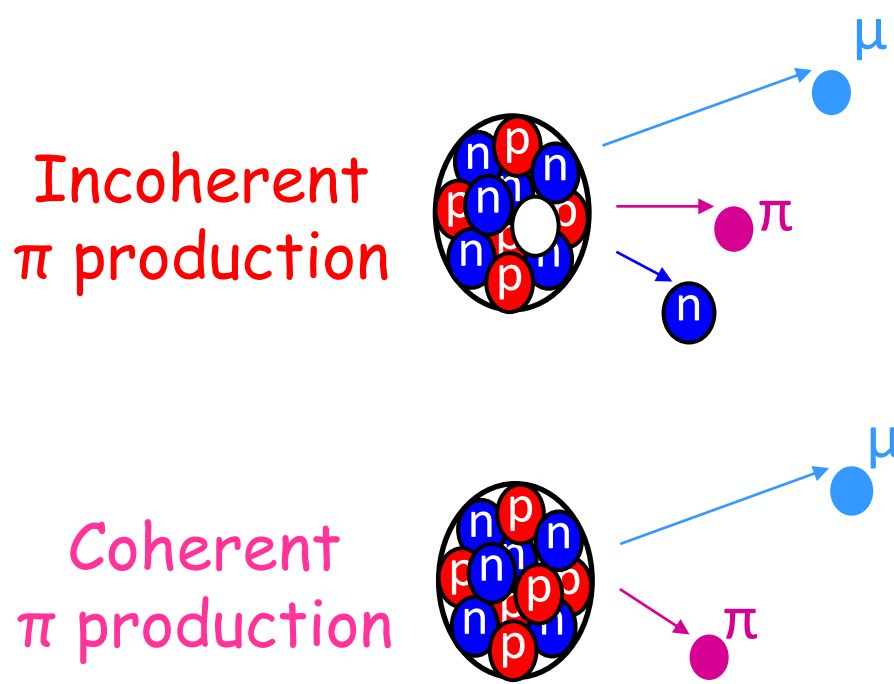
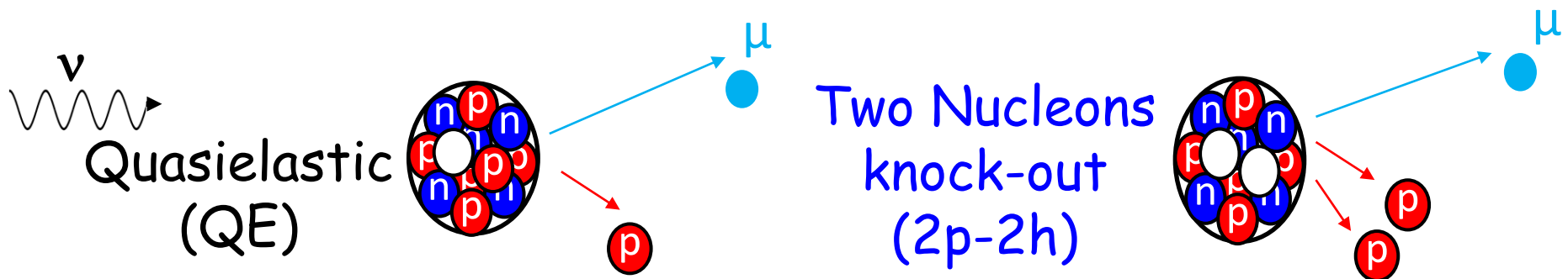
- Different reaction mechanisms contribute



- The neutrino energy is reconstructed from the final states of the reaction (often from CCQE events)

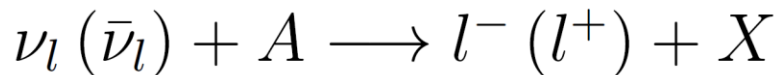


In this talk: Neutrino - nucleus interaction @ $E_\nu \sim O(1 \text{ GeV})$



Different processes are entangled

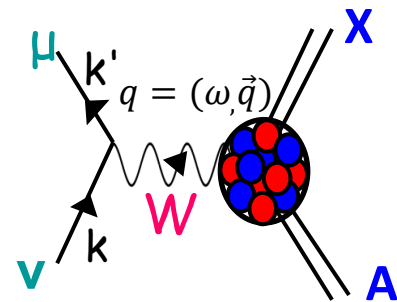
Charged current neutrino-nucleus cross section



$$\mathcal{L}_W = \frac{G_F}{\sqrt{2}} \cos \theta_C l_\mu J^\mu$$

Lab frame

$$\frac{d^2\sigma}{d\Omega_{k'} d\omega} = \frac{G_F^2 \cos^2 \theta_C}{4\pi^2} \frac{|\mathbf{k}'|}{|\mathbf{k}|} L_{\mu\nu} W^{\mu\nu}(\mathbf{q}, \omega)$$



$$L_{\mu\nu} = k_\mu k'_\nu + k'_\mu k_\nu - g_{\mu\nu} k \cdot k' \pm i \varepsilon_{\mu\nu\kappa\lambda} k^\kappa k'^\lambda \quad W^{\mu\nu} = \sum_f \langle 0 | J^{\mu\dagger}(q) | f \rangle \langle f | J^\nu(q) | 0 \rangle \delta^{(4)}(p_0 + q - p_f)$$

Leptonic tensor Hadronic tensor

The “inclusive” charged current cross section is a linear combination of 5 contributions

$$\frac{d^2\sigma}{d\Omega_{k'} d\omega} = \sigma_0 \left[L_{00} W^{00} + L_{33} W^{33} + (L_{03} + L_{30}) W^{03} + (L_{11} + L_{22}) W^{11} \pm (L_{12} - L_{21}) W^{12} \right]$$

A simplified expression particularly useful for illustration:

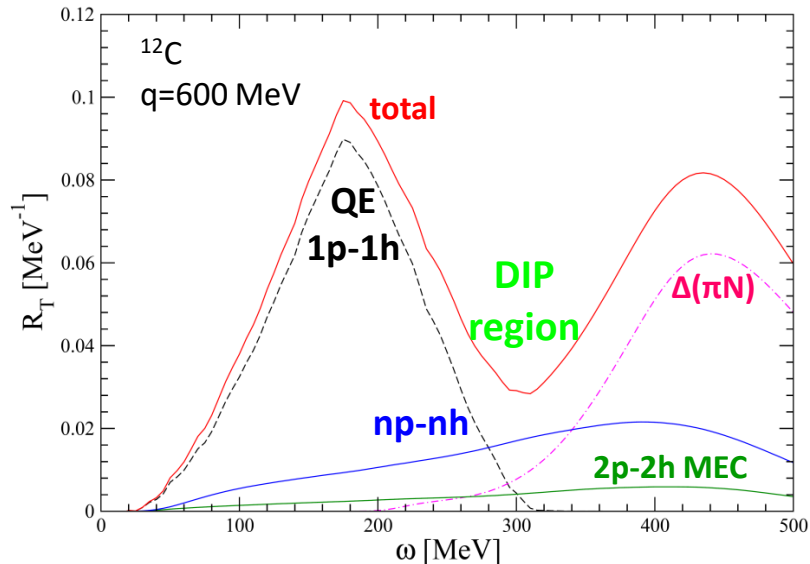
$$\frac{d^2\sigma}{d\cos\theta d\omega} = \frac{G_F^2 \cos^2 \theta_c}{\pi} |\mathbf{k}'| E'_l \cos^2 \frac{\theta}{2} \left[\frac{(\mathbf{q}^2 - \omega^2)^2}{\mathbf{q}^4} G_E^2 R_T(\mathbf{q}, \omega) + \frac{\omega^2}{\mathbf{q}^2} G_A^2 R_{\sigma\tau(L)}(\mathbf{q}, \omega) \right] + 2 \left(\tan^2 \frac{\theta}{2} + \frac{\mathbf{q}^2 - \omega^2}{2\mathbf{q}^2} \right) \left(G_M^2 \frac{\mathbf{q}^2}{4M_N^2} + G_A^2 \right) R_{\sigma\tau(T)}(\mathbf{q}, \omega) \pm 2 \frac{E_\nu + E'_l}{M_N} \tan^2 \frac{\theta}{2} G_A G_M R_{\sigma\tau(T)}(\mathbf{q}, \omega)$$

Explicitly appear:

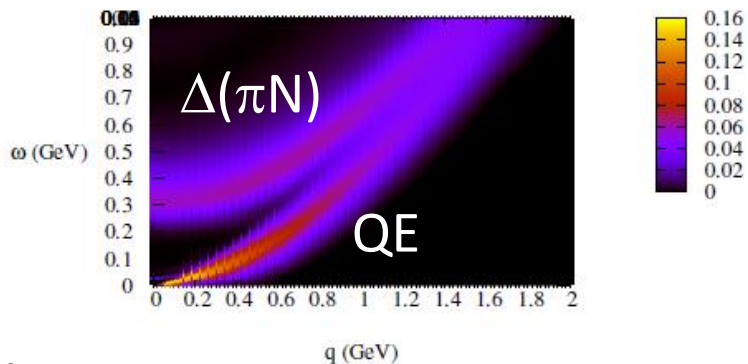
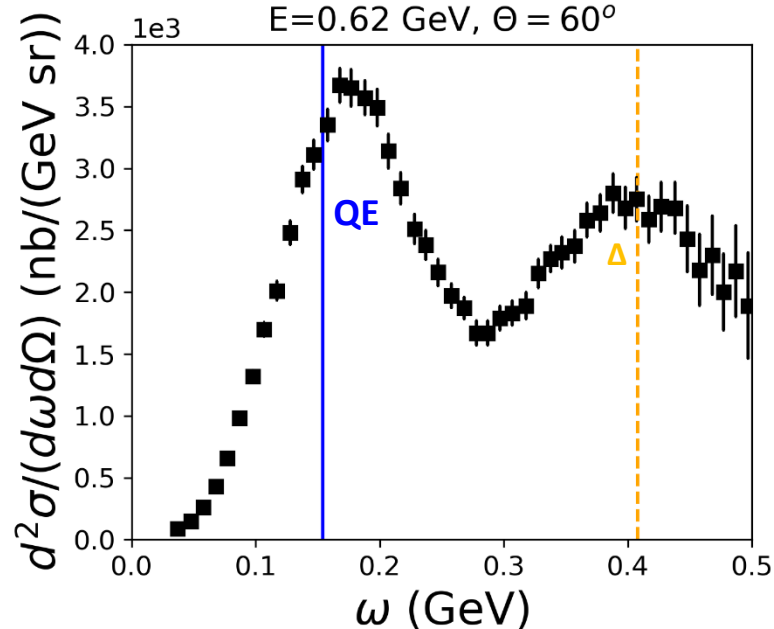
1. The different **kinematic variables** (related to the leptonic tensor)
2. The nucleon Electric, Magnetic, and Axial **form factors** (\leftrightarrow nucleon properties)
3. The **nuclear response functions** (\leftrightarrow nuclear dynamics)

Nuclear responses and inclusive electron and ν cross sections

Nuclear Responses



Monochromatic electron $d^2\sigma$



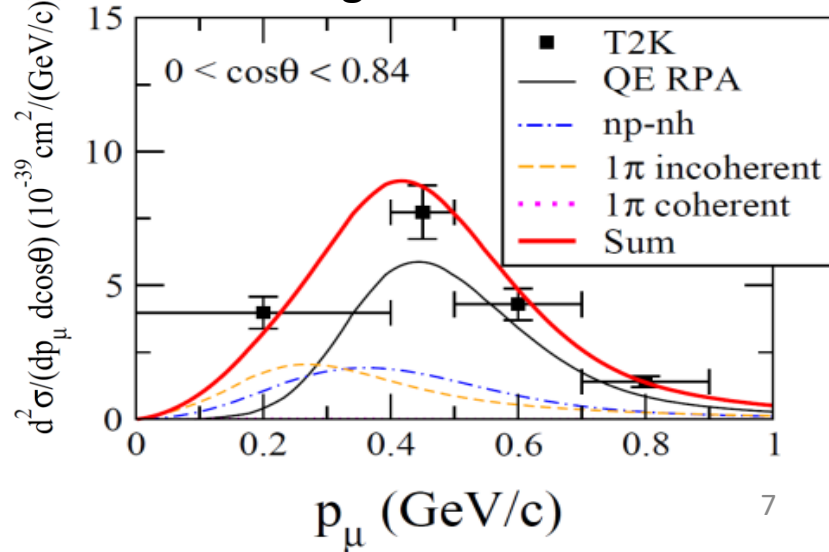
QE peak:

$$\omega = \sqrt{\mathbf{q}^2 + M_N^2} - M_N = \frac{Q^2}{2M_N} = \frac{\mathbf{q}^2 - \omega^2}{2M_N}$$

Δ peak:

$$\omega = \sqrt{\mathbf{q}^2 + M_\Delta^2} - M_N = \frac{Q^2}{2M_N} + \frac{M_\Delta^2 - M_N^2}{2M_N}$$

Flux-integrated neutrino $d^2\sigma$



The Form Factors

$$Q^2 = q^2 - \omega^2$$

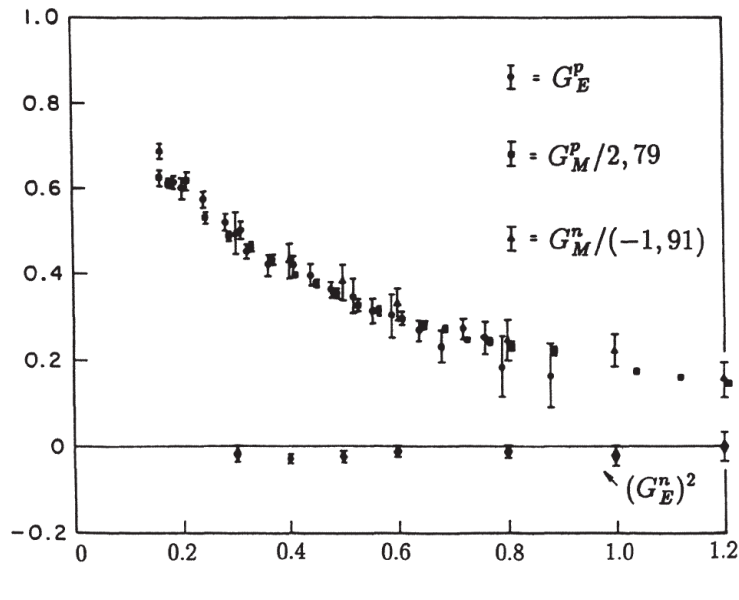
Vector form factors

$$G_E^P(Q^2) = \frac{G_M^P(Q^2)}{2.79} = \frac{G_M^n(Q^2)}{-1.91} = G^{\text{dipole}}(Q^2)$$

$$G^{\text{dipole}}(Q^2) = \left(1 + \frac{Q^2}{0.71 (\text{GeV}/c)^2} \right)^{-2}$$

Global dipole-like behavior

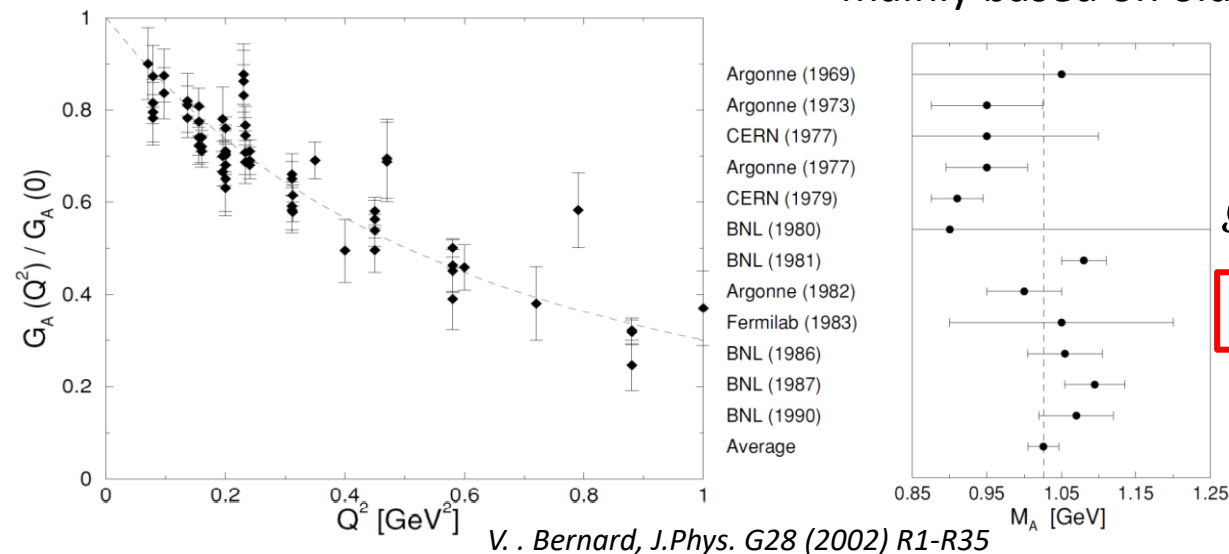
Weak vector form factors are well constrained by electron scattering experiments (CVC)



$Q^2(\text{GeV}^2/c^2)$

Q^2 evolution of the axial form factor is less well-known, mainly based on old bubble chamber data

Axial form factor



V. Bernard, J.Phys. G28 (2002) R1-R35

$$G_A(Q^2) = g_A (1 + Q^2 / M_A^2)^{-2}$$

$$g_A = 1.26 \text{ from neutron } \beta \text{ decay}$$

$$M_A = (1.026 \pm 0.021) \text{ GeV}/c^2$$

from ν - ^2H (bubble-chamber) CCQE
and
from π electroproduction

CCQE, CCQE-like and CC0 π

MiniBooNE CC Quasielastic cross section on Carbon and the M_A puzzle

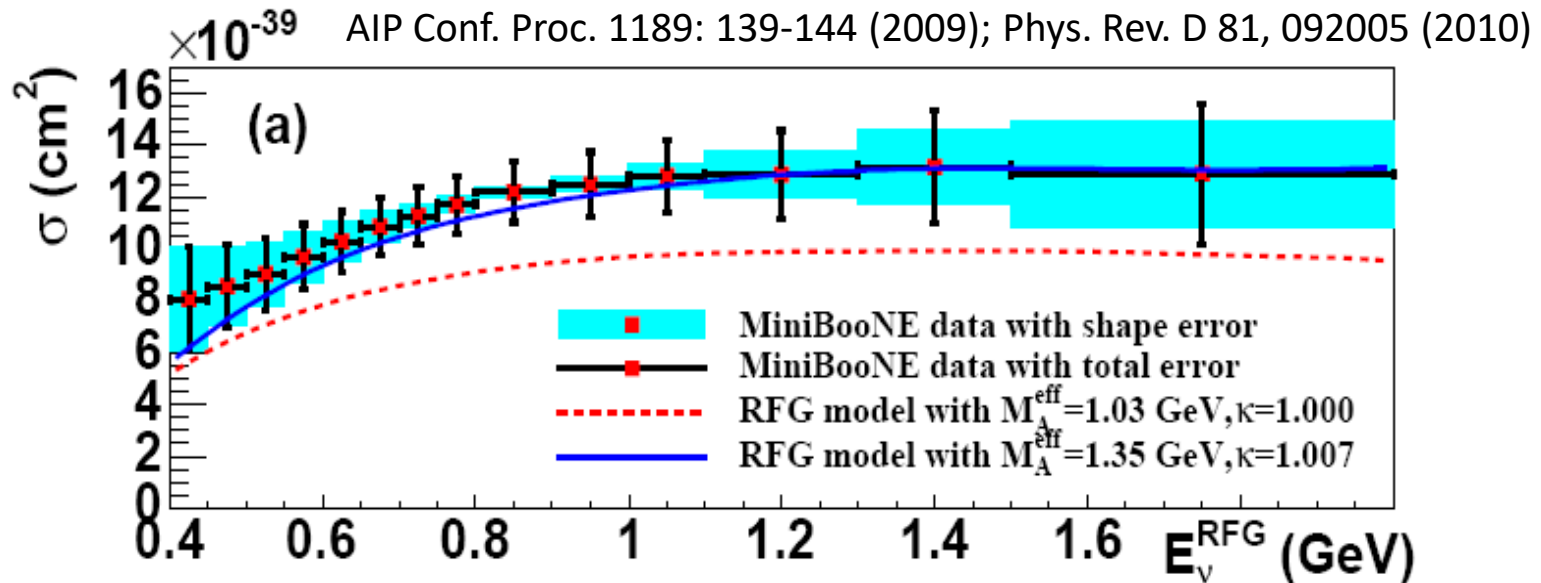
First Measurement of Muon Neutrino Charged Current Quasielastic (CCQE) Double Differential Cross Section

Cite as: AIP Conference Proceedings 1189, 139 (2009); <https://doi.org/10.1063/1.3274144>
Published Online: 02 December 2009

Tepepei Katori and MiniBooNE collaboration

PHYSICAL REVIEW D 81, 092005 (2010)

First measurement of the muon neutrino charged current quasielastic double differential cross section

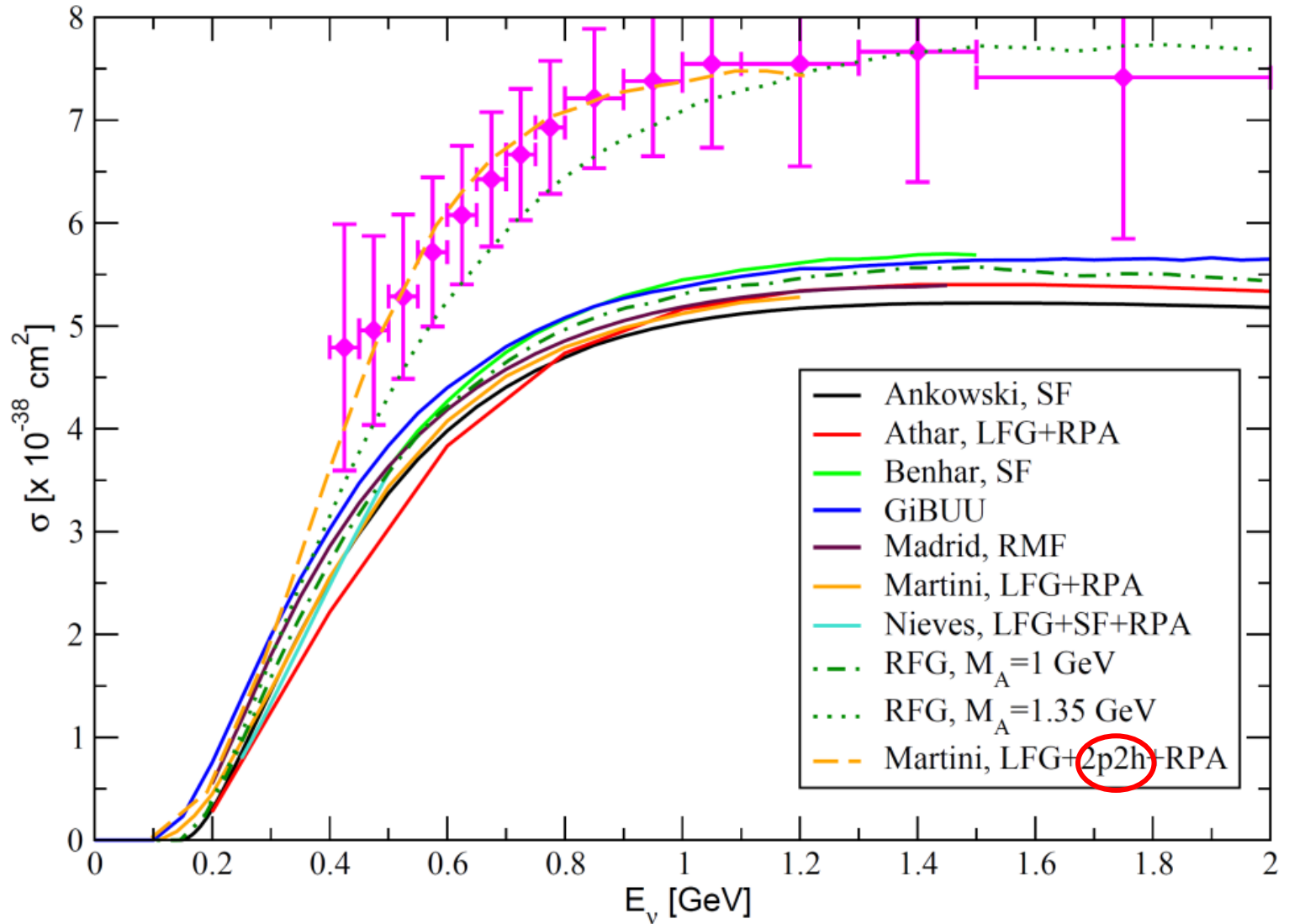


Comparison with a prediction based on Relativistic Fermi Gas (RFG) using $M_A=1.03$ GeV (standard value) reveals a discrepancy

In the Relativistic Fermi Gas (RFG) model an axial mass of **1.35 GeV** is needed to account for data **puzzle??**

Comparison of different theoretical models for Quasielastic

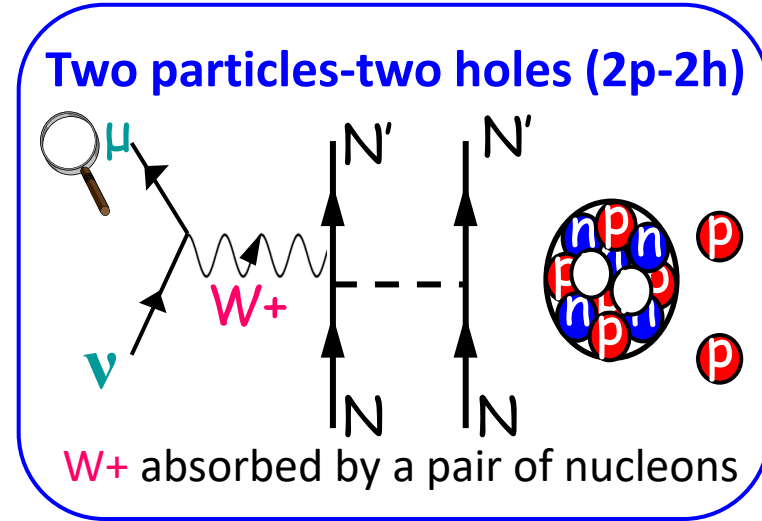
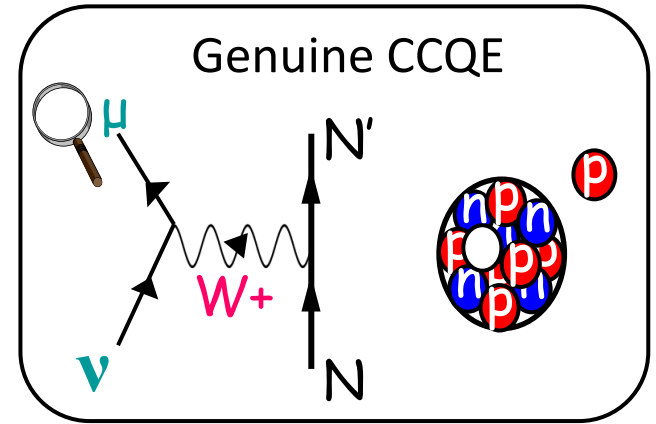
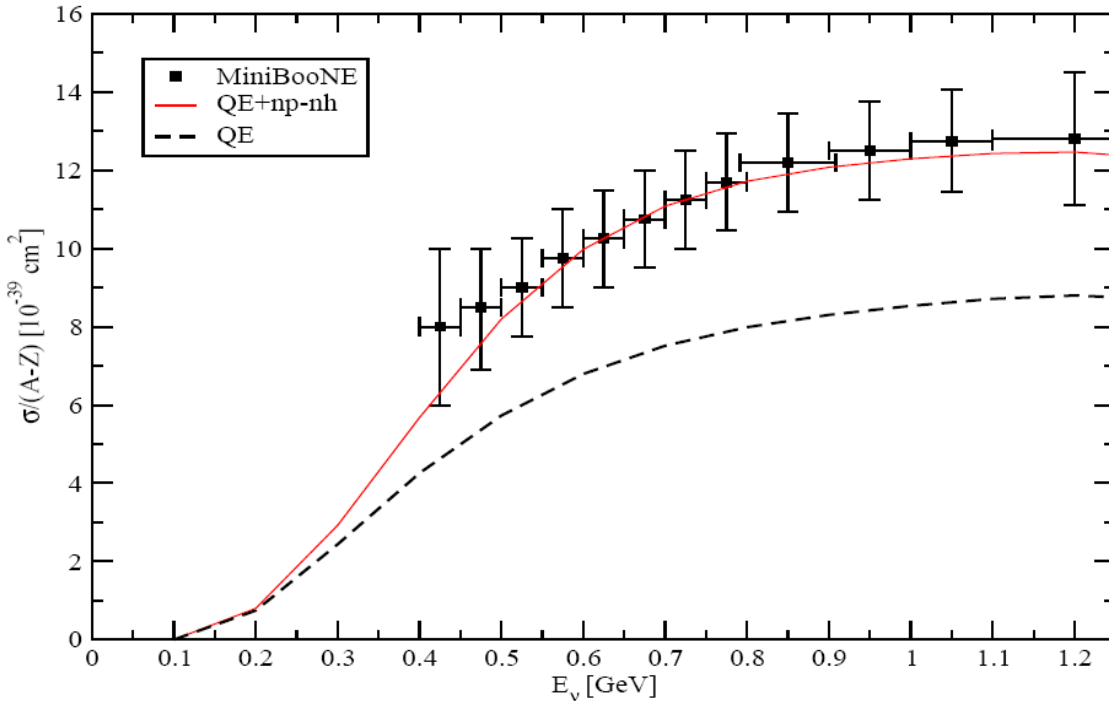
L. Alvarez-Ruso , arXiv:1012.3871 (Neutrino 2010)



puzzle??

An explanation of this puzzle

Inclusion of the multinucleon emission channel (np-nh = 2p-2h + 3p-3h)



CCQE-like = Genuine CCQE + np-nh

M. Martini, M. Ericson, G. Chanfray, J. Marteau, Phys. Rev. C 80 065501 (2009)

Agreement with MiniBooNE without increasing M_A

➡ MiniBooNE measured CCQE-like, not genuine CCQE

Flux-integrated double differential cross section

Unfolding matrix to remove detector effects

Number of observed events

Background contribution

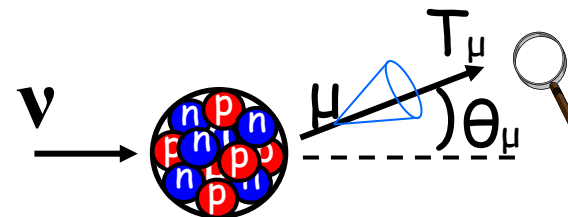
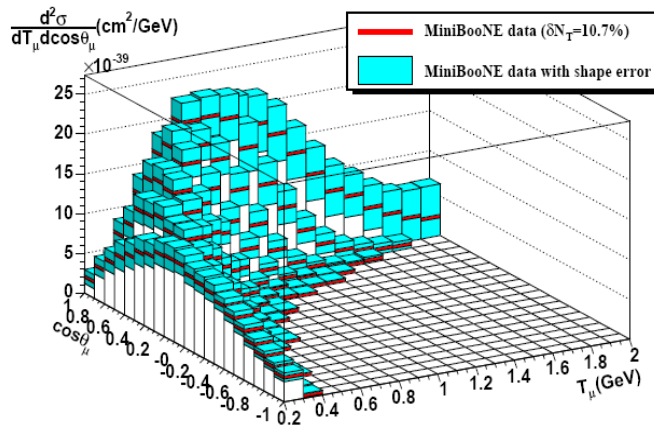
$$\left(\frac{d^2\sigma}{dT_l \cos\theta} \right)_i = \frac{\sum_j U_{ij} (d_j - b_j)}{\Phi \cdot T \cdot \epsilon_i \cdot (\Delta T_l, \Delta \cos\theta)_i}$$

Total integrated flux

Number of target nucleons in the Fiducial Volume

Efficiency

Bin widths



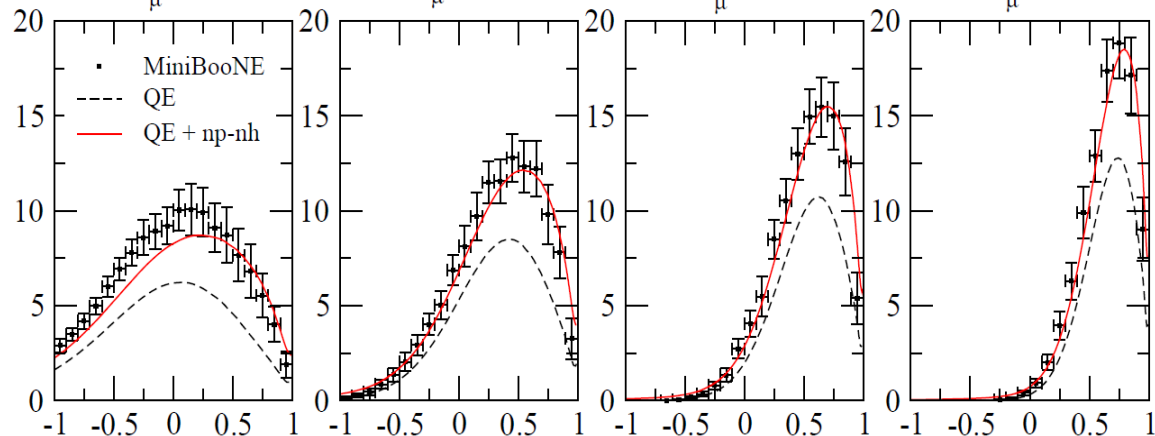
- Function of two measured variables
- Less model dependent than $\sigma(E_\nu)$: free from the neutrino energy reconstruction problem
- Flux dependent

Flux-integrated differential cross section is where theorists and experimentalists meet for ν interaction

MiniBooNE CCQE-like flux-integrated double differential cross section

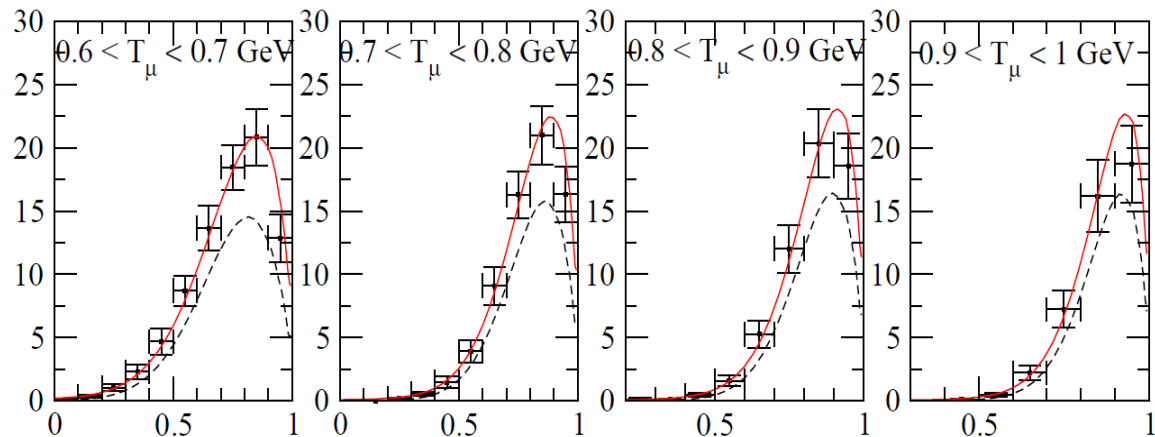
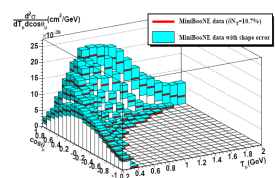
$$\frac{d^2\sigma}{dT_l d\cos\theta} = \frac{1}{\int \Phi(E_\nu) dE_\nu} \int dE_\nu \left[\frac{d^2\sigma}{d\omega d\cos\theta} \right]_{\omega=E_\nu-E_l} \Phi(E_\nu)$$

0.2 < T_μ < 0.3 GeV 0.3 < T_μ < 0.4 GeV 0.4 < T_μ < 0.5 GeV 0.5 < T_μ < 0.6 GeV



ν

$\frac{d^2\sigma}{dT_\mu d\cos\theta} (10^{-39} \text{ cm}^2/\text{GeV})$

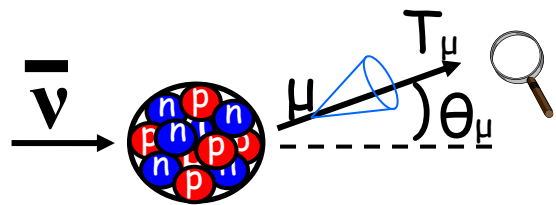


$\cos \theta$

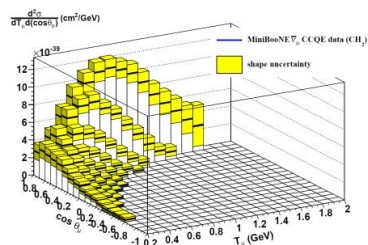
Martini, Ericson, Chanfray,
Phys. Rev. C 84 055502 (2011)

- Good agreement with data once multinucleon contributions are included
- Similar conclusions obtained by different theoretical calculations (see later)

MiniBooNE CCQE-like flux-integrated double differential cross section

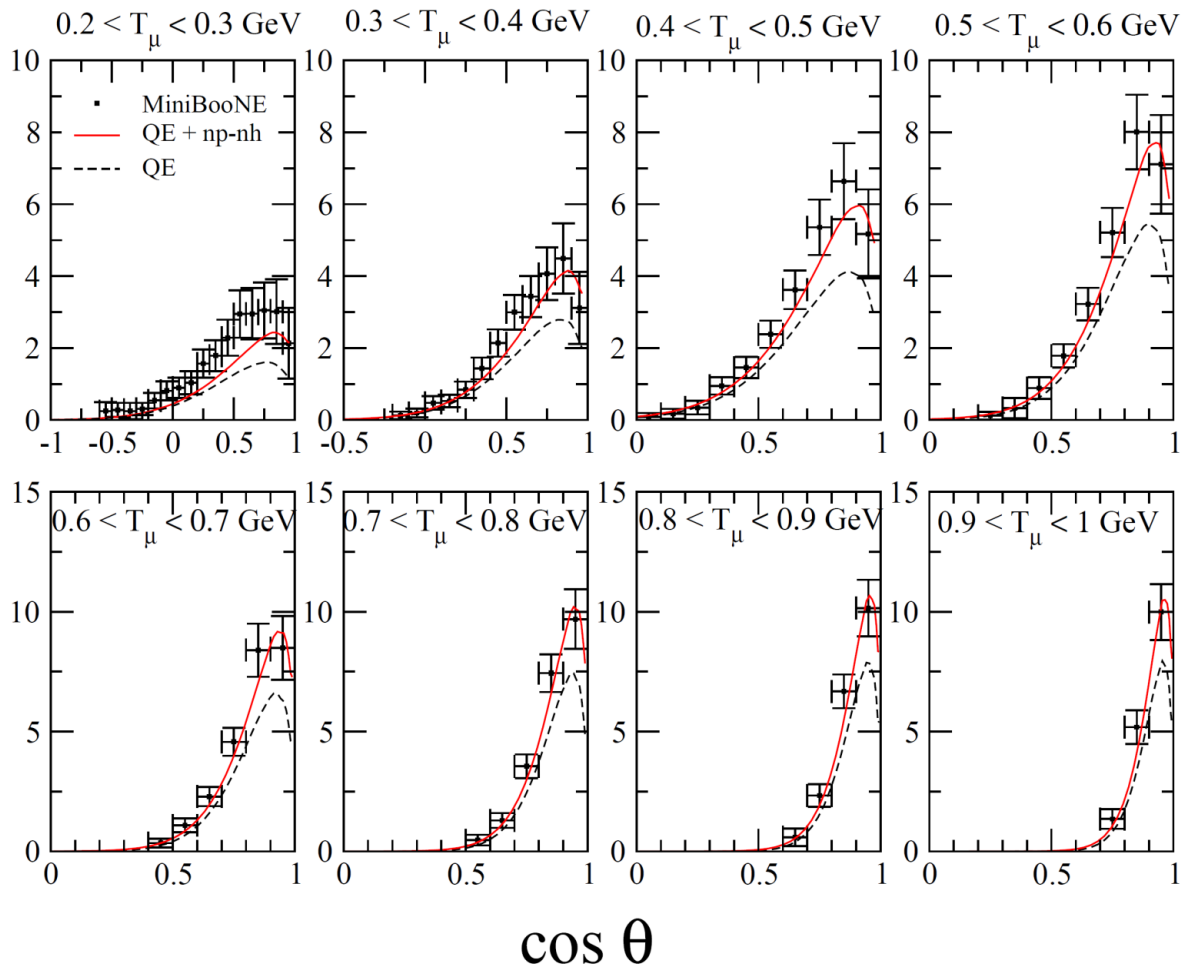


$\bar{\nu}$



MiniBooNE, *Phys. Rev. D* 88 032001 (2013)

$\frac{d^2 \sigma}{d \cos \theta / d T_\mu} (10^{-39} \text{ cm}^2 / \text{GeV})$



Martini, Ericson, *Phys. Rev. C* 87 065501 (2013)

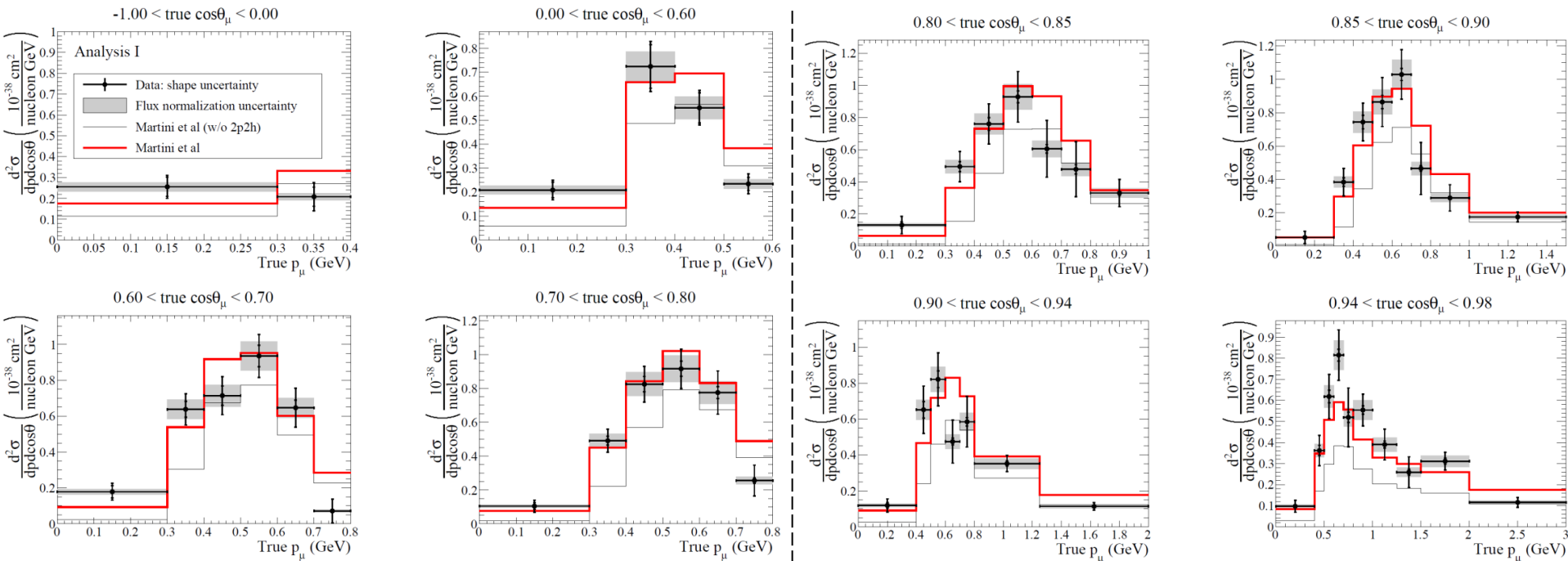
Similar conclusion also for the MiniBooNE CCQE-like antineutrino cross sections

The $CC0\pi$ measurement

After MiniBooNE, it has become more popular to present the data in terms of final state particles
 $CC0\pi = CCQE$ -like without subtraction of π absorption background ($CC0\pi \geq CCQE$ -like)

PHYSICAL REVIEW D **93**, 112012 (2016)

Measurement of double-differential muon neutrino charged-current interactions on C_8H_8 without pions in the final state using the T2K off-axis beam



— Including np - nh
 — Without np - nh

Better agreement including np - nh

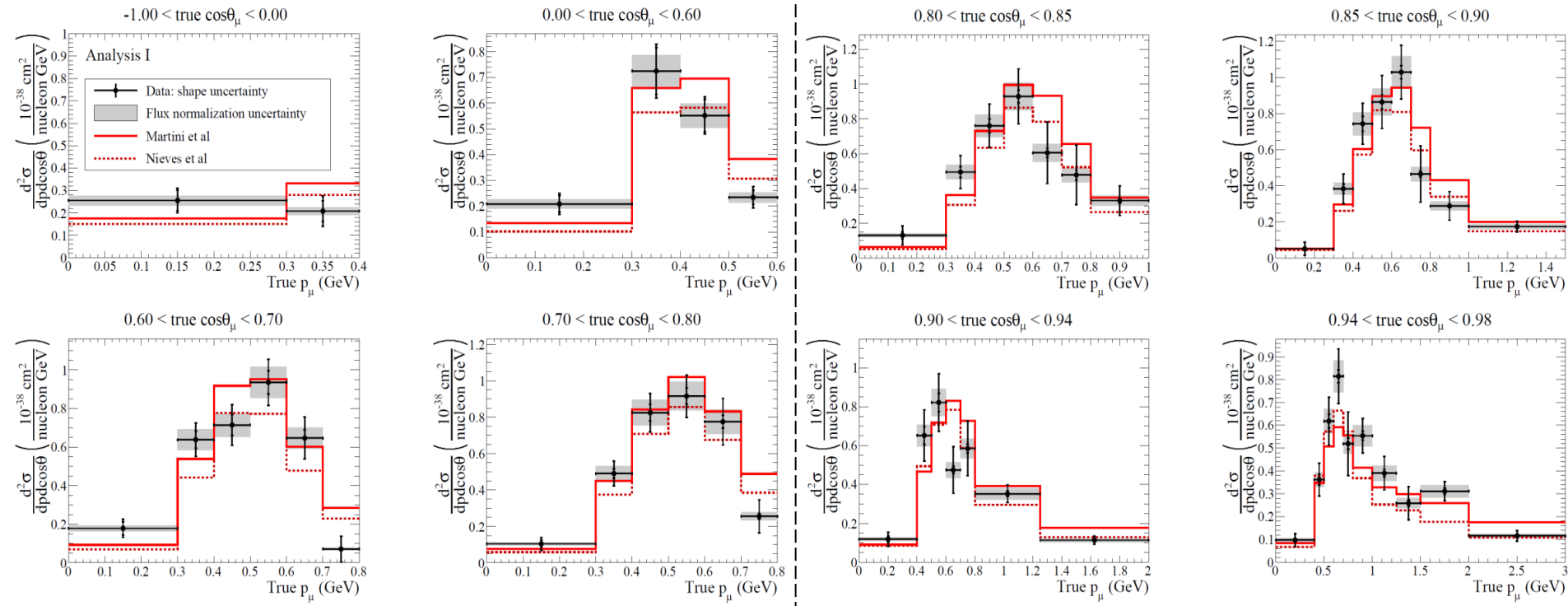
The $CC0\pi$ measurement

After MiniBooNE, it has become more popular to present the data in terms of final state particles

$CC0\pi = CCQE$ -like without subtraction of π absorption background

PHYSICAL REVIEW D **93**, 112012 (2016)

Measurement of double-differential muon neutrino charged-current interactions on C_8H_8 without pions in the final state using the T2K off-axis beam

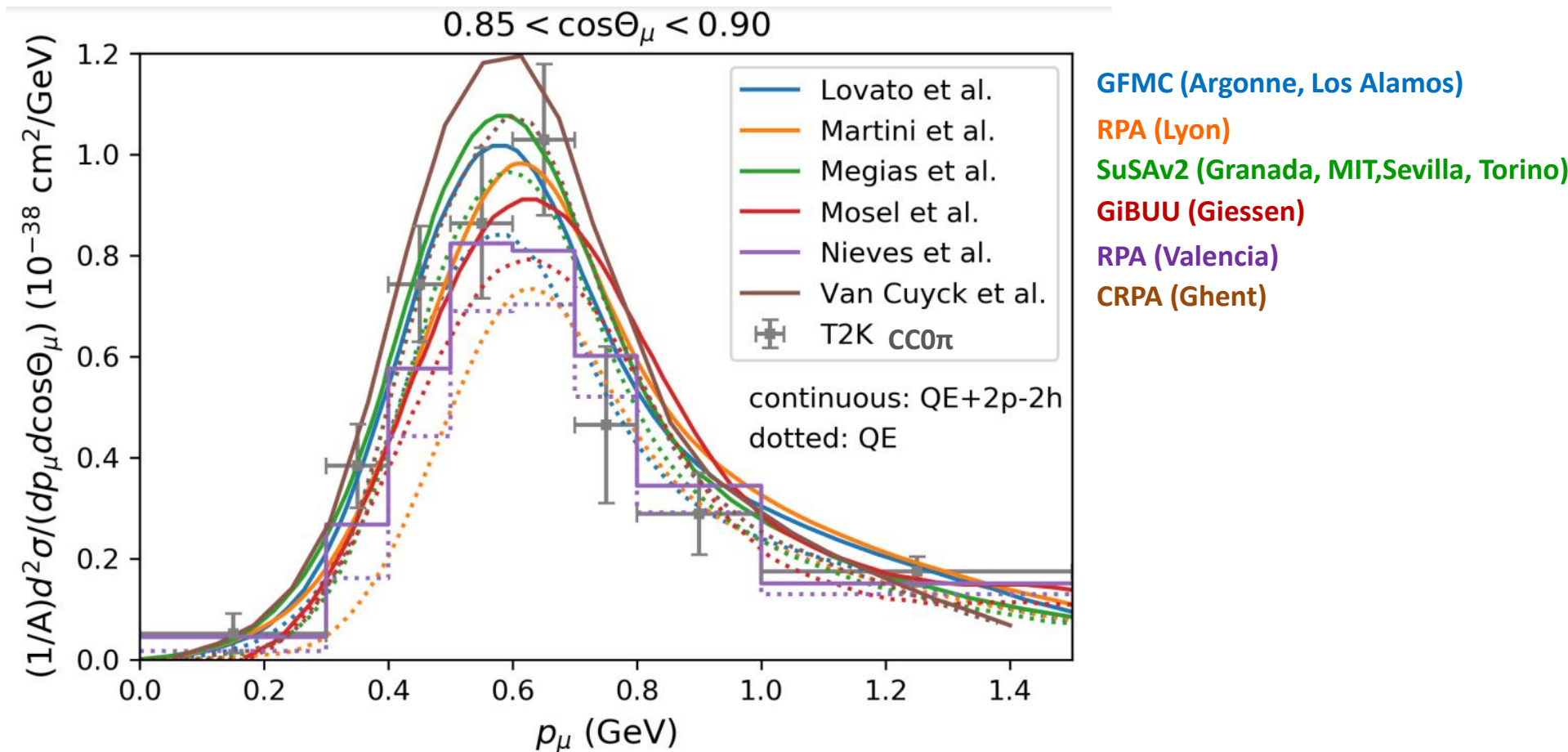


— Martini et al.
 Nieves et al.

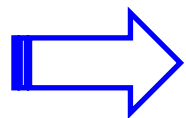
Differences between models' predictions

Comparison between different CCQE+2p-2h theoretical predictions

A. Branca et al. *Symmetry* 13 (2021) 9, 1625



Several theoretical calculations agree on the crucial role of 2p-2h to reproduce data but there are discrepancies between the different models' predictions

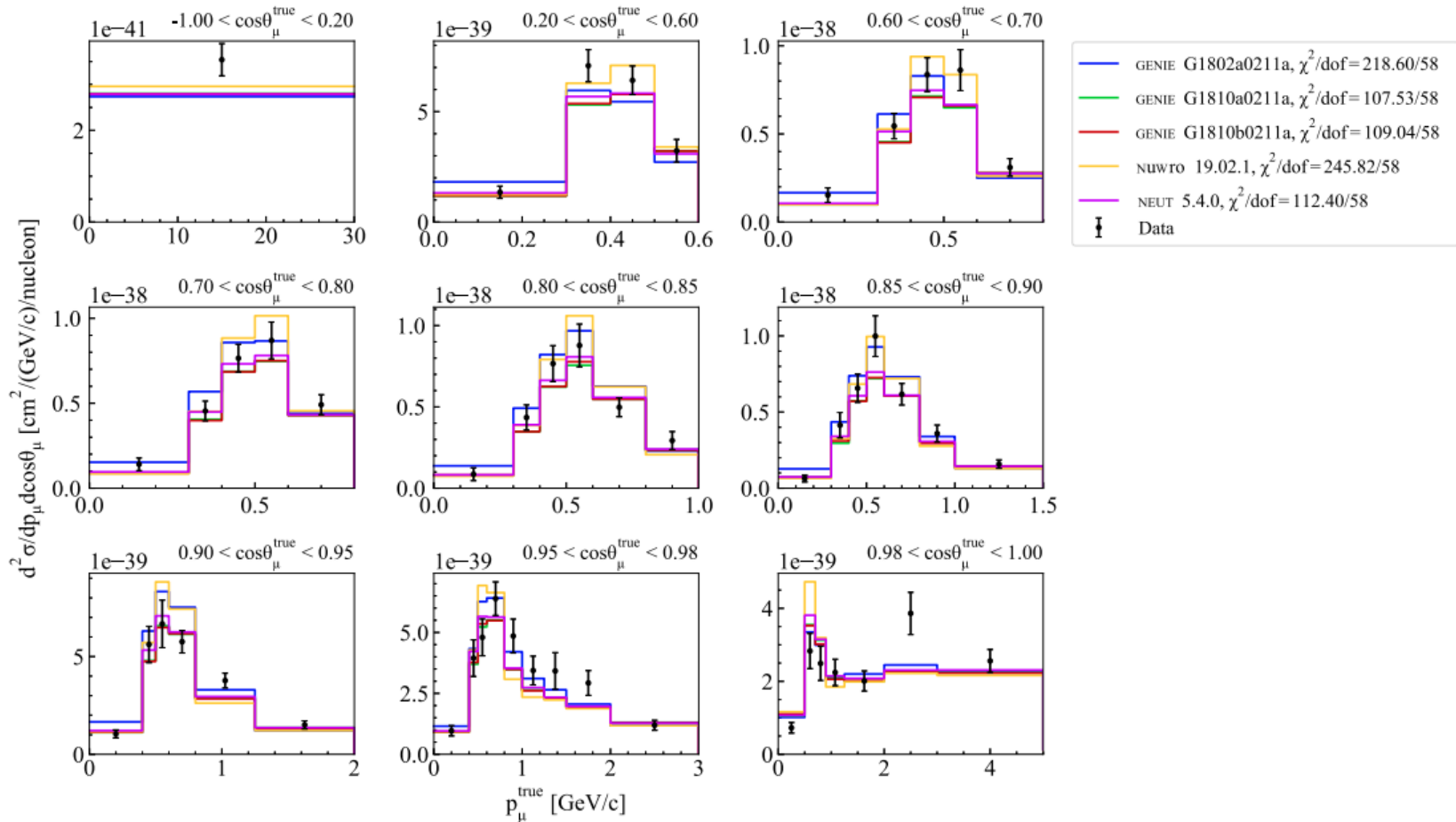


2p-2h are one of the most important source of the cross section uncertainties (systematic errors in oscillation experiments)

The T2K $\text{CC}0\pi$ data and the Monte Carlo predictions

M. BUIZZA AVANZINI *et al.*

PHYS. REV. D **105**, 092004 (2022)



Differences in the MC predictions (CCQE, 2p-2h and π absorption modeling)

p.s. The effort to implement different 2p-2h models in several Monte Carlo is still in progress

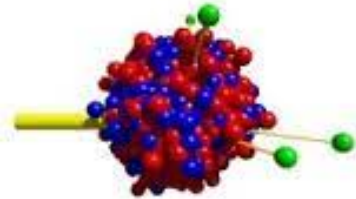
Monte Carlo Event Generators

Monte Carlo event generators connects theoretical models to experimental measurements

Main Event Generators for neutrino interactions:



GiBUU



NEUT



L. Alvarez-Ruso et al.,
EPJ Spec. Top. 230, 4449 (2021)

O. Buss et al.,
Phys.Rept. 512 1-124 (2012)

Y. Hayato and L. Pickering,
EPJ Spec. Top. 230, 4469 (2021)

T. Golan et al.,
NPB 229–232, 499 (2012)

PHYSICAL REVIEW D **105**, 092004 (2022)

Comparisons and challenges of modern neutrino-scattering experiments

M. Buizza Avanzini¹, M. Betancourt², D. Cherdack³, M. Del Tutto^{2,4}, S. Dytman⁵, A. P. Furmanski^{6,7},
S. Gardiner², Y. Hayato⁸, L. Koch⁹, K. Mahn¹⁰, A. Mastbaum¹¹, B. Messerly^{5,7}, C. Riccio^{12,13},
D. Ruterbories¹⁴, J. Sobczyk¹⁵, C. Wilkinson¹⁶ and C. Wret¹⁴

Main models implemented for the quasielastic and 2p-2h:

- Relativistic global and local Fermi Gas
- RPA
- Spectral Function
- SuperScaling (SuSAv2)

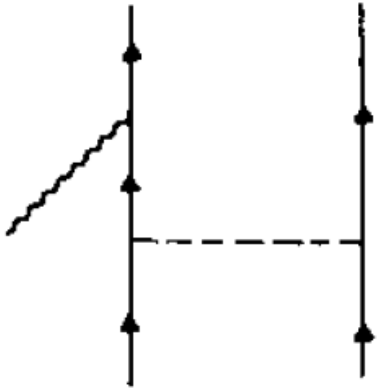
[For the illustration of the different models see for example the cross section lectures at the GIF school]

Some details on 2p-2h

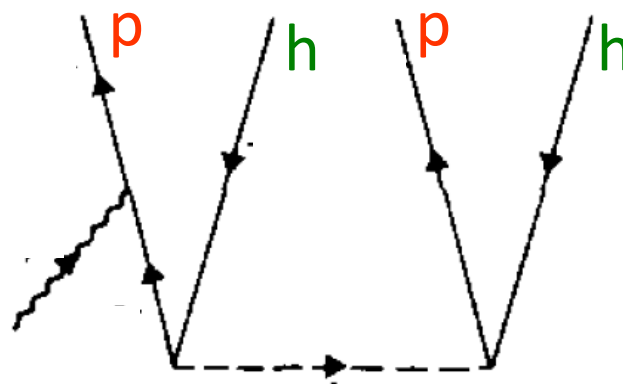
Two particle-two hole sector (2p-2h)

Three equivalent representations of the same process

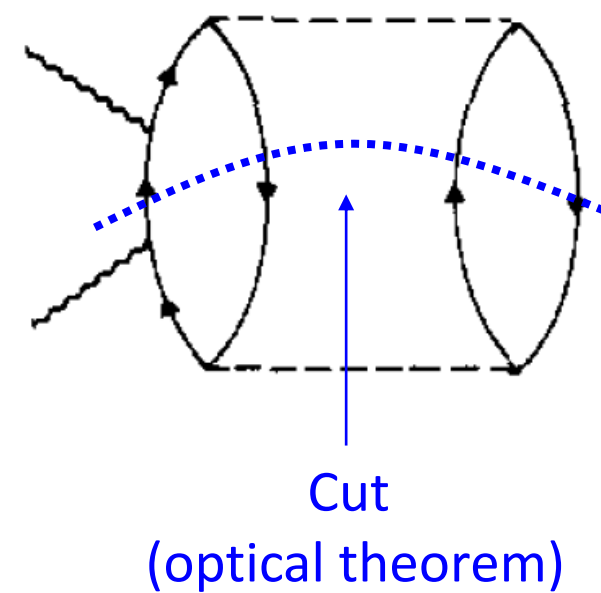
2 body current



2p-2h matrix element



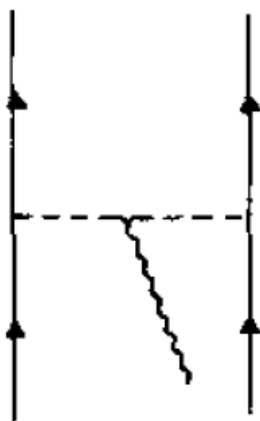
2p-2h response



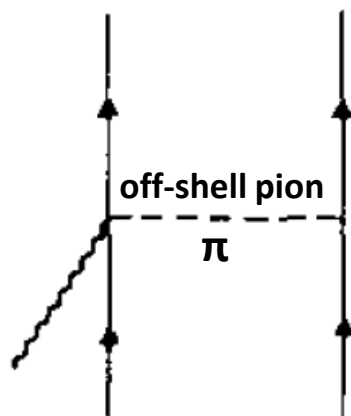
Final state: two particles-two holes

Diagrams for 2 body currents

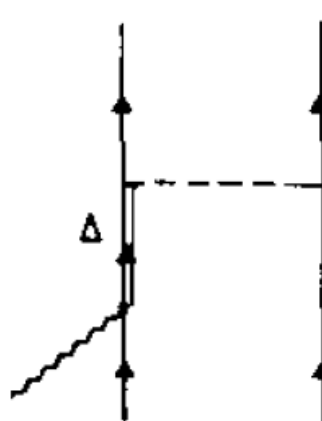
Meson Exchange Currents (MEC) J^{MEC}



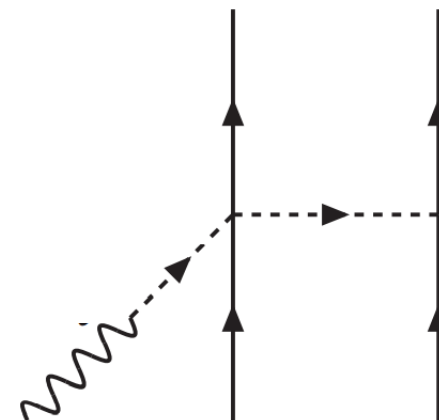
Pion in flight



Seagull or
Contact

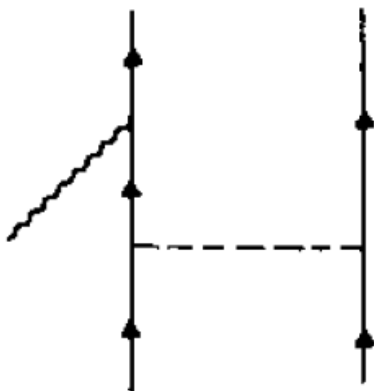


Delta



Pion pole
(purely axial)

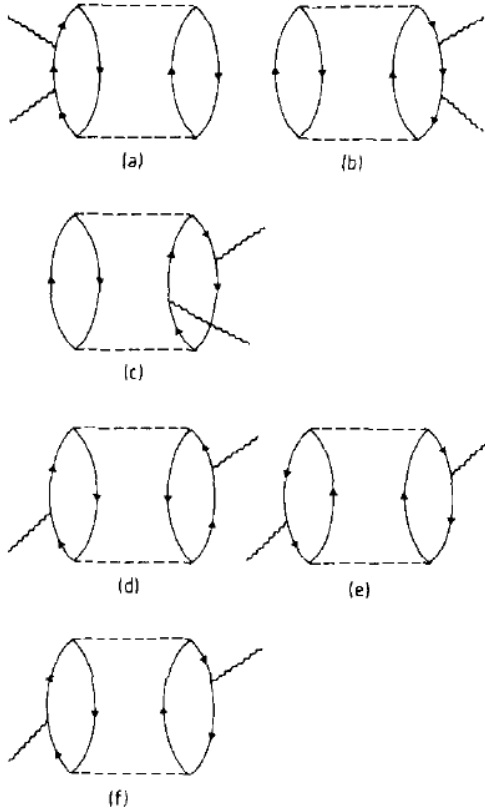
Nucleon-Nucleon Correlations (SRC) J^{corr}



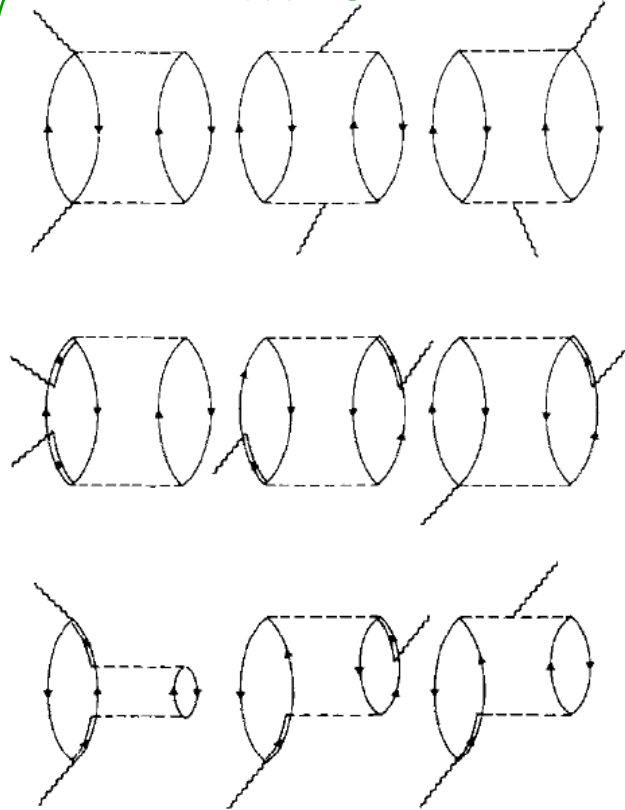
- An additional two-body current to be included in the framework of independent particle models for QE such as the Fermi Gas or Hartree-Fock.
- Absent in the approaches which start from the description of the nucleus in terms of correlated wave functions (such as CBF spectral function or GFMC) since the hadronic tensor of the one body current already includes this contribution.
- **There is a risk of a double counting of SRC in the Monte Carlo if different contributions to the neutrino cross sections are taken from different models.**

Some diagrams for 2p-2h responses

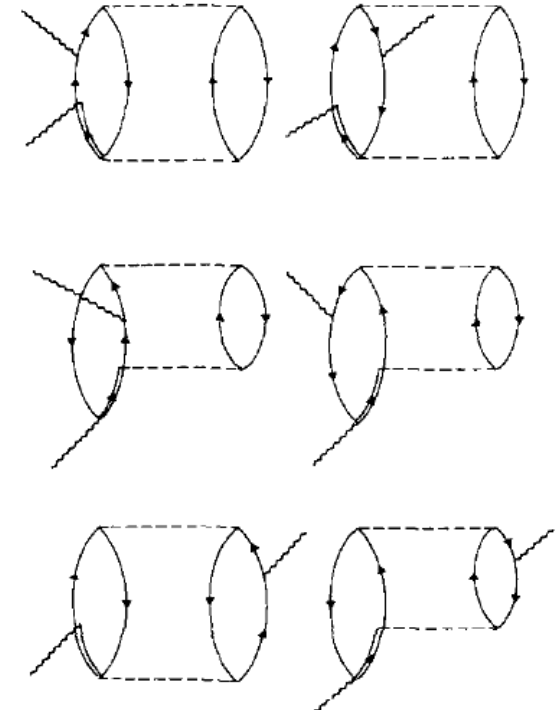
NN correlations



MEC



NN correlation-MEC interference



also called
1-body—2-body interference

Alberico, Ericson, Molinari, Ann. Phys. 154, 356 (1984)

Main difficulties in the np-nh sector

$$W^{\mu\nu}(\mathbf{q}, \omega) = W_{1p1h}^{\mu\nu}(\mathbf{q}, \omega) + W_{2p2h}^{\mu\nu}(\mathbf{q}, \omega) + \dots$$

$$W_{2p-2h}^{\mu\nu}(\mathbf{q}, \omega) = \frac{V}{(2\pi)^9} \int d^3p'_1 d^3p'_2 d^3h_1 d^3h_2 \frac{m_N^4}{E_1 E_2 E'_1 E'_2} \theta(p'_2 - k_F) \theta(p'_1 - k_F) \theta(k_F - h_1) \theta(k_F - h_2) \\ \underbrace{\langle 0 | J^\mu | \mathbf{h}_1 \mathbf{h}_2 \mathbf{p}'_1 \mathbf{p}'_2 \rangle \langle \mathbf{h}_1 \mathbf{h}_2 \mathbf{p}'_1 \mathbf{p}'_2 | J^\nu | 0 \rangle}_{\text{matrix elements}} \delta(E'_1 + E'_2 - E_1 - E_2 - \omega) \delta(\mathbf{p}'_1 + \mathbf{p}'_2 - \mathbf{h}_1 - \mathbf{h}_2 - \mathbf{q})$$

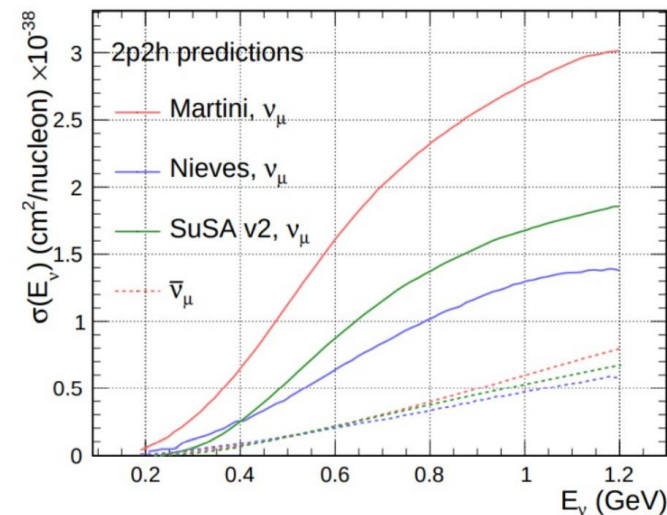
- 7-dimensional integrals $\int d^3h_1 d^3h_2 d\theta'_1$ of thousands of terms
- Huge number of diagrams and terms
- Divergences (angular distribution; NN correlations contributions)
- Calculations for all the kinematics compatible with the experimental neutrino flux

Computing very demanding

Hence different approximations by different groups:

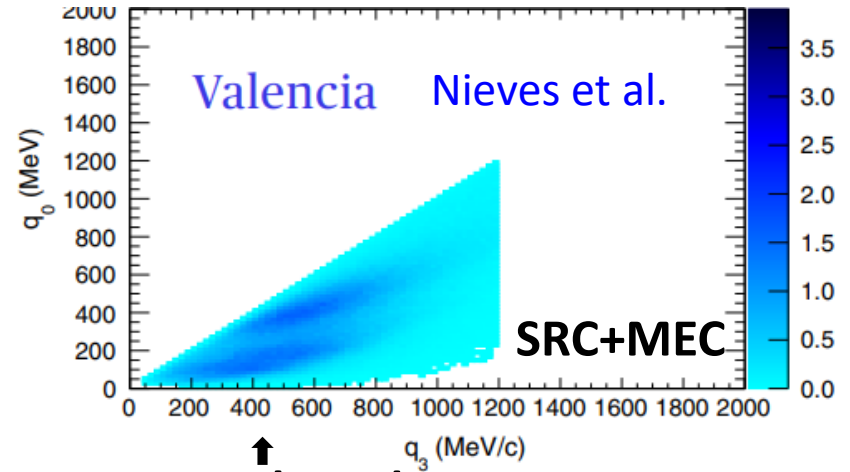
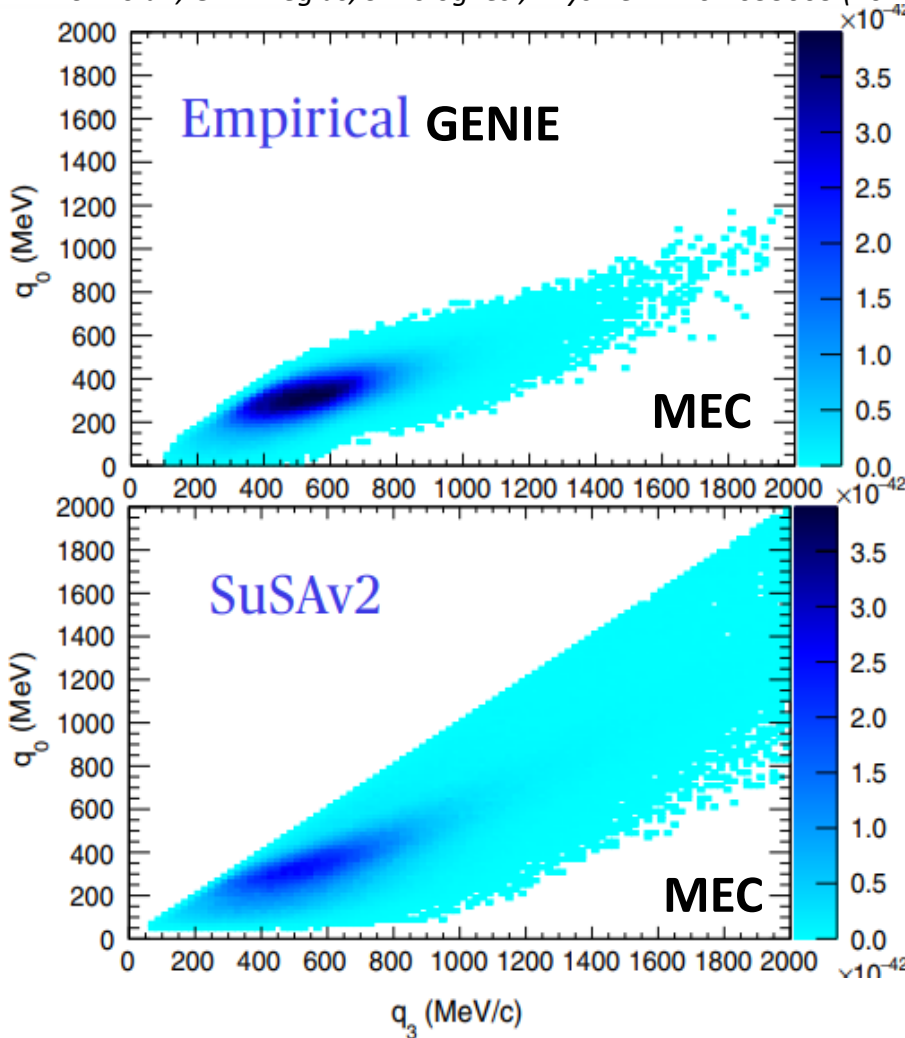
- choice of subset of diagrams and terms;
- different prescriptions to regularize the divergences;
- reduce the dimension of the integrals
(7D --> 2D if non relativistic; 7D --> 1D if $h_1 = h_2 = 0$)

⇒ Different final results by different groups



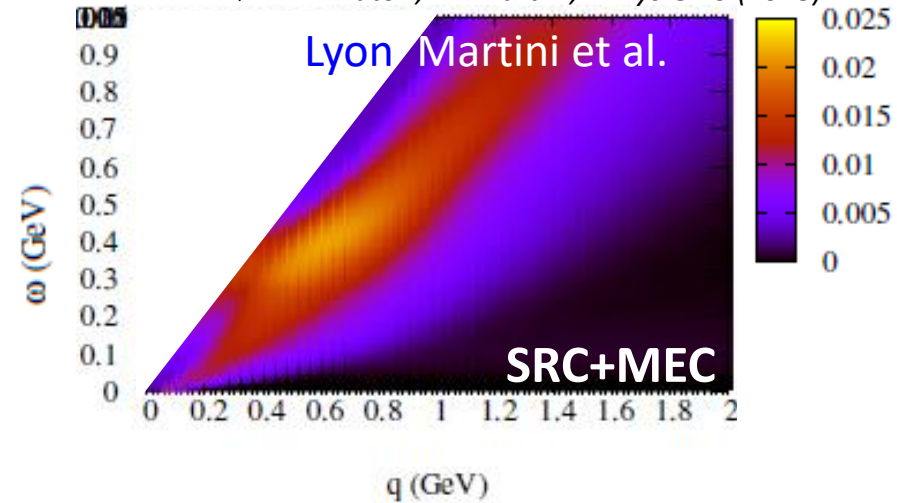
Example of different results for 2p-2h in the (q, ω) or (q_0, q_3) plane

S. Dolan, G.D. Megias, S. Bolognesi, *Phys.Rev.D* 101 033003 (2020)



RPA-based

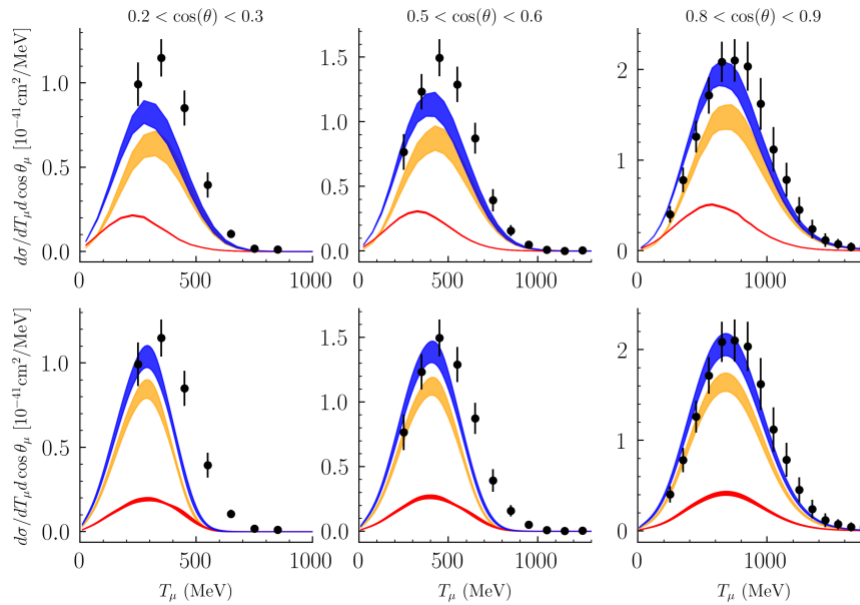
T. Katori, M. Martini, *J.Phys.G* 45 (2018)



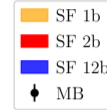
N.B. A one-to one correspondence between different exclusive channel's contributions can be misleading [e.g. NN SRC contributions are part of the 2p-2h channel in RPA-based approaches while they are included in QE in SuSA.]

Example of different results in recent Spectral Function and Green's Function Monte Carlo (ab-initio) calculations

MiniBoONE



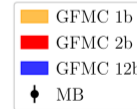
SF



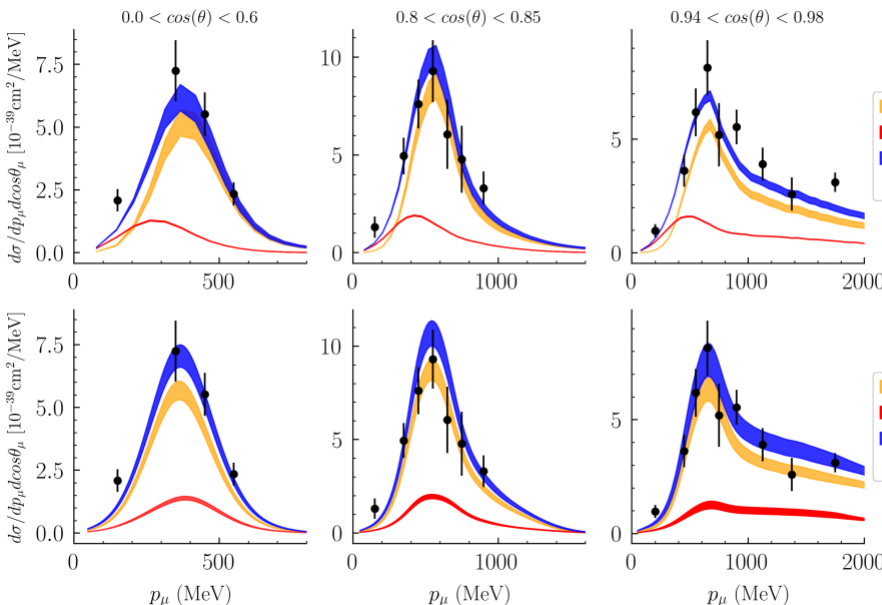
D. Simons et al. 2210.02455

N. Steinberg talk @ NUINT 2022

GFMC



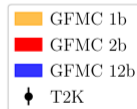
T2K



SF



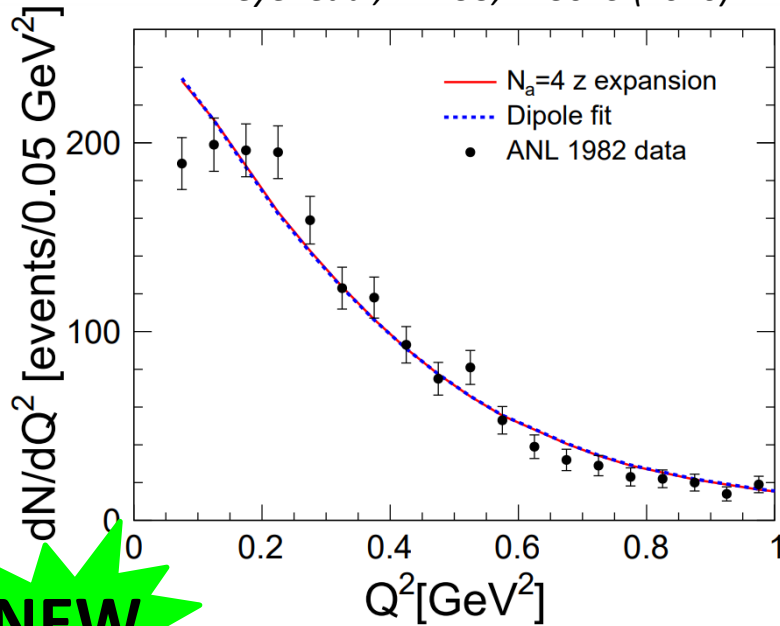
GFMC



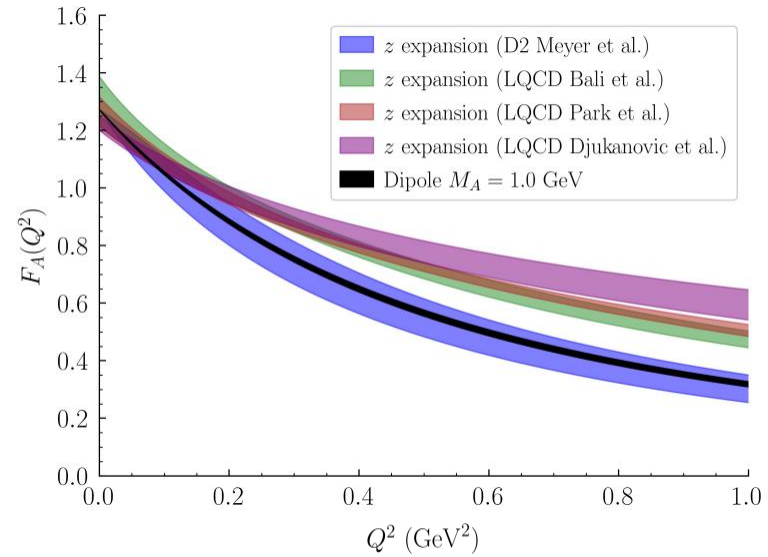
SF and GFMC 2-body contributions shifted because of different 1 body – 2 body interference effects

Axial Form factor and Lattice QCD predictions

A. Meyer et al, PRD93, 113015 (2016)

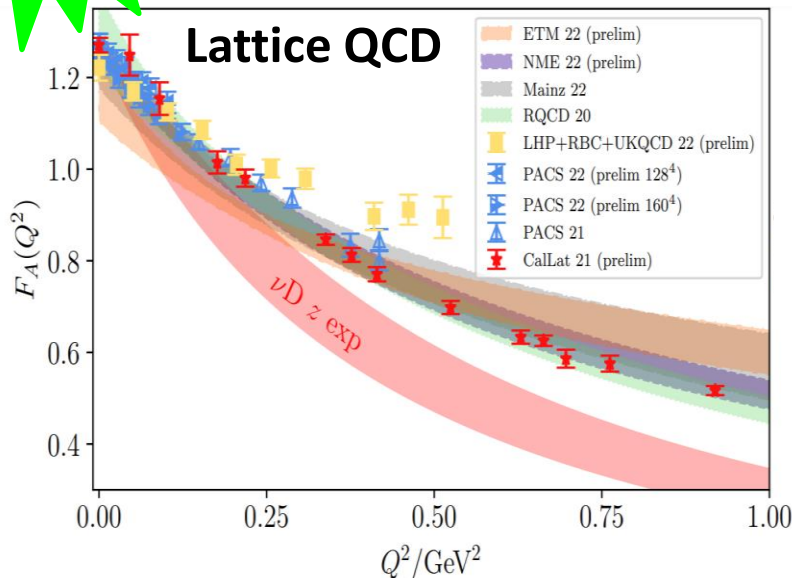


D. Simons et al. 2210.02455



NEW

A. Meyer talk @ NUINT 2022



- Dipole parameterization underestimates uncertainties
- Meyer et al. z -expansion: similar to dipole parameterization but larger errors
- Lattice QCD calculations show evidence of slow Q^2 falloff
- LQCD: much larger normalization at $Q^2 > 0.3$ GeV²

Impact of enhanced axial form factor from LQCD

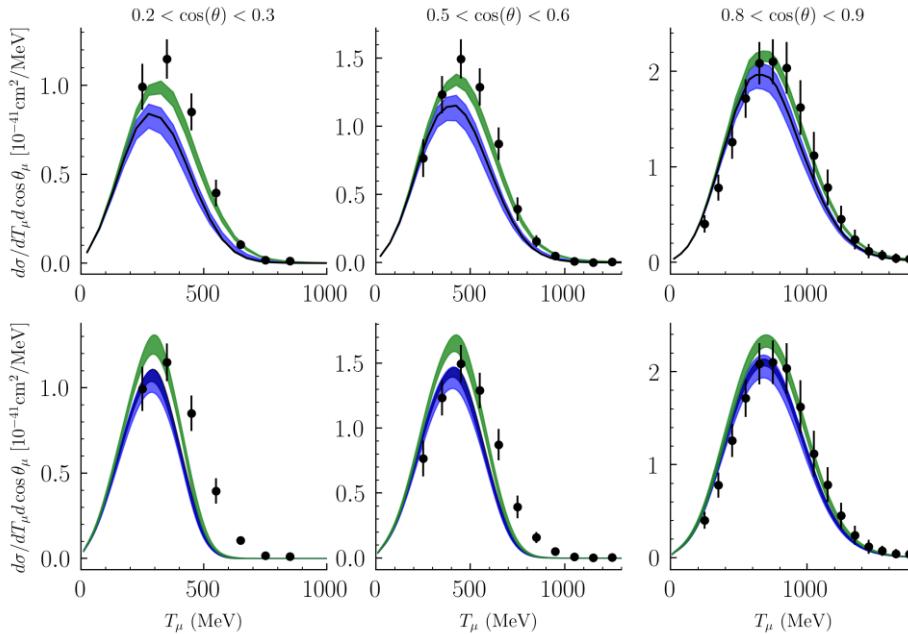
D. Simons et al. 2210.02455

N. Steinberg talk @ NUINT 2022

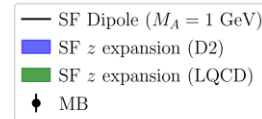


MiniBooNE:
Universal 10-20% increase
in normalization with LQCD

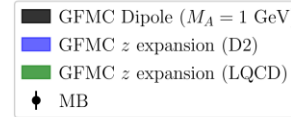
MiniBooNE



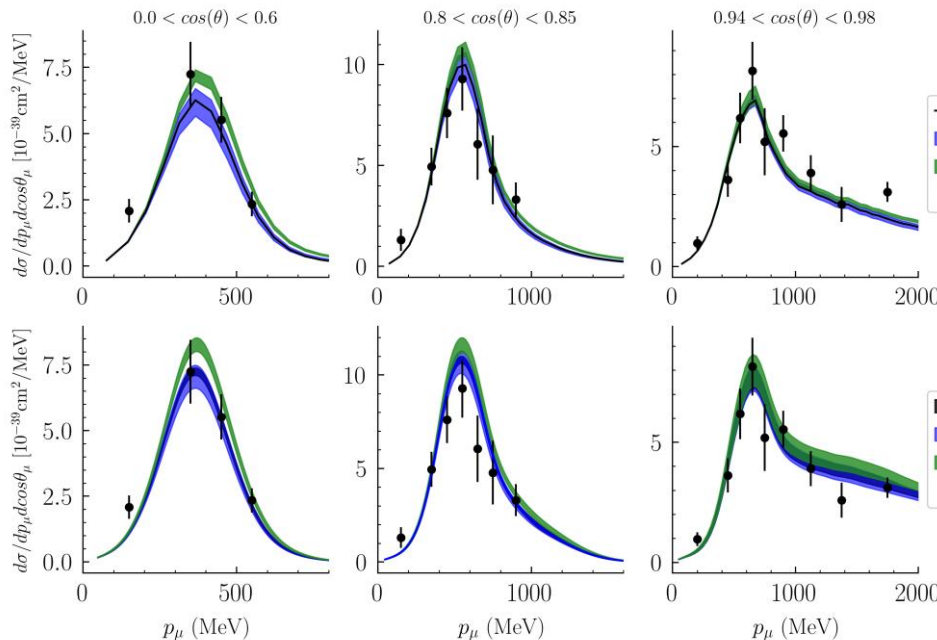
SF



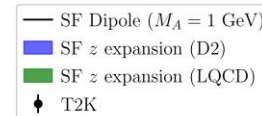
GFMC



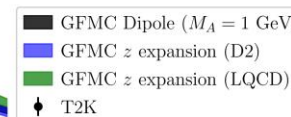
T2K



SF



GFMC



T2K:

Results fairly independent of
parameterization

Mostly due to T2K's lower
beam energy hence lower Q^2
where form factors agree

Data have room for both 2p-2h and
enhanced axial form factor for LQCD

Neutrino energy reconstruction

Energy reconstruction in neutrino oscillation experiments

Reconstructed ν energy

$$N_{\nu\beta}(\overline{E_\nu}) \sim \int \Phi_{\nu\alpha}(E_\nu) P_{\nu\alpha \rightarrow \nu\beta}(E_\nu, L, \{\Theta\}) \sigma_{\nu\beta}(E_\nu) \epsilon_{\text{det.}} d(E_\nu, \overline{E_\nu}) dE_\nu$$

True ν energy

Number of detected events

ν flux	ν oscillation probability	ν cross section	Detector efficiency	Migration matrix
------------	-------------------------------	---------------------	---------------------	-------------------------

Two methods for ν energy reconstruction

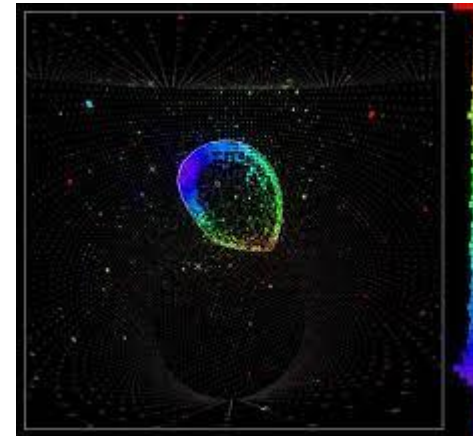
Tracking detectors

- Use all the detected particles
- Calorimetric method



Cherenkov detectors

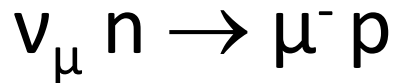
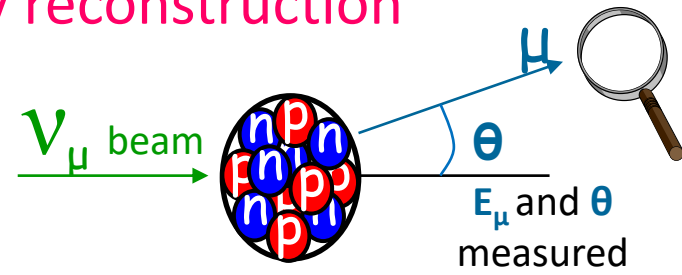
- Use only lepton (1 ring signal)
- Quasielastic-based method



Quasielastic-based neutrino energy reconstruction

Reconstructed neutrino energy

$$\overline{E}_\nu = \frac{m_p^2 - (m_n - E_b)^2 - m_\mu^2 + 2(m_n - E_b)E_\mu}{2(m_n - E_b - E_\mu + p_\mu \cos \theta_\mu)}$$

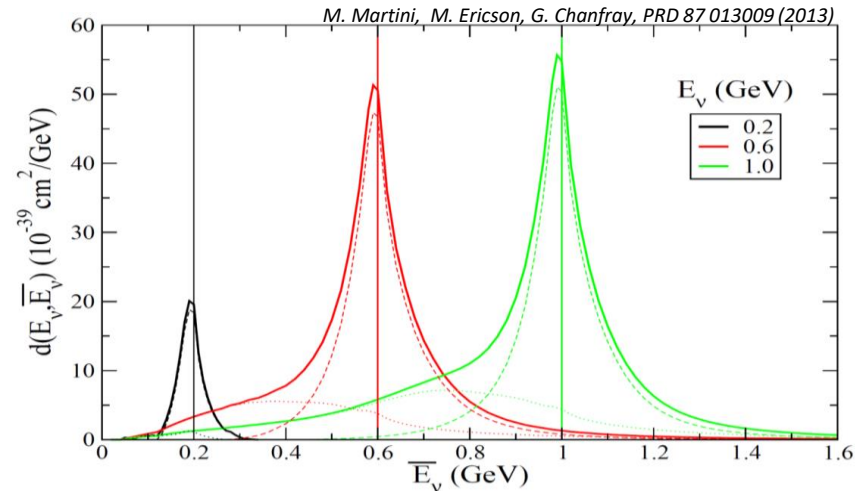


via two-body kinematics

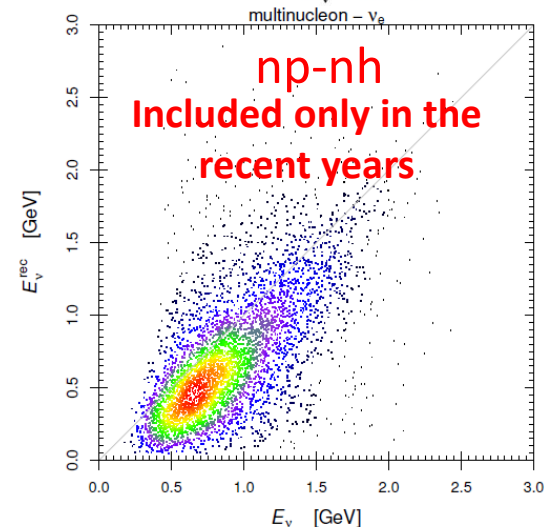
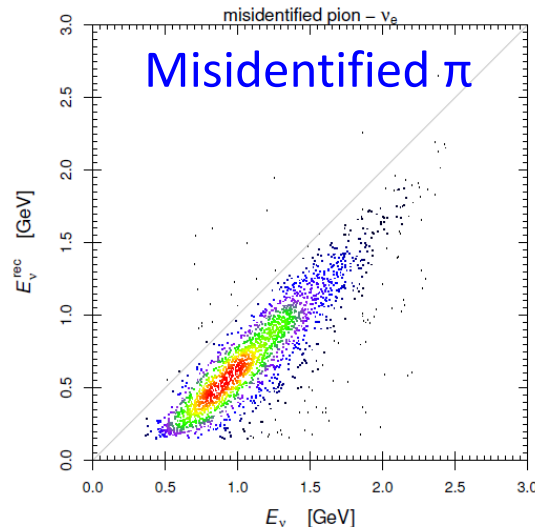
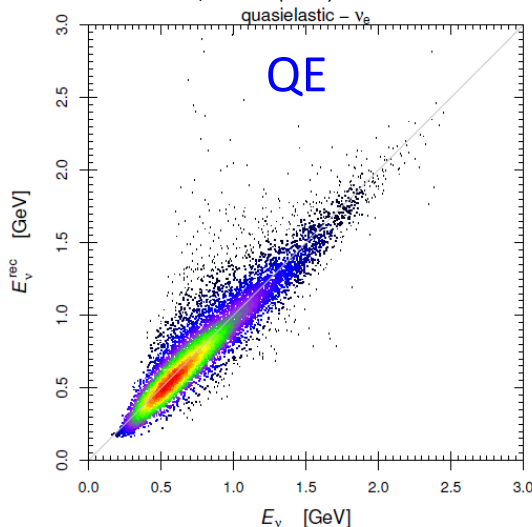
$\overline{E}_\nu = E_\nu$ exact only for CCQE with free nucleon

$$d(E_\nu, \overline{E}_\nu)$$

Migration matrix:
to take into account
nuclear effects

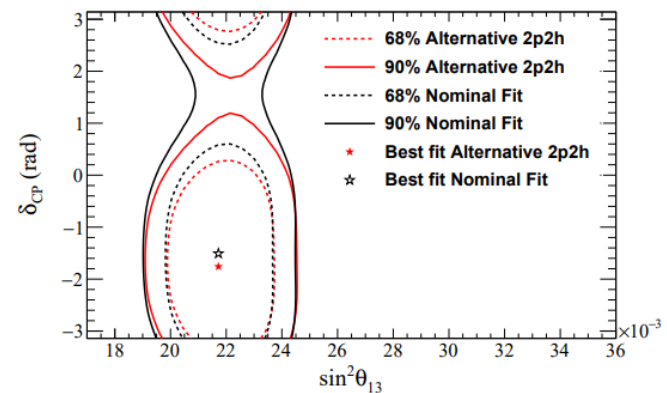
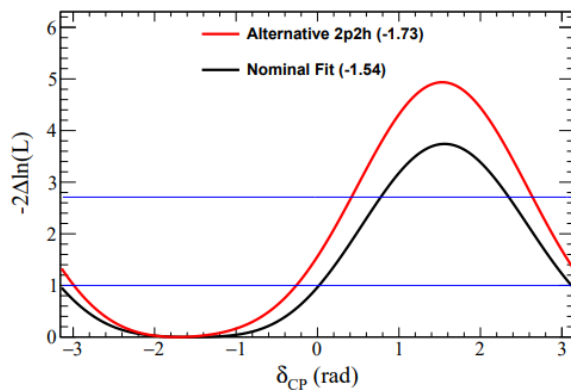
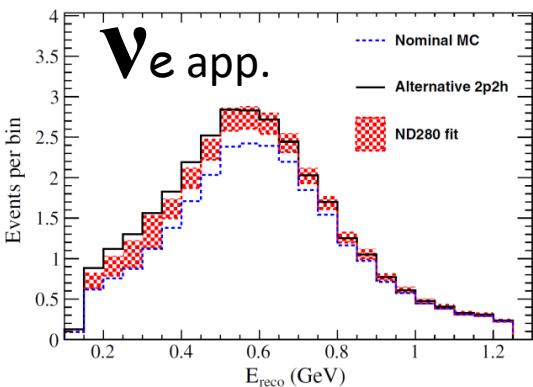
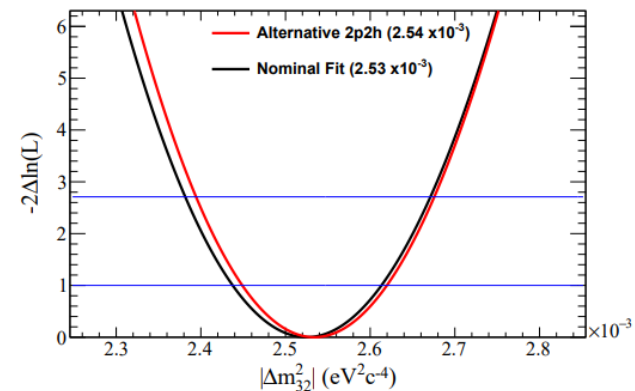
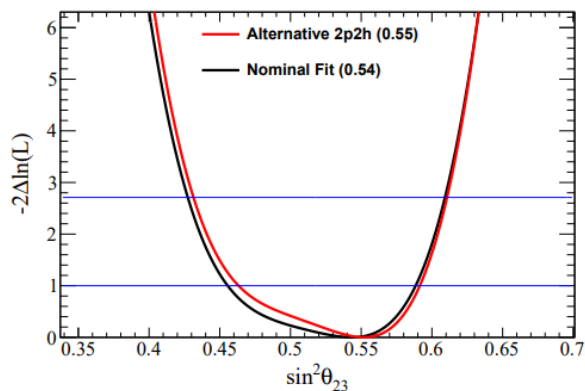
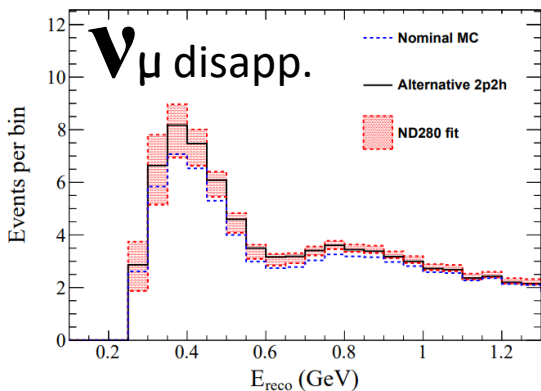


M. Ericson et al. PRD 93, 073008 (2016)



Impact of 2p-2h modeling on T2K oscillation analysis

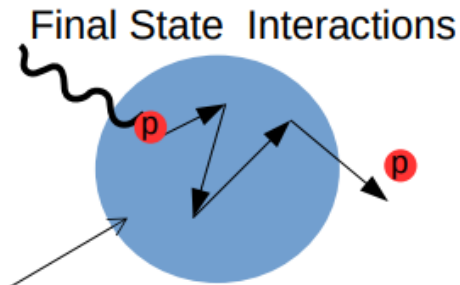
T2K Phys.Rev.D 96 (2017) 9, 092006



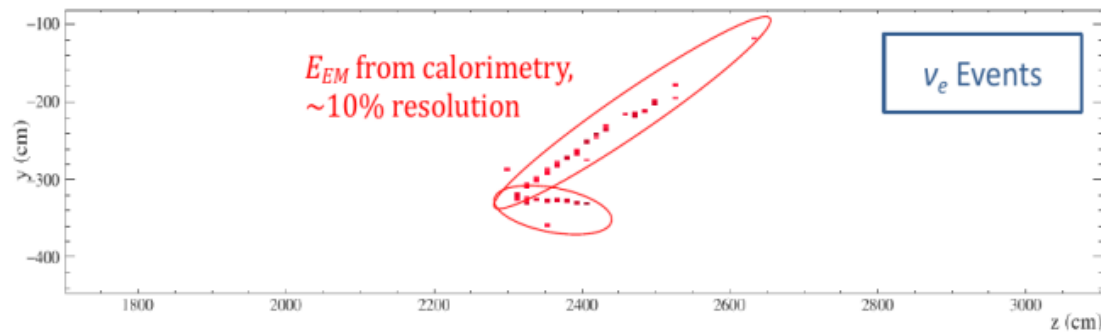
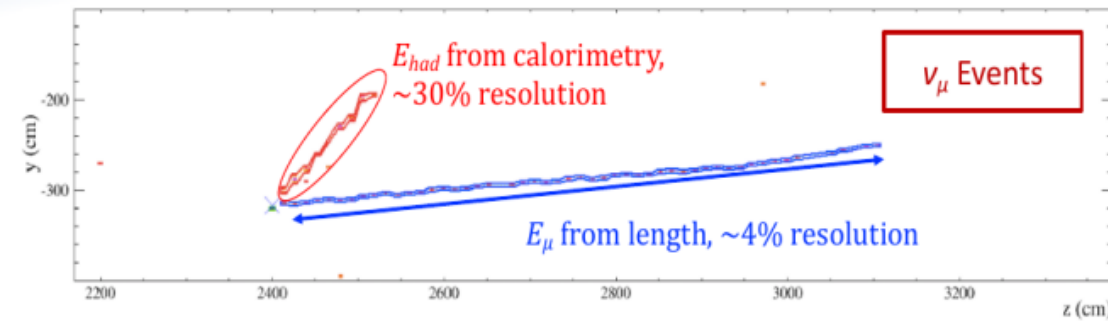
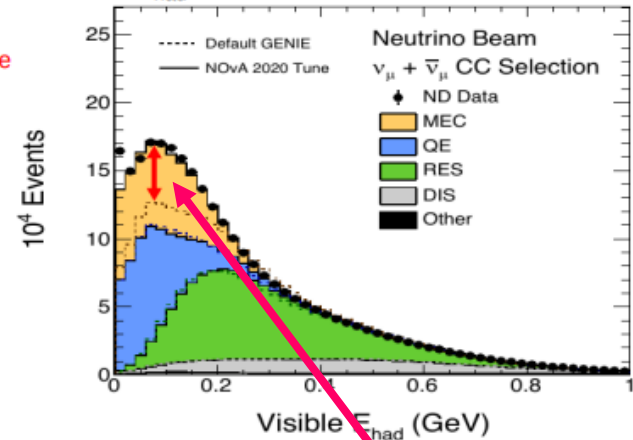
E_ν reconstruction NOvA

Calorimetric method

- E_ν reconstructed with hadronic deposits:
 - important difference $\nu - \bar{\nu}$: proton vs neutron (~undetected)
 - proton/pion energy smeared by Final State Interactions
- Different reconstruction and energy resolution for ν_μ and ν_e



Important to tune model predictions for E_{had} **NOvA Preliminary**



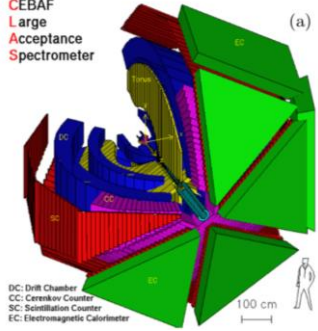
S. Bognesi @ GIF school 119

Electron-beam energy reconstruction for ν oscillation measurements

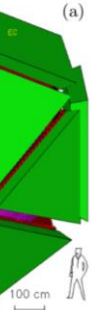
$e4\nu$



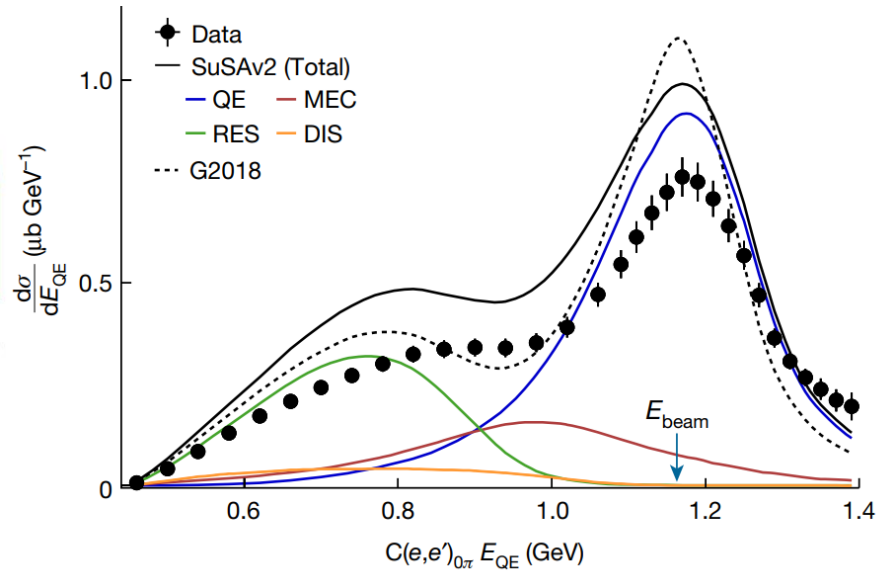
CEBAF
Large
Acceptance
Spectrometer



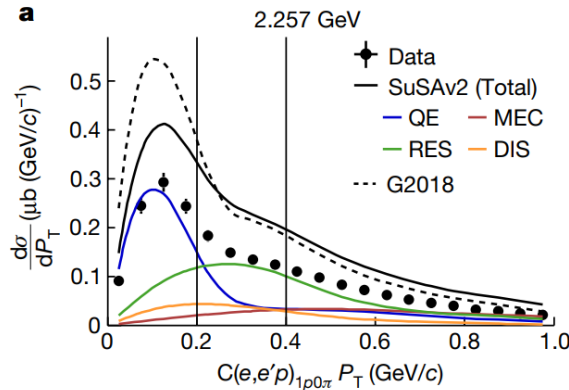
DC: Drift Chamber
CC: Cerenkov Counter
SC: Scintillation Counter
EC: Electromagnetic Calorimeter



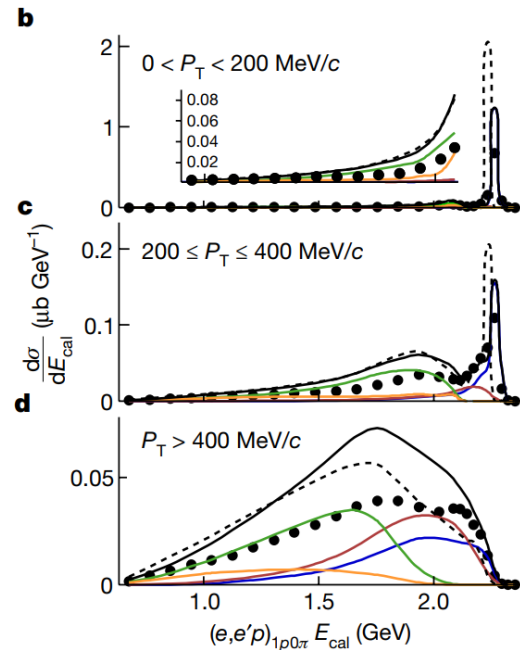
Nature 599 (2021) 7886, 565-570



QE-based
(e, e')



$$\mathbf{P}_T = \mathbf{P}_T^{e'} + \mathbf{P}_T^p$$

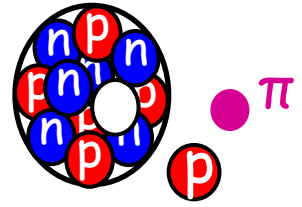


Calorimetric
-based
($e, e'p$)

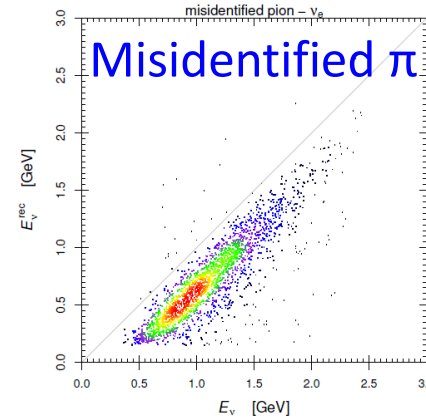
1π production

The one pion production channel

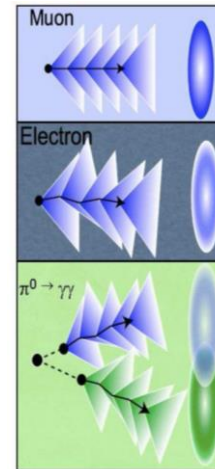
Important for several reasons:



- Misidentified π is part of the ν energy migration matrix



- In Cherenkov detectors $\text{NC}1\pi^0$ can mimic electron-like signal in $\nu_\mu \rightarrow \nu_e$ oscillation search

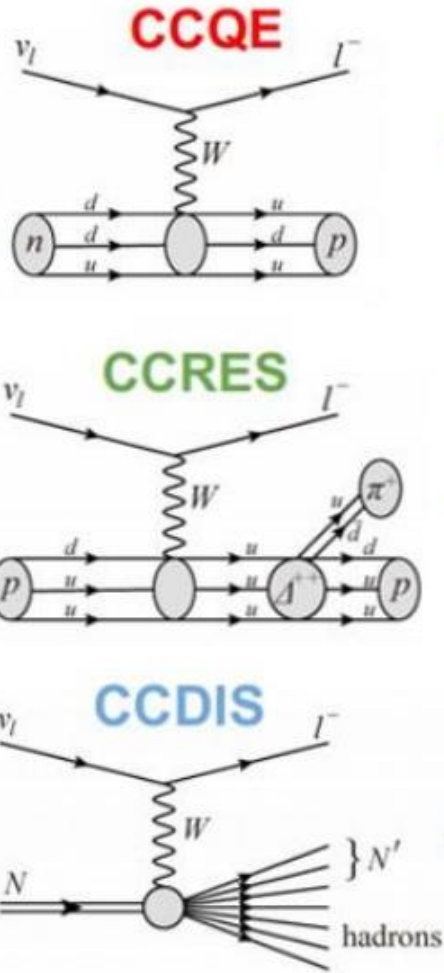


- There is an increasing interest on CC 2-ring signal (charged lepton and π) at Super-Kamiokande

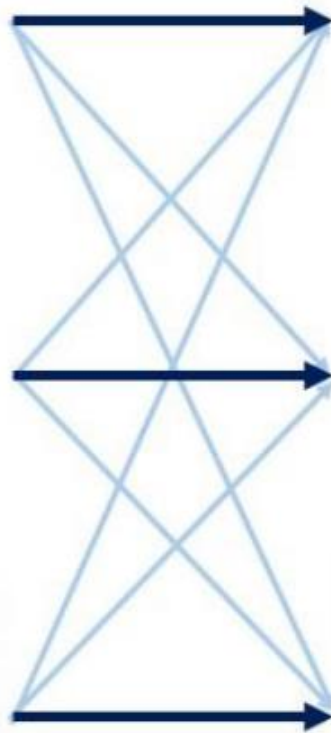
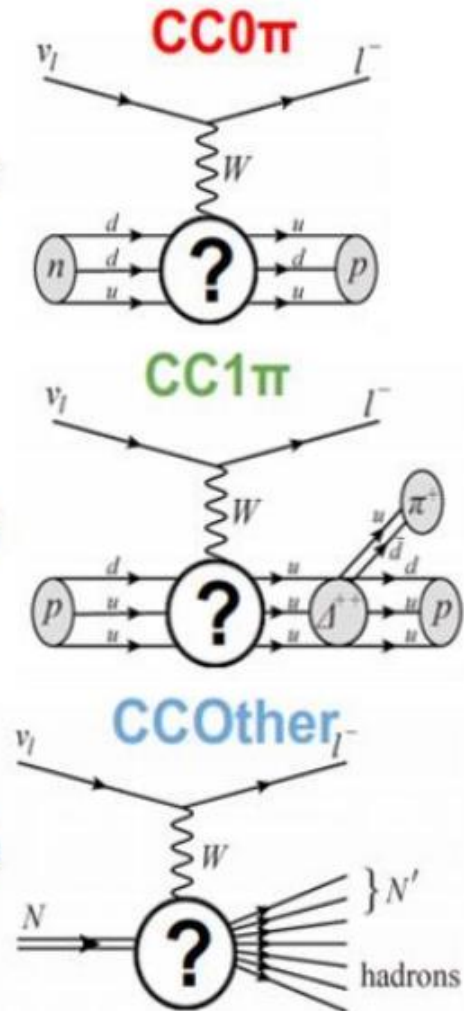
$$E_{\nu_{\text{reco}}} = \frac{m_p^2 - (m_p - E_{\text{bind}} - E_\mu - E_\pi)^2 + |\vec{P}_\mu + \vec{P}_\pi|^2}{2\{m_p - E_{\text{bind}} - E_\mu - E_\pi + \hat{k}_\nu(\vec{P}_\mu + \vec{P}_\pi)\}}$$

Elementary vertices .vs. detection topologies

Elementary vertices
(nucleon level)



Detection topologies
(nucleus level)



Nuclear Effects
and Final State
Interactions

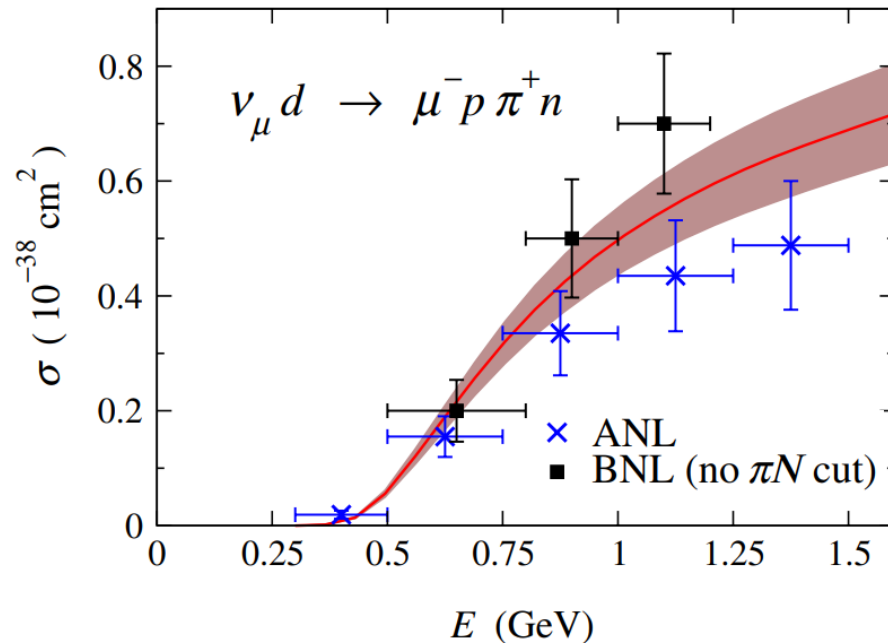
Figure from Dr. Stephen Dolan

Different interaction vertices can lead to the same final state due to nuclear effects and FSI

1π production in neutrino-deuteron scattering

- Discrepancies between “old” deuteron bubble-chamber data (Argonne ANL and Brookhaven BNL)
- Both ANL and BNL data suffer from a large flux-normalization error

E. Hernandez et al. Phys. Rev. D 87, 113009 (2013)



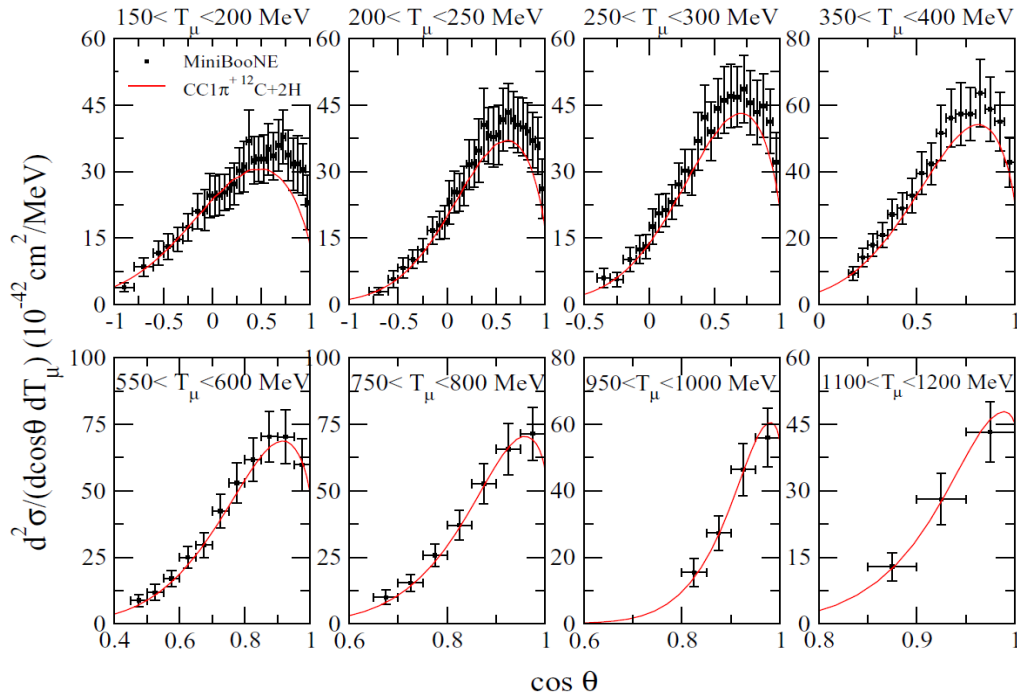
As for the CCQE, also for the 1π production there is a strong desire to repeat bubble-chamber experiments to better determine the axial form factors (in particular the C_5^A)

$$C_5^A(Q^2) = \frac{C_5^A(0)}{(1 + Q^2/M_{A\Delta}^2)^2}$$

CC1 π^+ flux-integrated differential cross sections on carbon

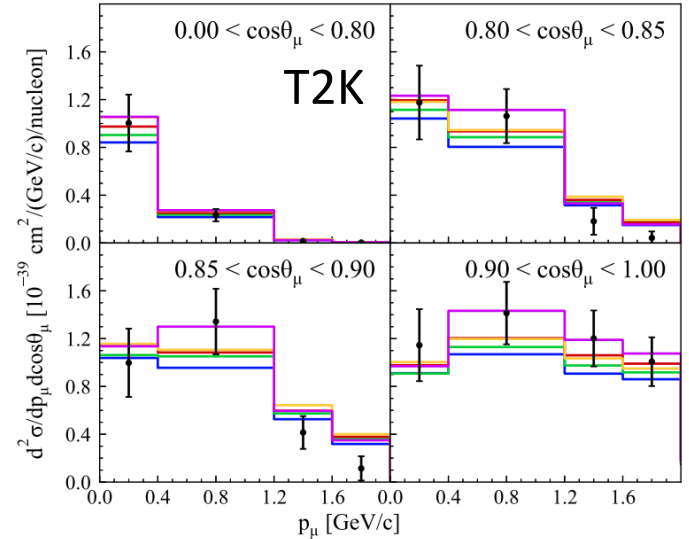
Results in terms of muon variables

MiniBooNE

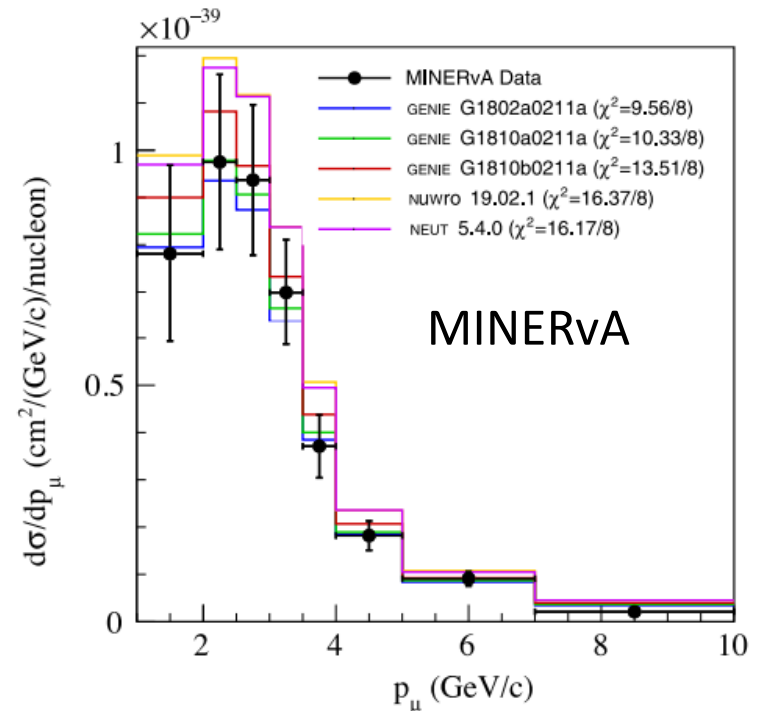


M. Martini, M. Ericson, *Phys. Rev. C* 90 025501 (2014)

Reasonable agreement between models and data



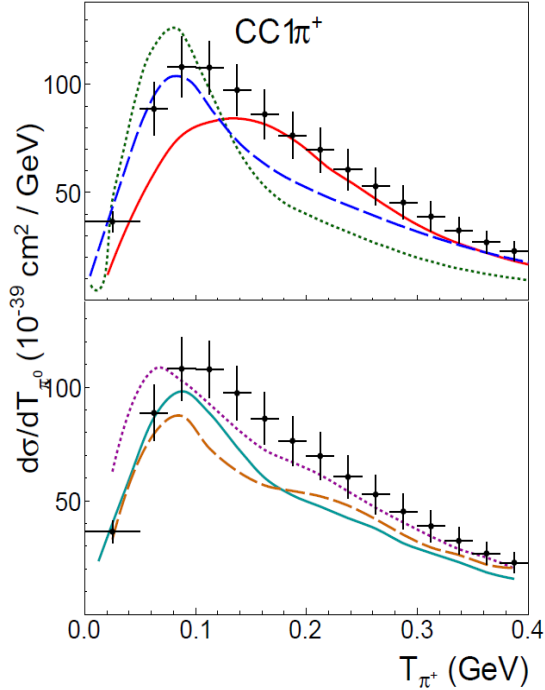
M. Buizza Avanzini et al. *PRD* 105, 092004 (2022)



CC1 π results in terms of pion variables

MiniBooNE

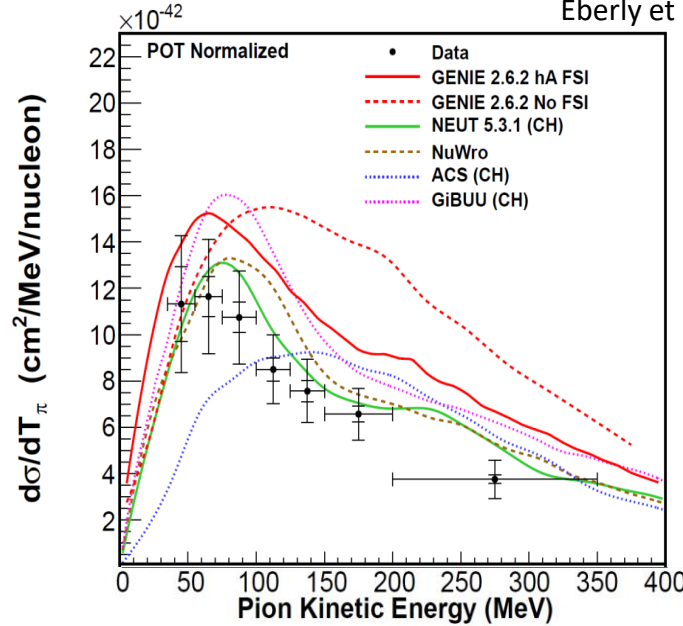
Rodrigues, AIP Conf. Proc. 1663 (2015)



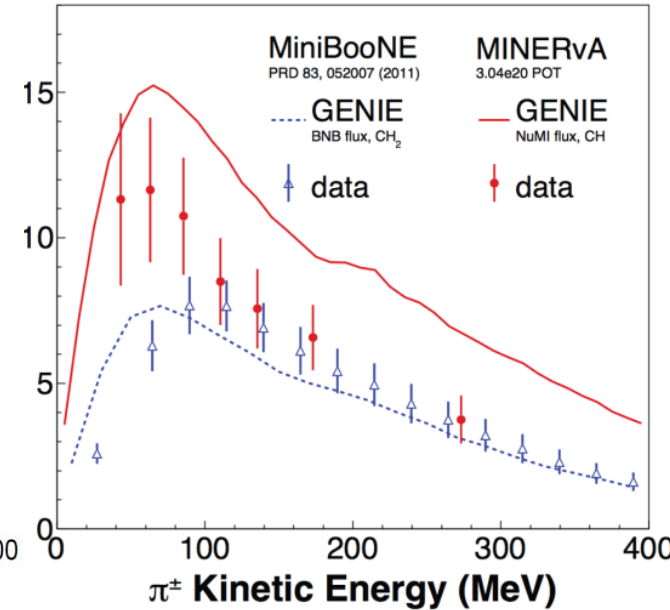
— Athar *et al.* - - - Nieves *et al.* - - - GiBUU — NuWro
 - - - GENIE — NEUT — + MB data

MINERvA

Eberly *et al.*, PRD 92 (2015)



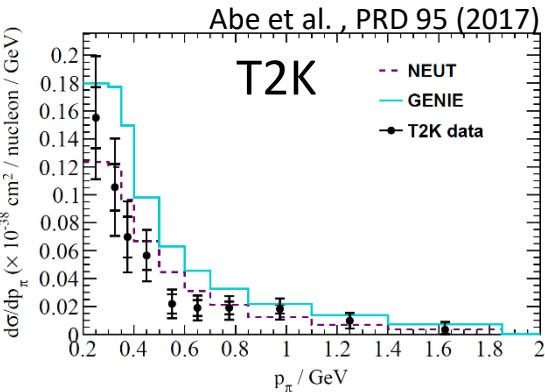
MiniBooNE - MINERvA



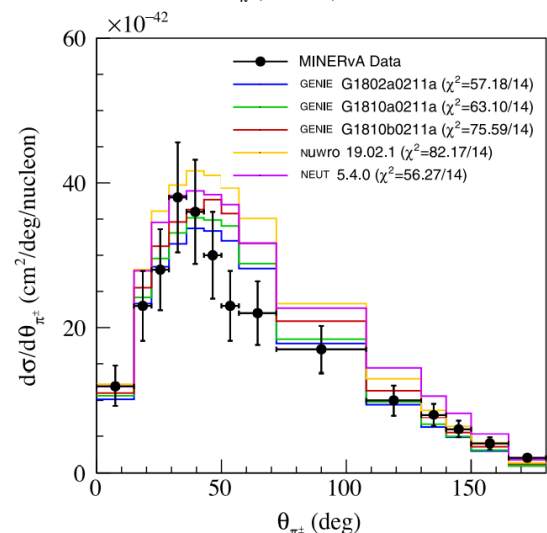
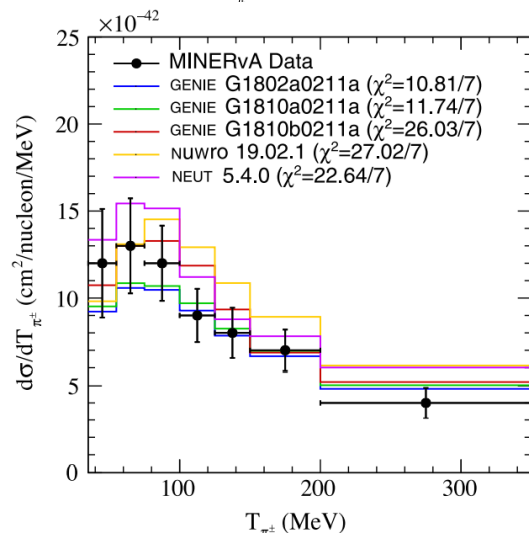
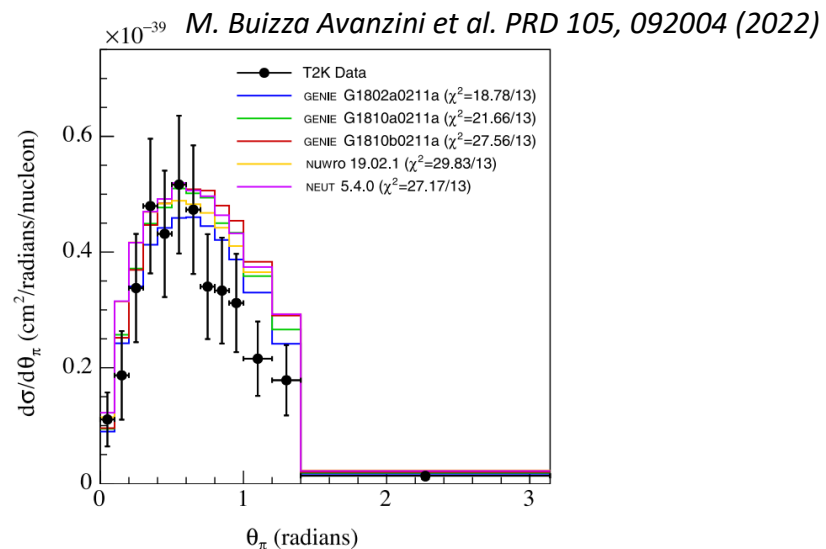
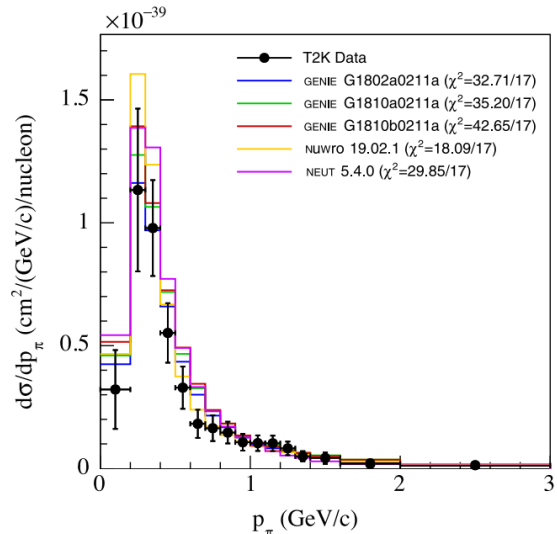
Historically many tensions

- models .vs. data ??
- models .vs. models??
- data .vs. data (through models)??

the 1 π puzzle



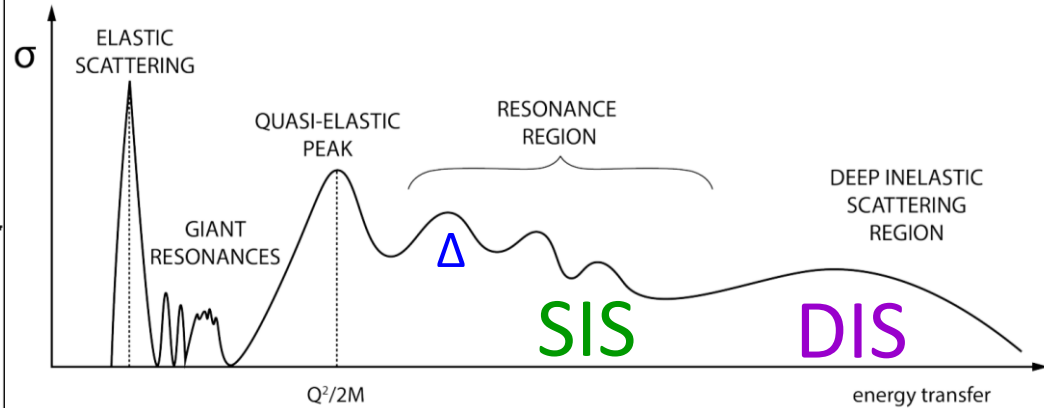
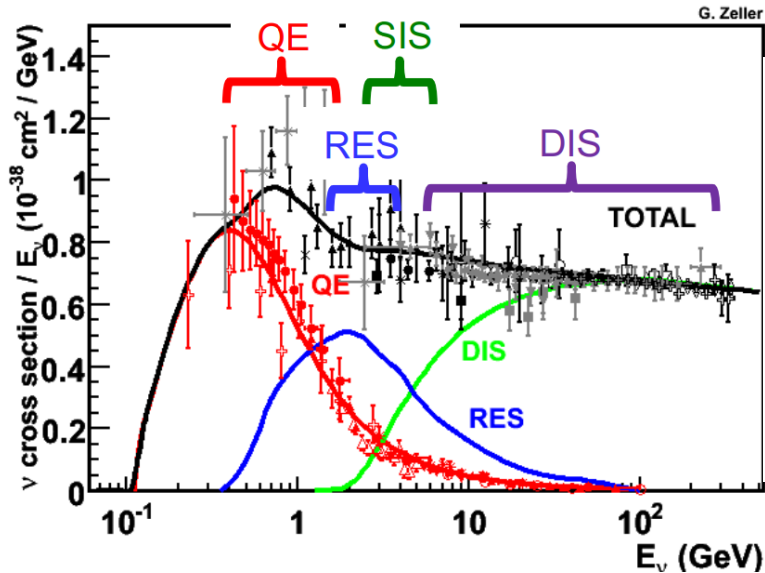
Pion puzzle – T2K and MINERvA data .vs. Monte Carlo (2022)



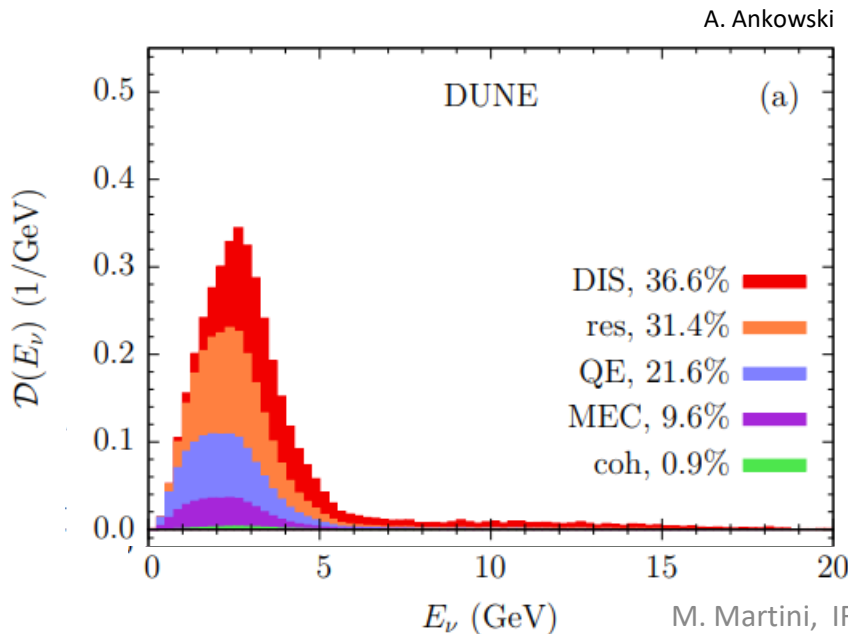
Tensions remain

- The generators used to extract the cross section is often the one with the best description of the data
- Experimental collaborations have more advanced analyses in progress (T2K Vargas and MINERvA McFarland @ NuInt22)
- These Monte Carlo results are based on Δ dominated models
- None of the common event generators include nuclear medium effects for the Δ

Beyond Δ resonance



- The complications of pion data analyses lay not only on the modeling of primary production and pion FSI but also on the fact that all hadronic processes related to shallow inelastic scattering (SIS) and DIS regions must be modeled correctly
- **SIS and DIS have been minimally studied both experimentally and theoretically with neutrino scattering**
- **A major challenge, important in particular for DUNE**



- T. Katori, M. Martini, J.Phys.G 45 1, 013001 (2018)*
- L. Alvarez-Ruso et al. Prog. Part. Nucl. Phys. 100, 1–68 (2018)*
- M. Sajjad Athar, J. G. Morfín, J.Phys. G 48, 034001 (2021)*

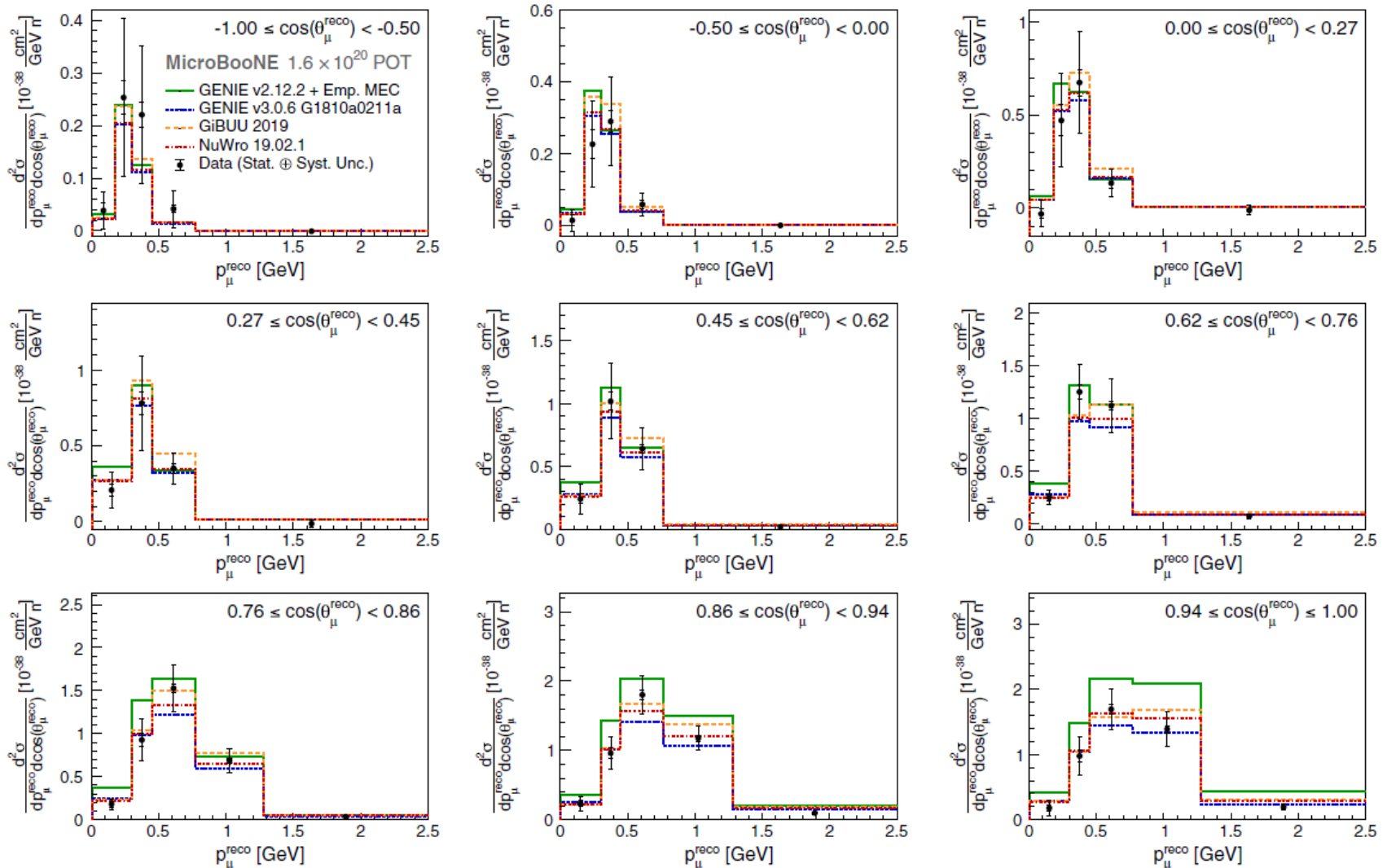
Recent hot topics:

- Argon cross sections (MicroBooNE)
- Semi-inclusive processes (proton detection)
- Single Transverse Kinematics Imbalance

First MicroBooNE measurement on Argon: inclusive $d^2\sigma/dp_\mu d\cos\theta_\mu$

- CC Inclusive: only the charged lepton is detected. All reaction mechanisms contribute

PHYSICAL REVIEW LETTERS **123**, 131801 (2019)

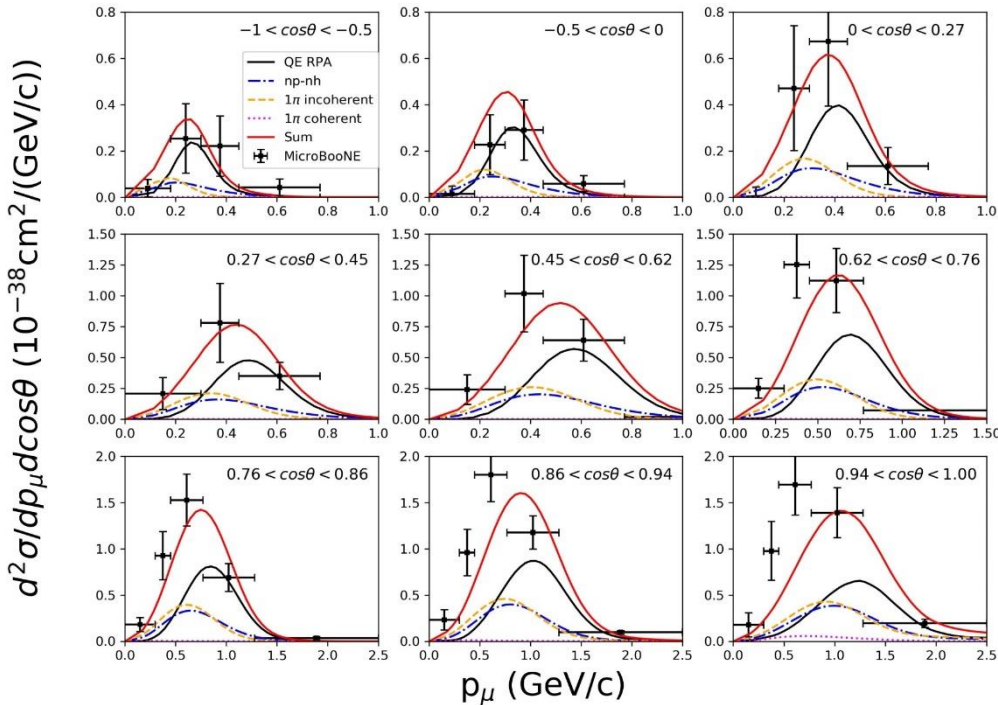


RPA and SuSAv2 calculations of MicroBooNE inclusive $d^2\sigma$ on argon

RPA

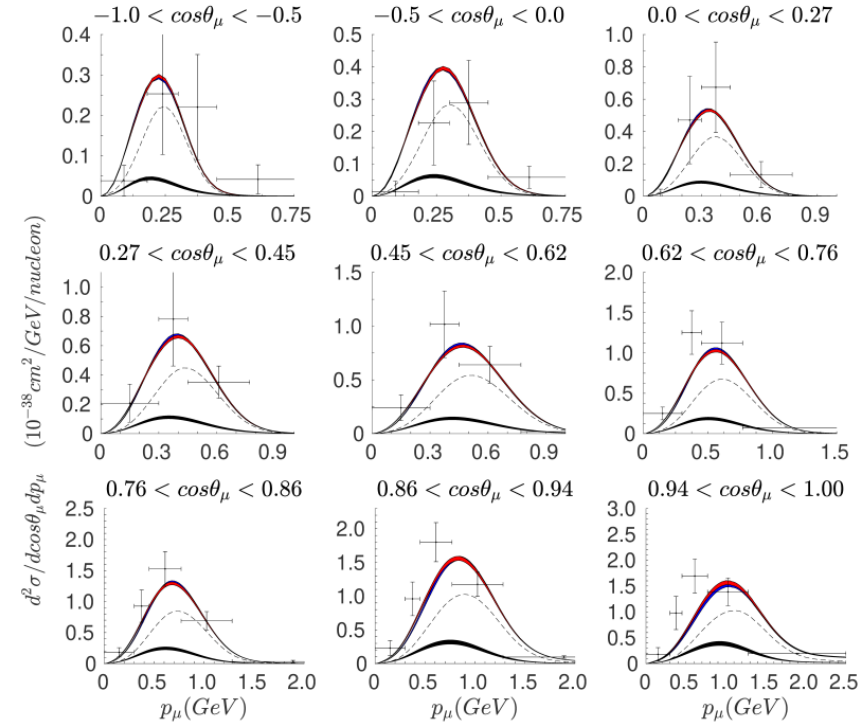
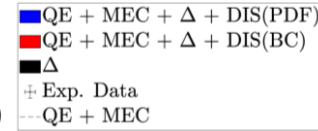
Total = QE + np-nh + 1π inc. + 1π coh.

M. Martini, M. Ericson, G. Chanfray, PRC 106 (2022)



SuSAv2

Gonzalez-Rosa et al. PRD 105 (2022)



Results also with SuSA
Barbaro et al. Universe 7 (2021)

- Reasonable overall agreement, though not as good as in the ^{12}C T2K inclusive case (see next slide)
- At backward angles the predictions of the different models are slightly shifted to lower values of p_μ , whereas the reverse occurs at forward angles

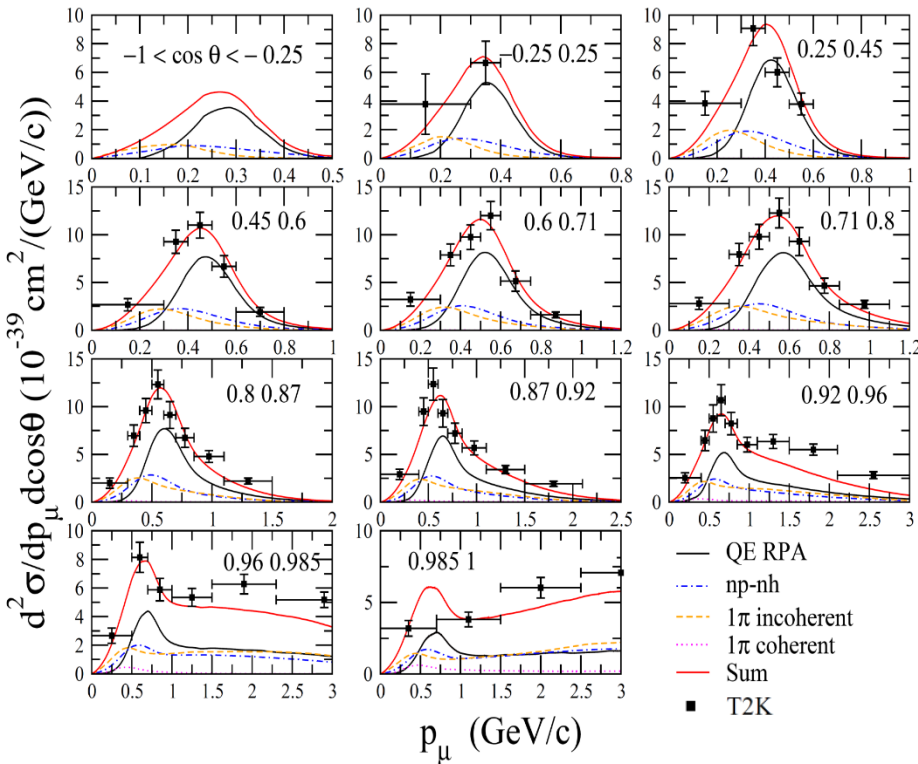
RPA and Monte Carlo calculations of T2K inclusive $d^2\sigma$ on carbon

PHYSICAL REVIEW D **98**, 012004 (2018)

Measurement of inclusive double-differential ν_μ charged-current cross section with improved acceptance in the T2K off-axis near detector

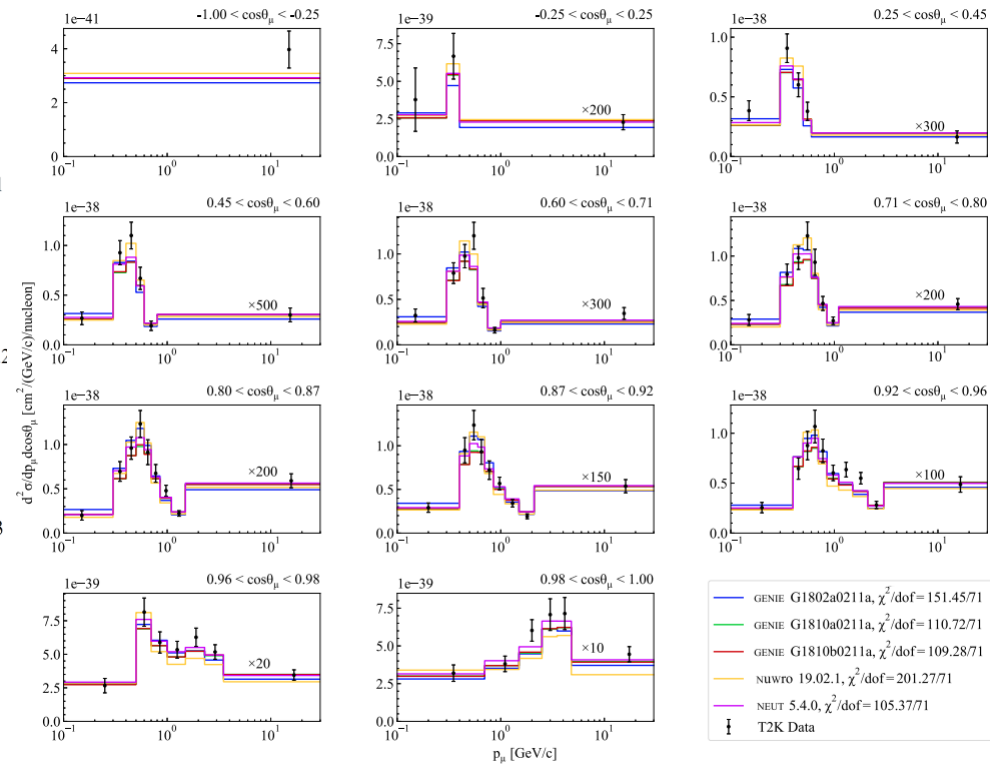
RPA

M. Martini, M. Ericson, G. Chanfray, PRC 106, 015503 (2022)



Monte Carlo

M. Buizza Avanzini et al. PRD 105, 092004 (2022)

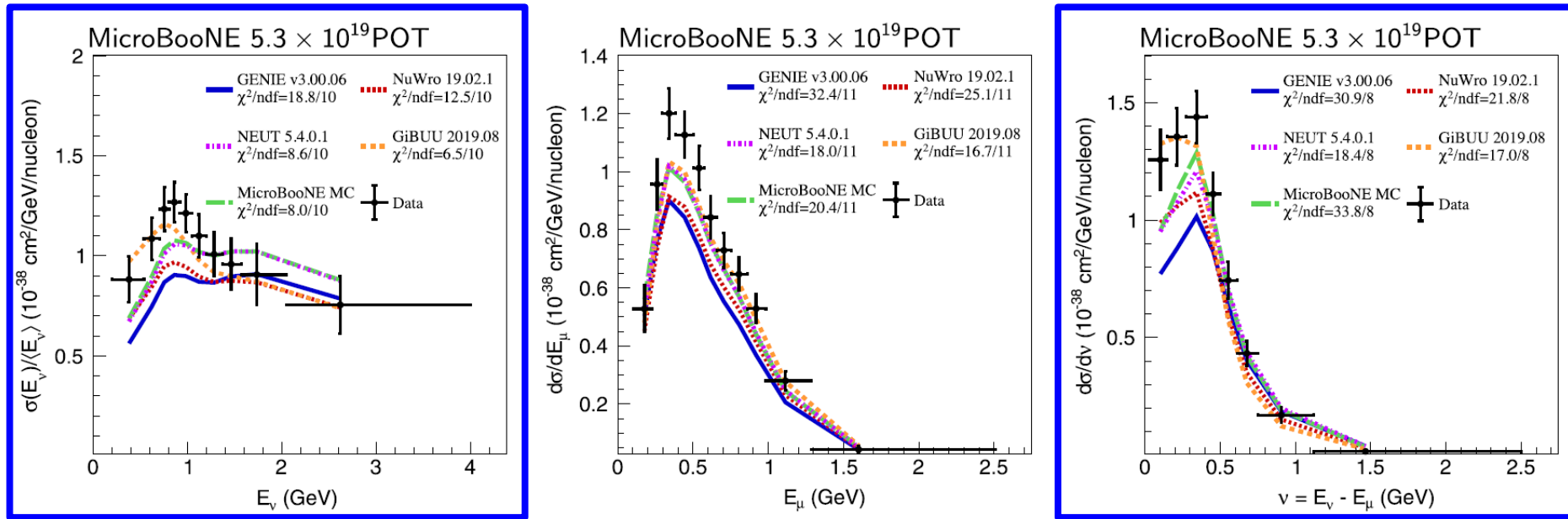


Remarkable agreement

Recent energy-dependent inclusive MicroBooNE cross sections on argon

PHYSICAL REVIEW LETTERS **128**, 151801 (2022)

First Measurement of Energy-Dependent Inclusive Muon Neutrino Charged-Current Cross Sections on Argon with the MicroBooNE Detector

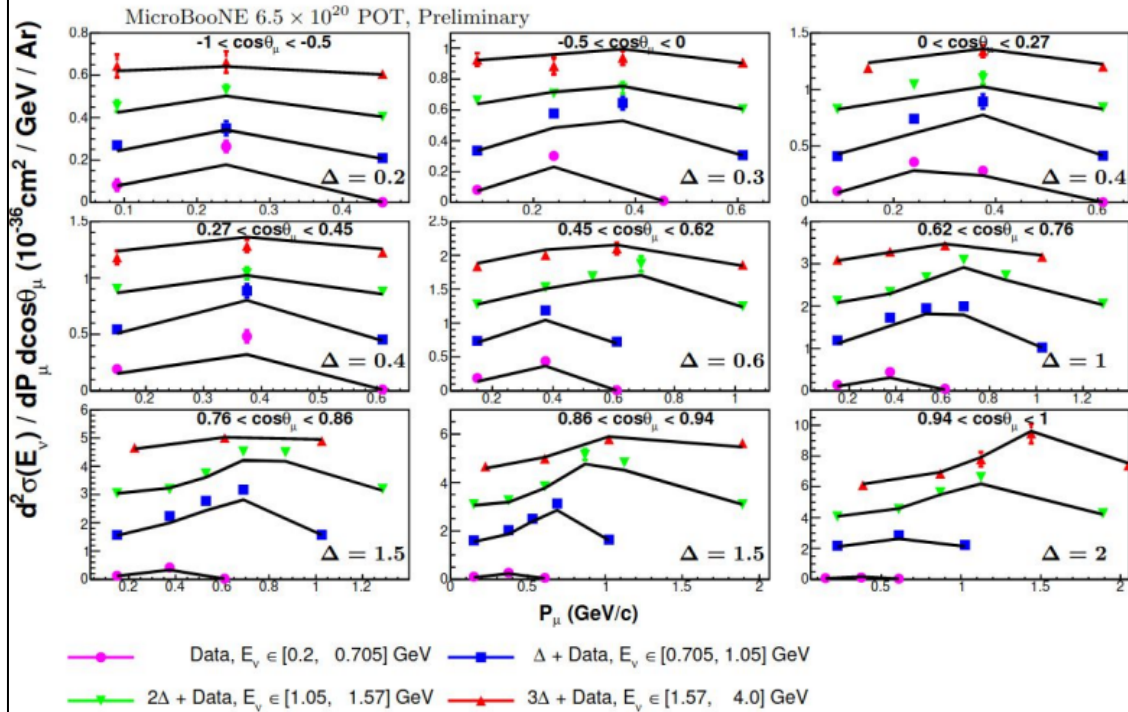


Results presented for the first time as a function of true neutrino energy E_ν and transferred energy (ν or ω)

This has been made possible by a new procedure (based on the comparison between the data and the Monte Carlo predictions constrained on the lepton kinematics) allowing the mapping between the true E_ν and ω on one hand, and the reconstructed neutrino energy E_ν^{rec} and hadronic energy $E_{\text{had}}^{\text{rec}}$ on the other hand



Unfolded Measurement in 3D



Data plotted against NuWro prediction
 E_ν slices overplot with offset $N\Delta$ for each angle slice
 Δ in same units of $d^2\sigma(E_\nu)/dP_\mu d\cos(\theta_\mu)(10^{-36}\text{cm}^2/\text{GeV}/\text{Ar})$

Model Generator	χ^2/ndf
Genie v2.12.10	740.8/138
Genie v3.0.6 (MicroBooNE Tune)	313.9/138
Genie v3.0.6 (Untuned)	309.7/138
GIBUU 2021	265.6/138
NEUT v5.4.0.1	233.1/138
NuWro v19.02.01	200.9/138

Descending χ^2/ndf →

3D measurement contains wealth of information → all model central value predictions are now in tension with data

More powerful than 1D measurement, which was consistent with some models

17

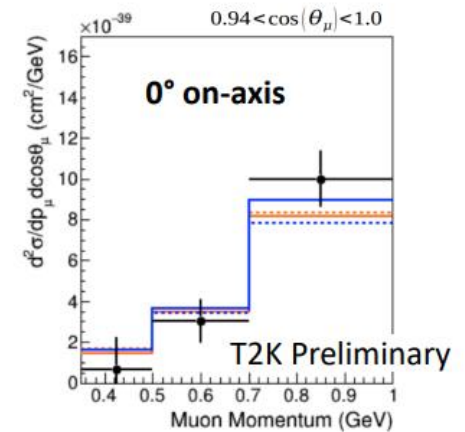
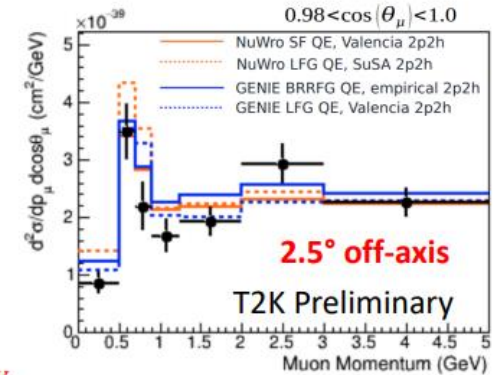
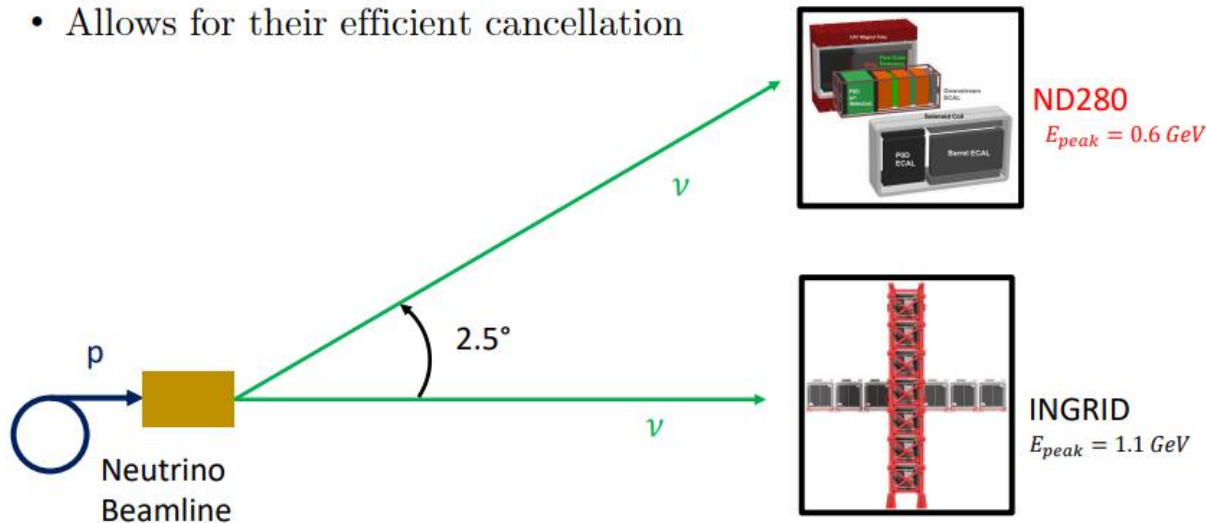
London Cooper-Troendle (MicroBooNE) talk @ NuInt22



Direct probe of E_ν dependence

Sneak Peek: Joint On-/Off-Axis CC0 π Cross Section

- First T2K multi-detector cross section measurement
- Direct probe of E_ν dependence
- Exploits correlations between the systematic uncertainties of the samples
 - Allows for their efficient cancellation

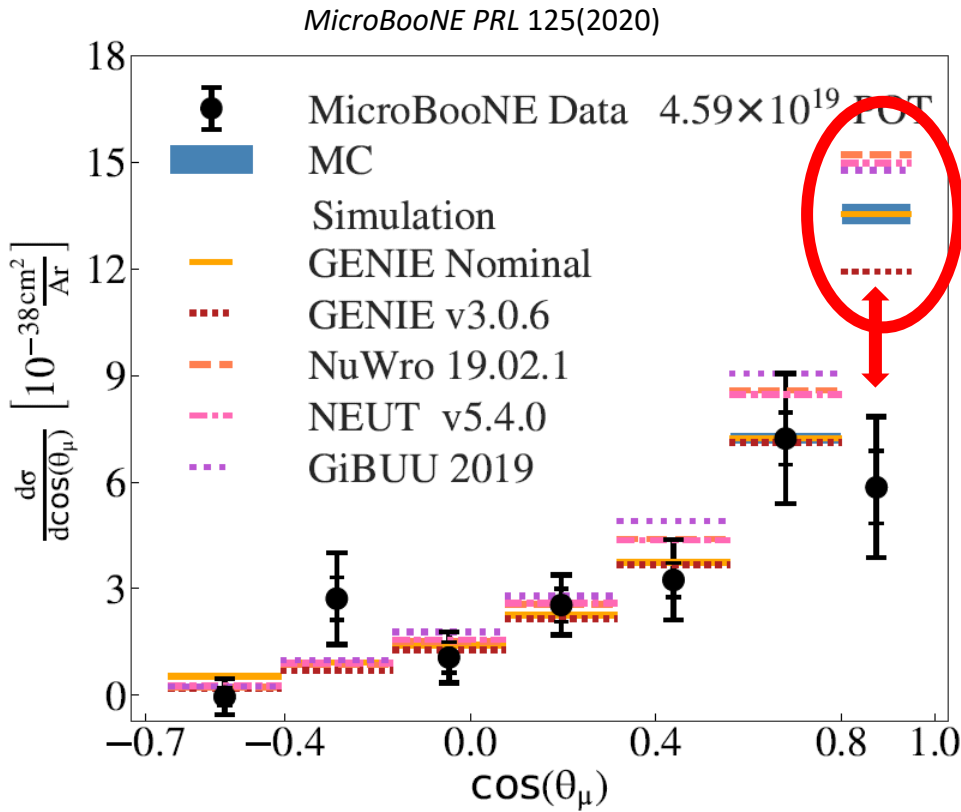


MicroBooNE semi-inclusive CC0 π 1p on argon

PHYSICAL REVIEW LETTERS **125**, 201803 (2020)

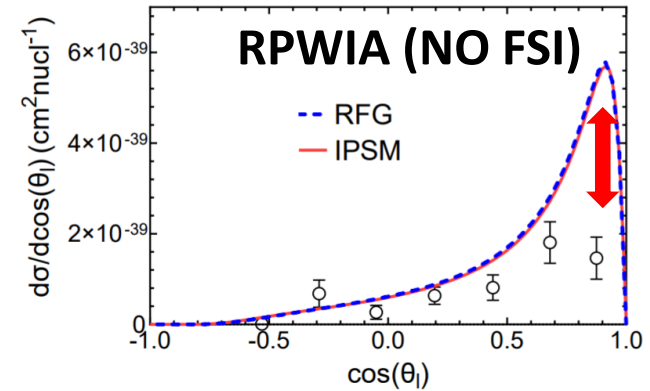
First Measurement of Differential Charged Current Quasielasticlike ν_μ -Argon Scattering Cross Sections with the MicroBooNE Detector

?! CCQE-like with another meaning than in the past

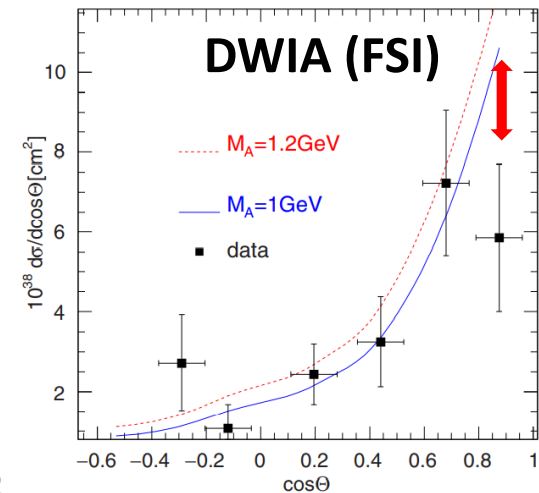


Overestimation in the muon forward direction

J. M. Franco-Patino et al. PRD 104 (2021) 7, 073008

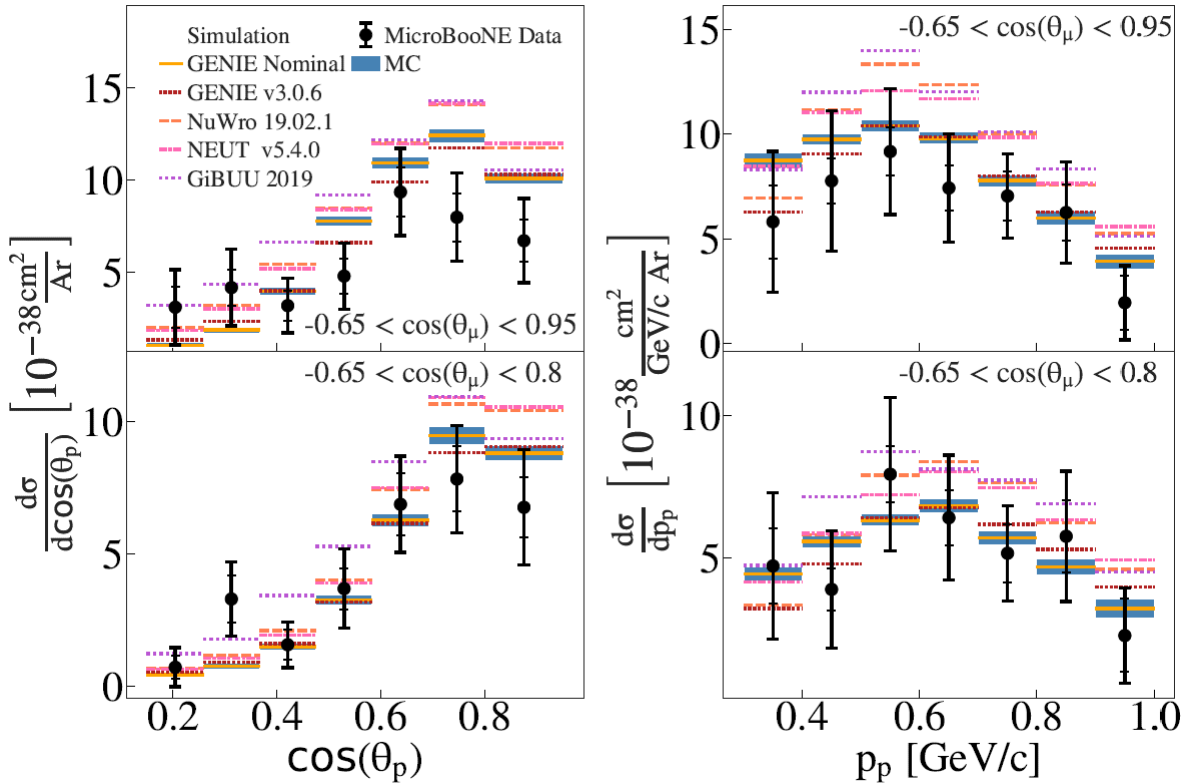


A.V. Butkevich PRC 105 (2022) 2, 025501



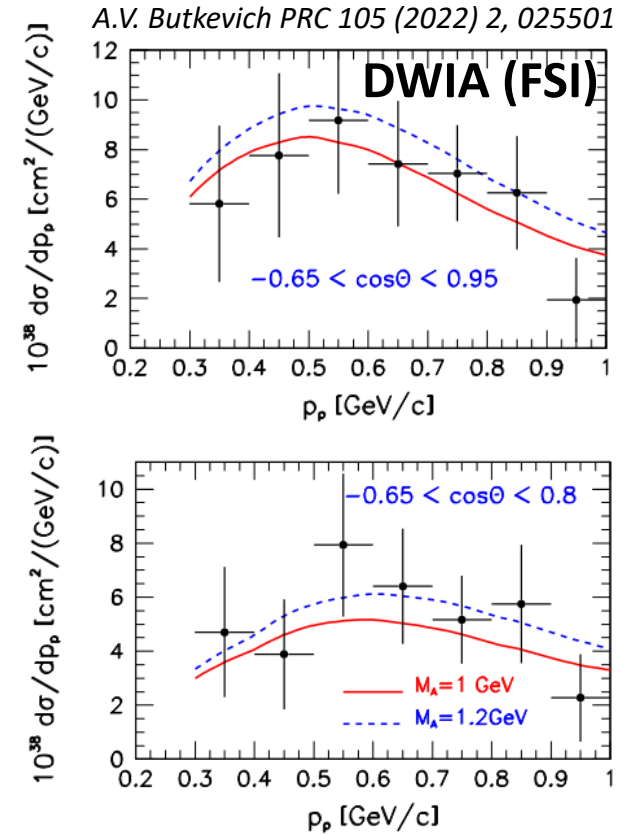
MicroBooNE semi-inclusive CC0 π 1p on argon versus proton variables

MicroBooNE PRL 125(2020)



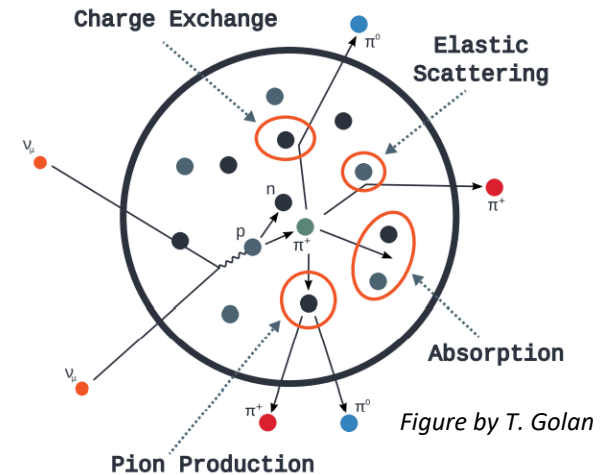
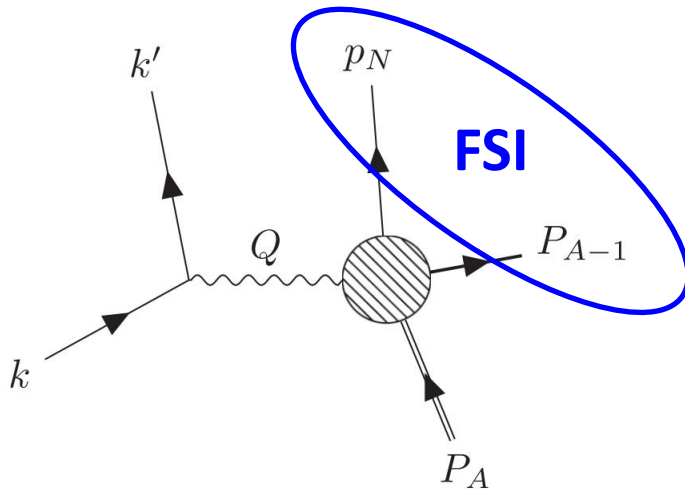
- Poor Monte Carlo – data agreement
- Spread of Monte Carlo predictions

How good are the current approximations (use “inclusive” models, factorization,...) of the Monte Carlos for the semi-inclusive processes?



Final State Interactions

FSI between the knocked-out particle(s) and the residual nucleus



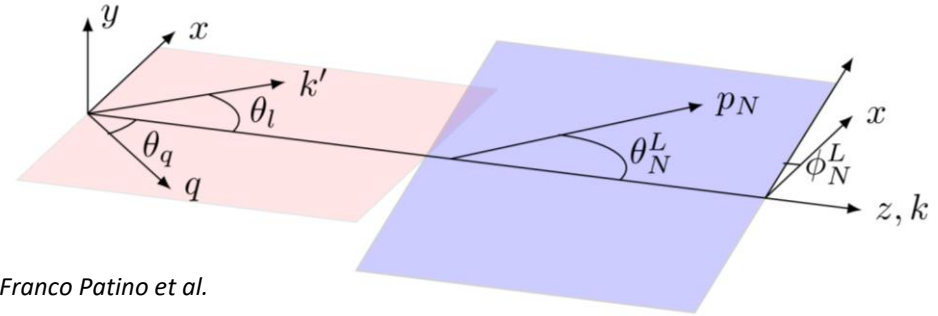
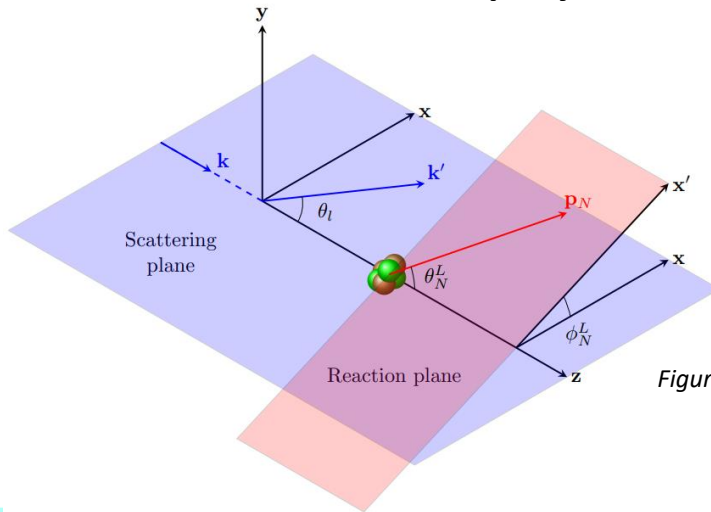
- Monte Carlo event generators includes different models of intra-nuclear cascades: particles are assumed to be classical and move along a straight line
- FSI between the knocked-out nucleon and the residual nucleus can be microscopically treated using different approaches: Optical Potential, RMF, Energy-Dependent RMF

The inclusion of FSI effects is extremely important for the description of semi-inclusive data

[Some recent references: *R. Gonzalez-Jimenez et al., PRC 101, 015503 (2020)* ; *J. Isaacson et al., PRC 103 015502 (2021)*; *A. Nikolakopoulos et al. PRC 105, 054603 (2022)*; *A. Ershova et al., PRD 106 032009 (2022)*]

The semi-inclusive neutrino cross section

There is a rapidly increasing interest on semi-inclusive cross sections



Figures by J. M. Franco Patino et al.

M. B. Barbaro talk @NUFACT 2021

$$\begin{aligned} \mathcal{F}_\chi^2 &= L_{\mu\nu} W^{\mu\nu} \\ &= V_{CC} R^{CC} + 2V_{CL} R^{CL} + V_{LL} R^{LL} + V_T R^T + V_{TT} R^{TT} + V_{TC} R^{TC} + V_{TL} R^{TL} + \chi (V_T R^T + V_{TC} R^{TC} + V_{TL} R^{TL}) \end{aligned}$$

The $(\nu_\mu, \mu p)$ cross section is decomposed in **10 independent response functions** of **5 variables** $(\omega, q, \mathbf{p}_N)$.

More complex structure than in the **inclusive** (ν_μ, μ) case: **5 new responses**, which vanish after integration over the final nucleon variables

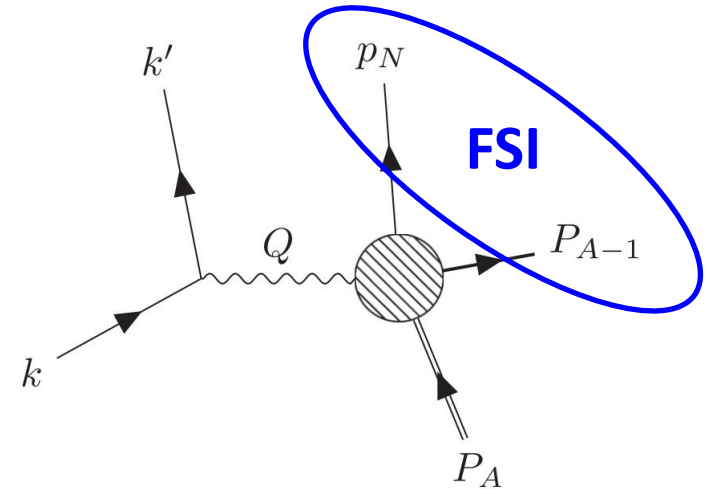
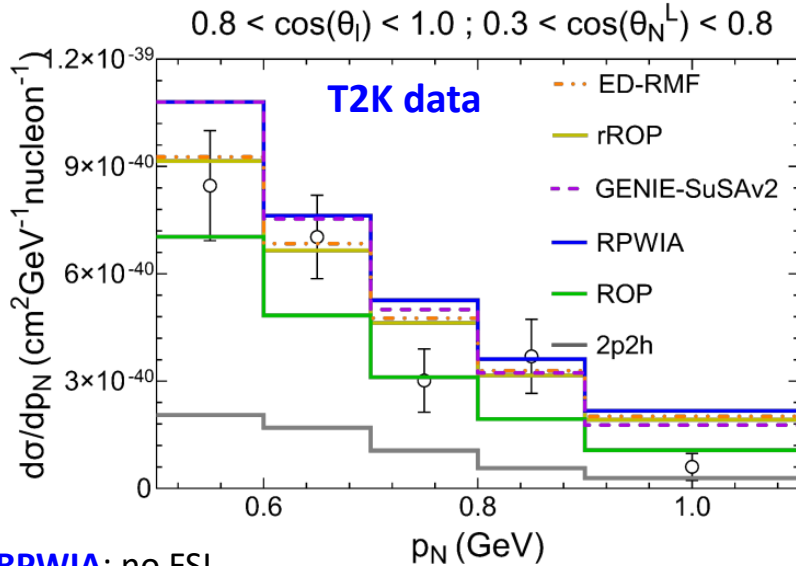
$$R^{TT,TC,TL,TC',TL'} \propto \cos(\phi), \cos(2\phi) \quad \phi \text{ outgoing nucleon azimuthal angle}$$

Semi-inclusive \rightarrow Inclusive (but not viceversa!)

Theoretical situation:

- few models and papers for genuine CCQE [J. M. Franco Patino et al, PRC 102 (2020); PRD 104 (2021), 2207.02086; A. V. Butkevich PRC 105 (2022)]
- one (incomplete due to the absence of Δ -MEC) model for 2p-2h [T. Van Cuyck et al. PRC 94 (2016); PRC 95 (2017)]

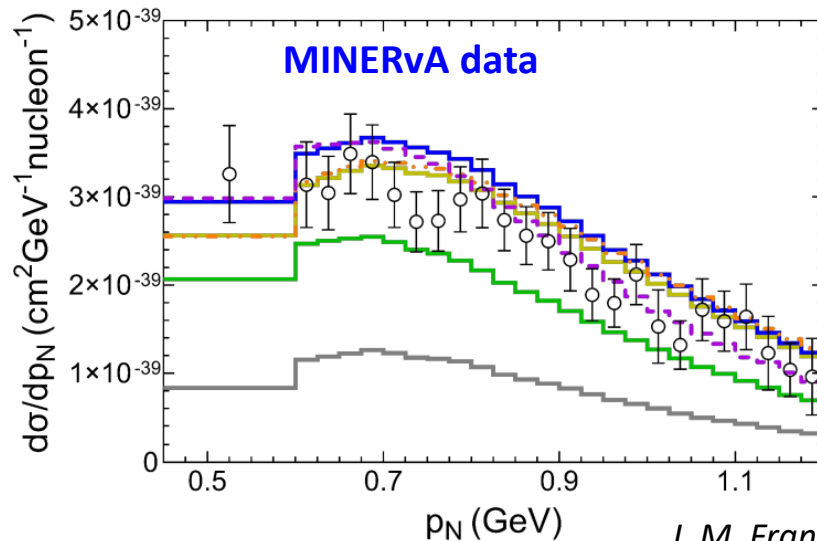
Semi-inclusive CC0 π cross section on carbon: role of proton FSI



RPWIA: no FSI

GENIE-SuSAv2: include FSI but from inclusive model (factorization)

ED-RMF, rROP, ROP: different theoretical approaches for FSI

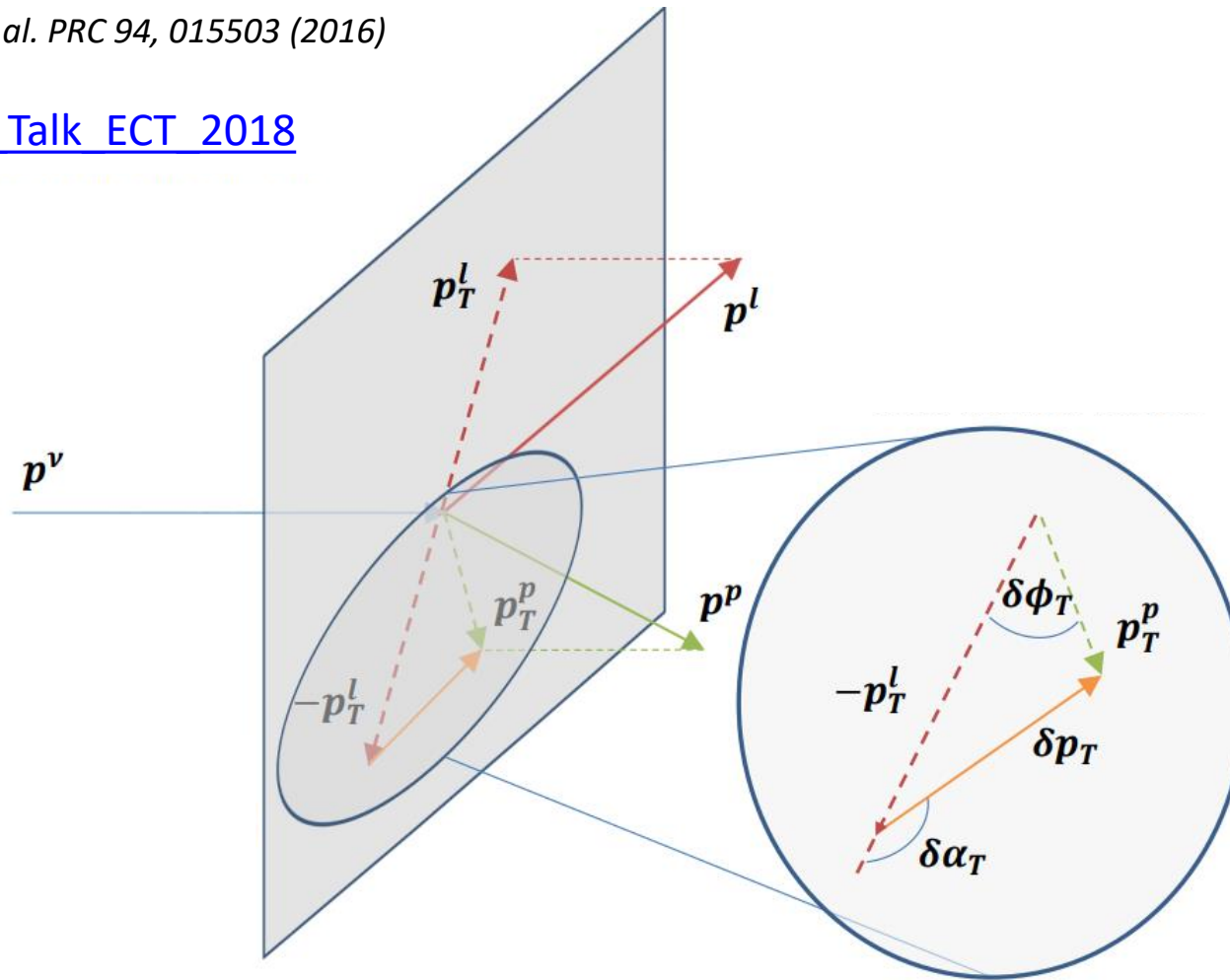


- FSI improve the agreement with data with respect to the RPWIA (no FSI) prediction
- Too large data error bars to discriminate between different FSI models

Single Transverse Kinematic Imbalance (STKI) – 3 variables (STV)

X. -G. Lu et al. PRC 94, 015503 (2016)

[S Dolan Talk ECT 2018](#)



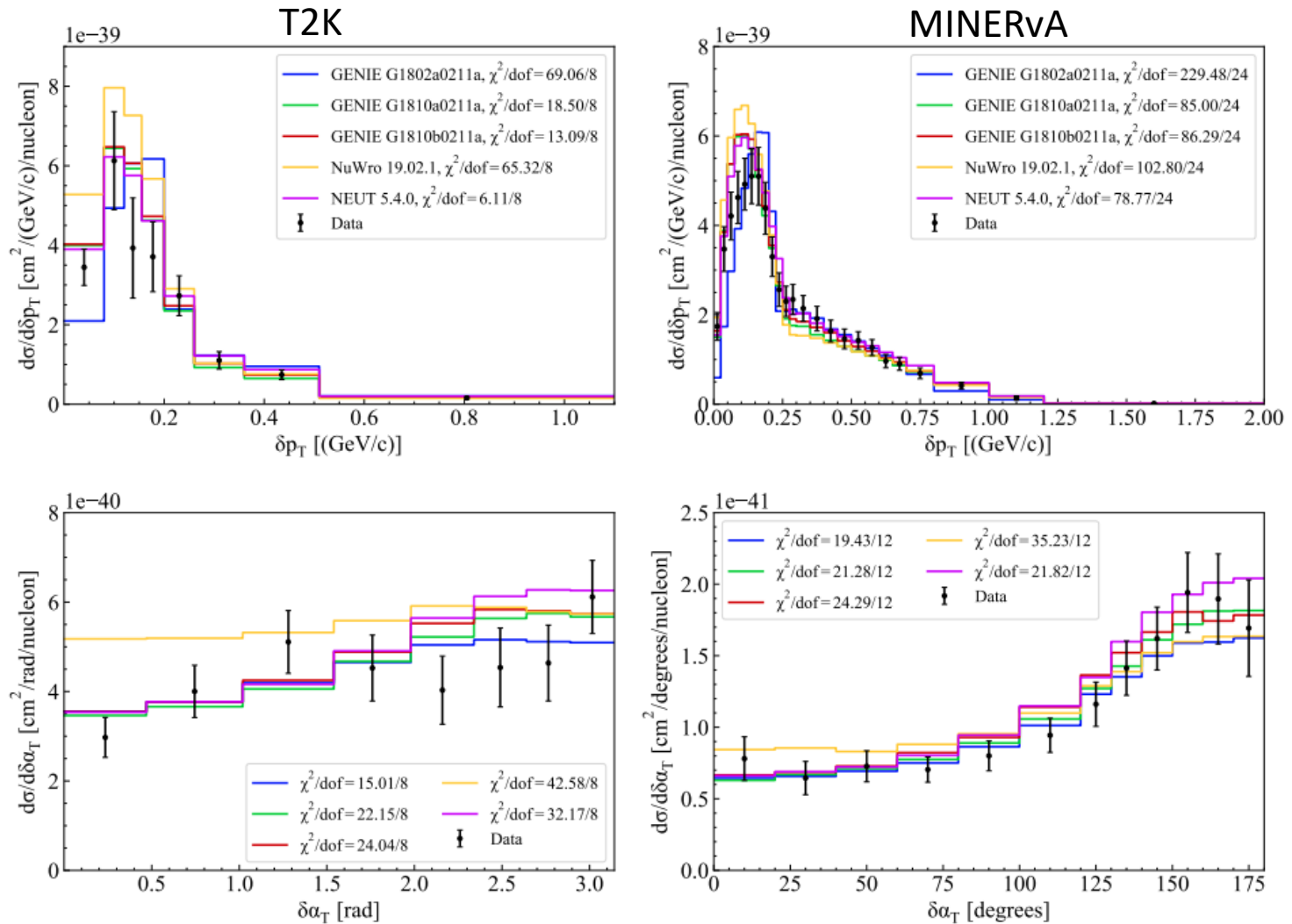
Scattering on a free nucleon at rest: $\vec{p}_T^p = -\vec{p}_T^l$

$\delta p_T = 0$; $\delta \phi_T = 0 \longrightarrow$ peaked distributions

$\delta \alpha_T$ undefined \longrightarrow flat distribution

Deviations (imbalance) from these behaviors “measure” nuclear effects

Semi-inclusive $CC0\pi$ $d\sigma$ on carbon versus STKI Variables: Monte Carlo predictions



M. Buizza Avanzini et al. PRD 105, 092004 (2022)

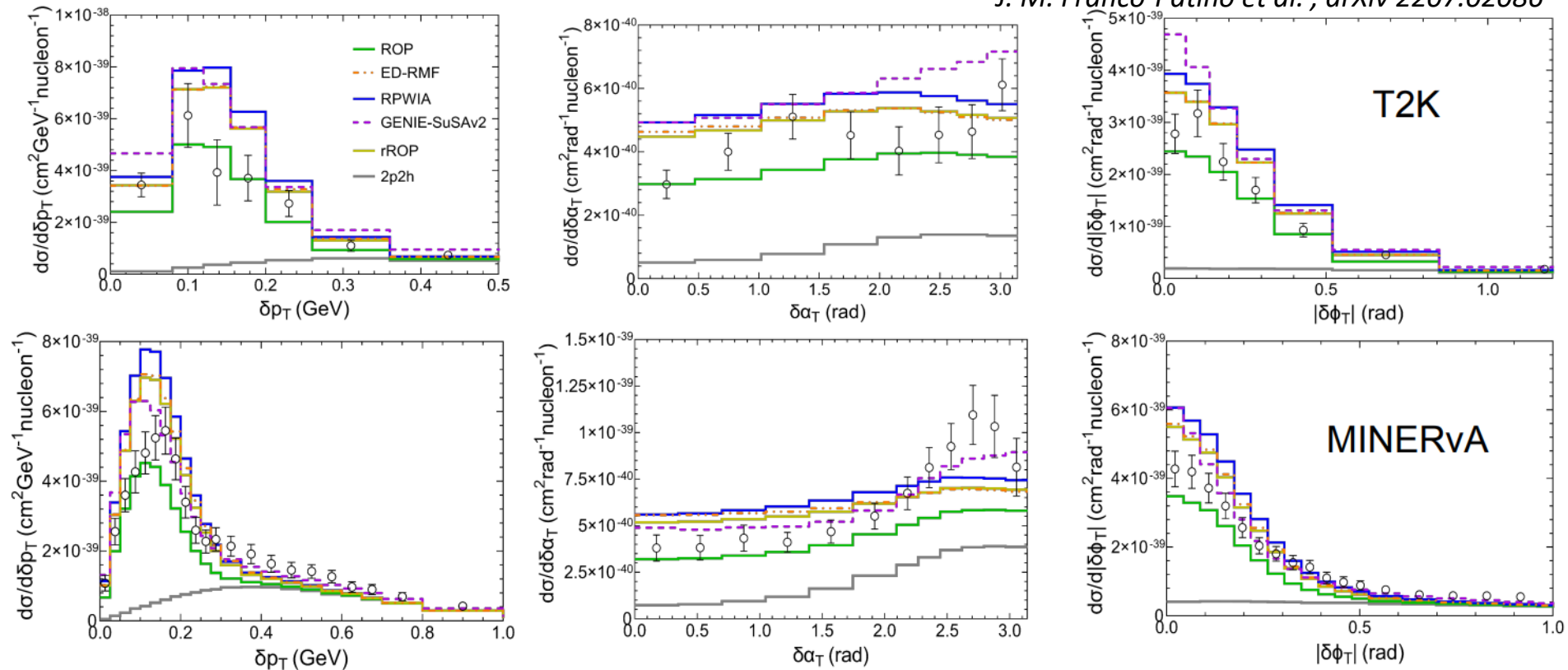
None of the generators correctly reproduces all the data in the STKI variables without tuning

This is not a surprise since these generators implement “inclusive” microscopic models 57

Semi-inclusive $CC0\pi$ $d\sigma$ on carbon versus STKI Variables: discrimination of FSI microscopic modeling

A recent theoretical study

J. M. Franco-Patino et al., arXiv 2207.02086



RPWIA: no FSI

GENIE-SuSAv2: include FSI but from inclusive model (factorization)

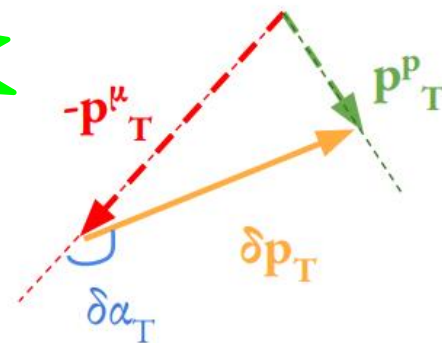
ED-RMF, rROP, ROP: different theoretical approaches for FSI

- FSI improve the agreement with data respect to the RPWIA prediction
- STKI Variables helps to discriminate between different FSI models: data (at least T2K) seem to prefer **ROP**
- 2p2h (from an inclusive-based model) give non-negligible contribution

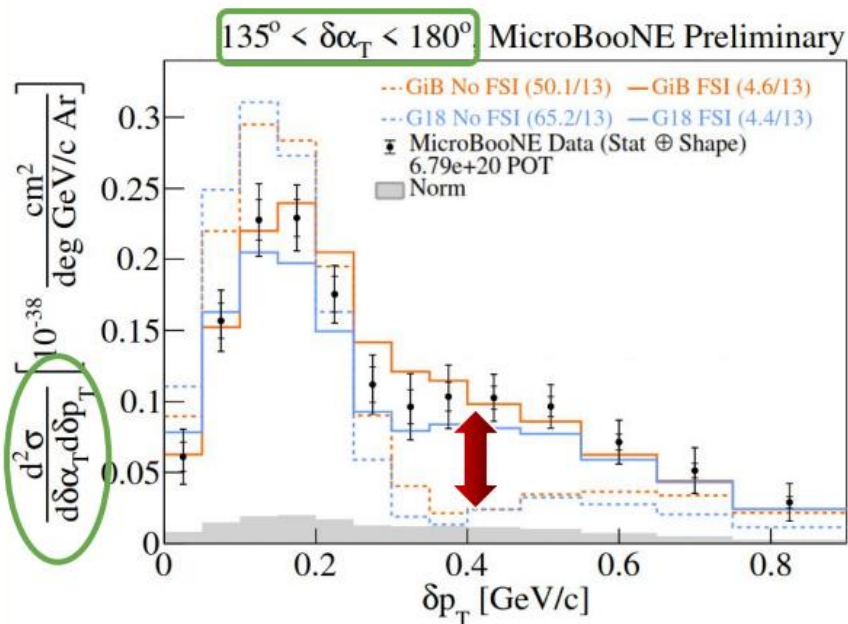
New (NuInt22) Semi-inclusive $CC0\pi$ $d\sigma$ on Argon versus STKI Variables

2D results for the first time on any neutrino target

High Statistics → Into the Multiverse!



- **Extension to 2D** for the first time on any neutrino target
- Probe regions with greater model discrimination power



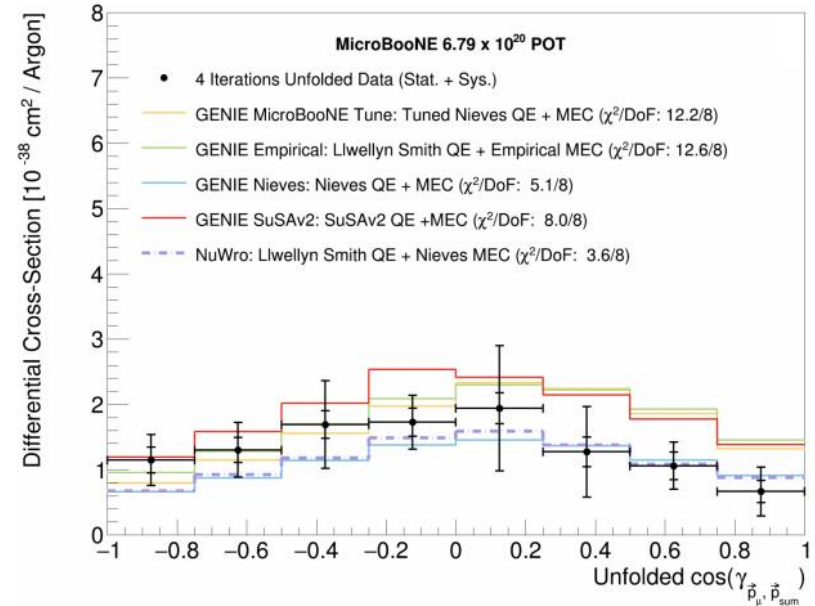
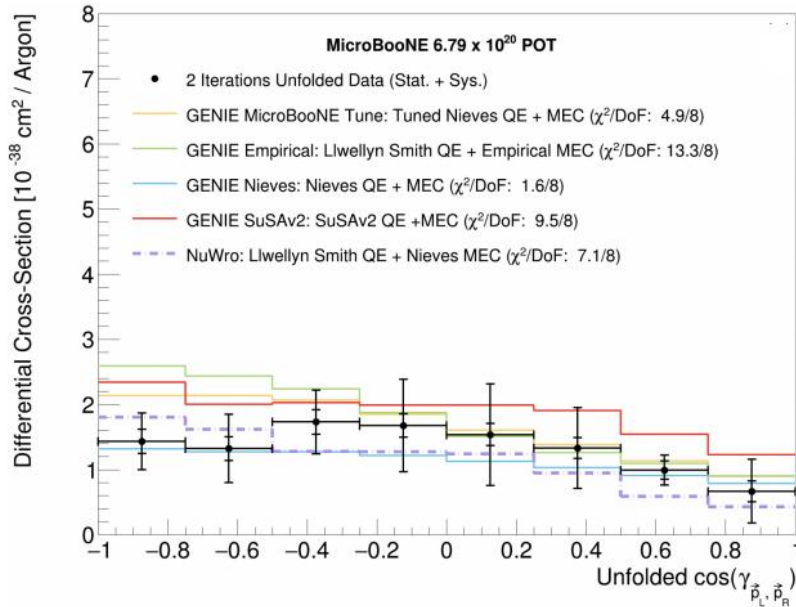
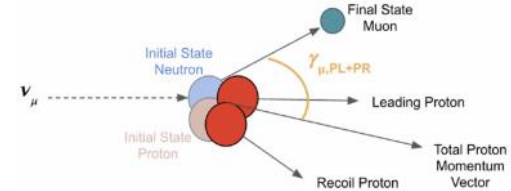
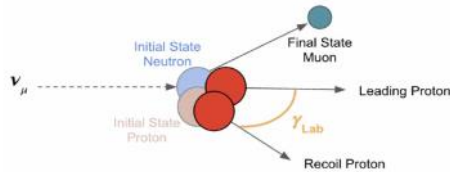
- FSI predictions in good agreement with data
- Minimal no-FSI contributions at high δp_T
- High $\delta\alpha_T$ & high δp_T part of phase-space ideal to test FSI / multinucleon effect sensitivity

MICROBOONE-NOTE-1108-PUB G18 = GENIE v3.0.6 G18_10a_02_11b + T2K Tune, GiB = GiBUU 2021

17

Afroditi Papadopoulou (MicroBooNE) talk at NuInt 22

Unfolded CC 2p0 π Cross Section and Model comparison



Michael Kirby (MicroBooNE) talk at NuInt 22

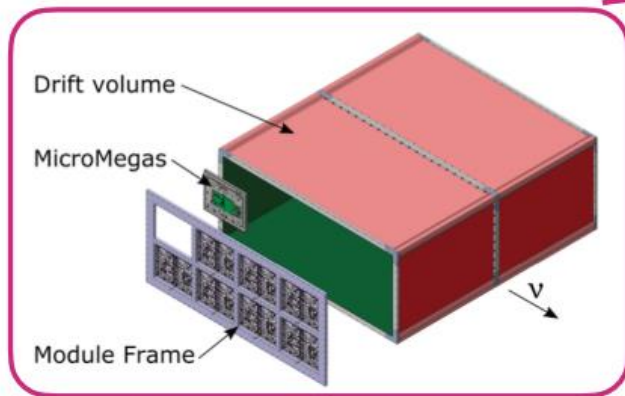
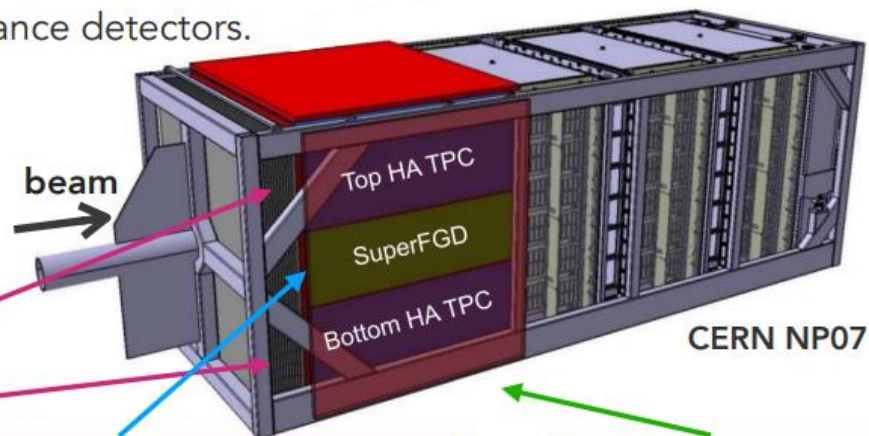
P. Abratenko et al. 2211.03734

ND280 Upgrade

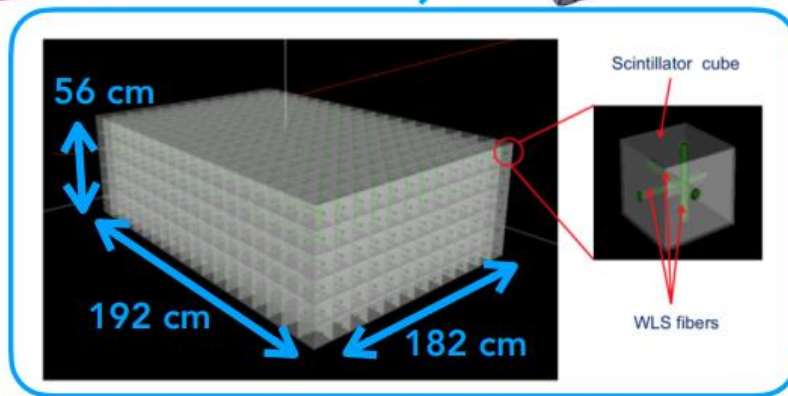
- Pi-0 detector will be replaced with new 4π acceptance detectors.

- **SuperFGD** : fully active plastic scintillator.
- **High-Angle TPC**: high resolution tracking of charged particles.
- **Time-of-Flight** : Provide time information.

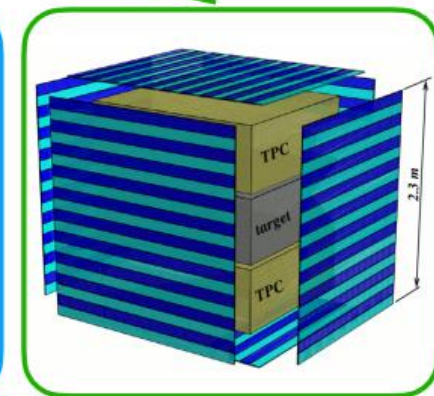
- Technical Design Report on [arXiv:1901.03750](https://arxiv.org/abs/1901.03750)



High-Angle TPC (HATPC)



Super Fine-Grained Detector (SuperFGD)



Time-of-Flight (TOF)

[A Eguchi T2KND280upgrade NuFACT2022 \(fnal.gov\)](https://arxiv.org/abs/1901.03750)

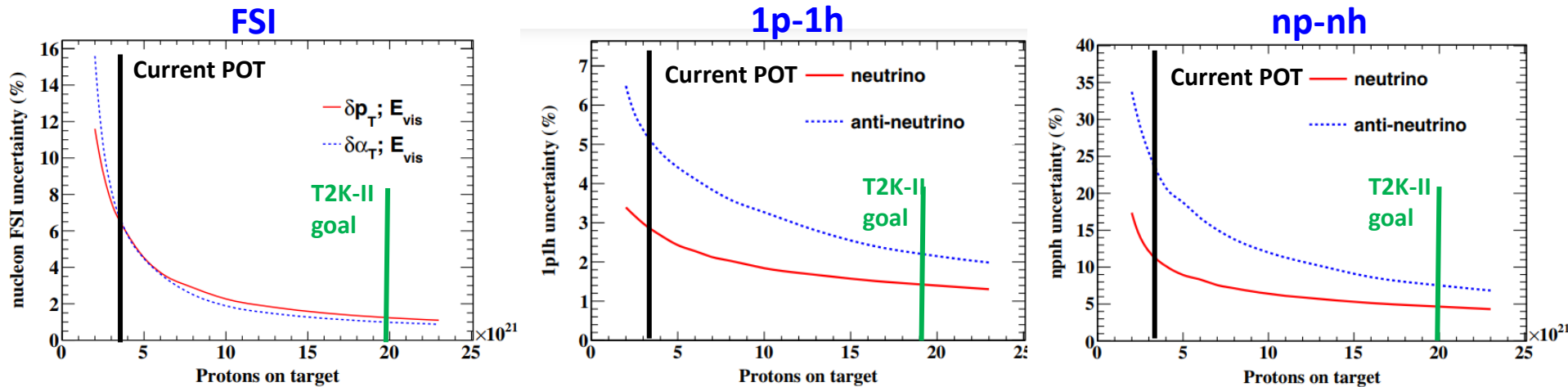
The T2K ND280 Upgrade – Physics sensitivity studies

- More mass, more data, better acceptance
- Improved reconstruction at high and backward lepton angles
- Better reconstruction of outgoing nucleons

The Upgrade opens the door to new multi-dimensional analyses (e.g. δp_T in bins of $\delta \alpha_T$)

PHYSICAL REVIEW D **105**, 032010 (2022)

Sensitivity of the upgraded T2K Near Detector to constrain neutrino and antineutrino interactions with no mesons in the final state by exploiting nucleon-lepton correlations



Significant decrease of the nuclear effects uncertainties

Neutrino cross sections: summary of status and challenges

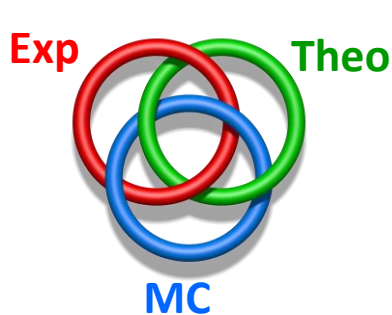
A) Cross sections in terms of muon variables (CC inclusive, CC0 π)

- **Significant progress in the last 15 years**
- Many experimental and theoretical results
- Still we have to tackle currently existing degeneracies:
 1. between cross sections and flux uncertainties
 2. between nucleon uncertainties and nuclear effects
 3. between different nuclear models and approximations

B) Cross sections in terms of hadronic variables (CC1 π , CC0 π 1p, CC0 π Np, CCOther)

We are only at the beginning!

- Few experimental and theoretical results
- The one pion puzzle is still there
- SIS and DIS have been minimally studied
- Theoretical models and Monte Carlo implementation of semi-inclusive processes are needed



Needs:

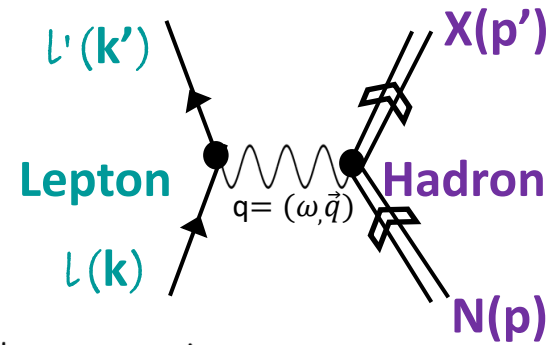
- More neutrino data on nuclei and nucleons
- Further theory efforts
- Generators equipped with more detailed (/consistent/adapted) models

Close collaboration between theorists, experimentalists and generator developers is crucial

In the precision era of neutrino physics new intriguing results, like CP violation, necessary passes through a precise knowledge of neutrino-nucleus cross sections

BACKUP

Electroweak transition matrix elements



Electromagnetic transition $\ell^- N \rightarrow \ell^- X$

$$-i\mathcal{M} = -\underbrace{(ie)^2 \bar{u}(k') \gamma_\mu u(k)}_{\text{e.m. lepton current}} \frac{-ig^{\mu\nu}}{q^2} \underbrace{\langle X(p'_f) | J_\nu(0) | N(p) \rangle}_{\text{hadronic current (Vector)}}$$

Charged current transition $\nu N \rightarrow \ell^- X$

$$-i\mathcal{M} = \left(\frac{-ig}{2\sqrt{2}}\right)^2 \cos \theta_C \underbrace{\bar{u}(k') \gamma_\mu (1 - \gamma^5) u(k)}_{\text{weak lepton current}} \frac{ig^{\mu\nu}}{M_W^2} \underbrace{\langle X(p'_f) | J_\nu(0) | N(p) \rangle}_{\text{hadronic current (Vector-Axial)}}$$

θ_C

Cabibbo angle

$$\frac{g^2}{8M_W^2} = \frac{G_F}{\sqrt{2}}$$

Fermi coupling constant

The leptonic tensor

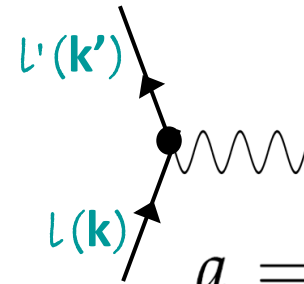
$$L_{\mu\nu} = \frac{1 + |a|}{2} \sum_{s_i} \sum_{s_f} j_\mu^\dagger j_\nu = \frac{1 + |a|}{2} \sum_{s_i} \sum_{s_f} \bar{u}(k) \tilde{l}_\mu u(k') \bar{u}(k') l_\nu u(k)$$

$$= \frac{1 + |a|}{2} \text{Tr} \left[(\not{k} + m_\ell) \tilde{l}_\mu (\not{k}' + m_{\ell'}) l_\nu \right]$$

Leptonic component of the electroweak current

$$j_\mu = \bar{u}(k') l_\mu u(k)$$

$$l_\mu = \gamma_\mu (1 - a \gamma^5) \quad \tilde{l}_\mu = \gamma_0 l_\mu^\dagger \gamma_0$$



$$\not{p} = \gamma_\mu p^\mu$$

$$a = 0 \text{ EM}$$

$$a = 1 (-1) \text{ CC and NC}$$

Electron scattering

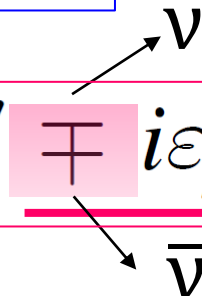
$$L_{\mu\nu} = k_\mu k'_\nu + k'_\mu k_\nu - g_{\mu\nu} (k \cdot k' - m_e^2)$$

$$g_{\mu\nu} = (+, -, -, -)$$

$$\epsilon_{0123} = +1$$

Neutrino scattering

$$L_{\mu\nu} = k_\mu k'_\nu + k_\nu k'_\mu - g_{\mu\nu} k \cdot k' \mp i \epsilon_{\mu\nu\alpha\beta} k^\alpha k'^\beta$$



The hadronic tensor

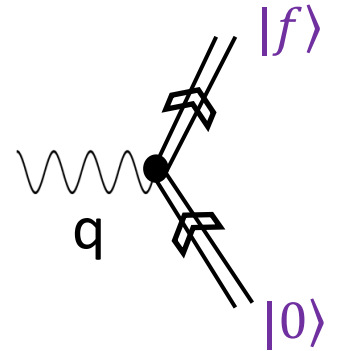
The hadronic tensor contains all the information on the target response

$$W^{\mu\nu} = \sum_f \langle 0 | J^{\mu\dagger}(q) | f \rangle \langle f | J^\nu(q) | 0 \rangle \delta^{(4)}(p_0 + q - p_f)$$

$|0\rangle$ hadronic initial state

$|f\rangle$ hadronic final state

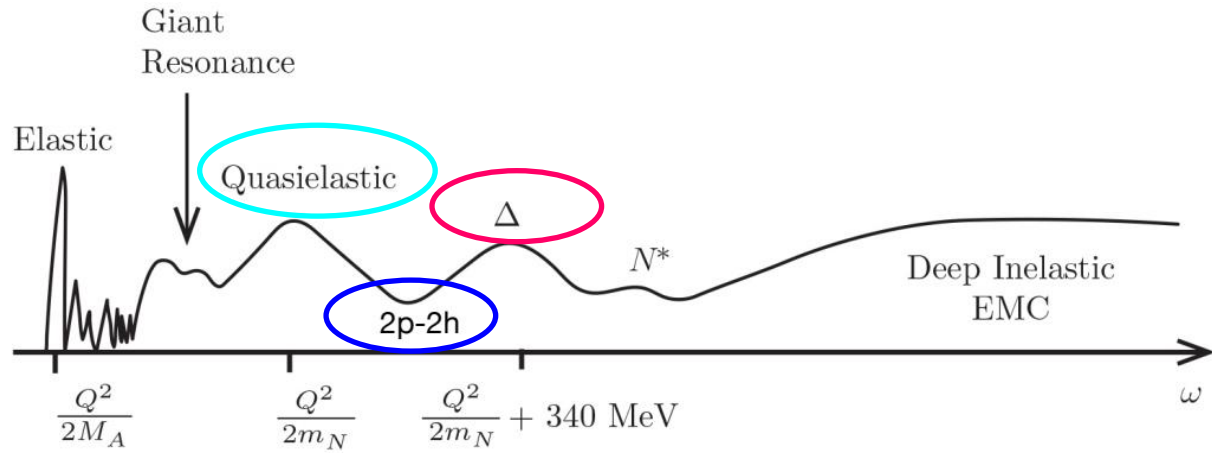
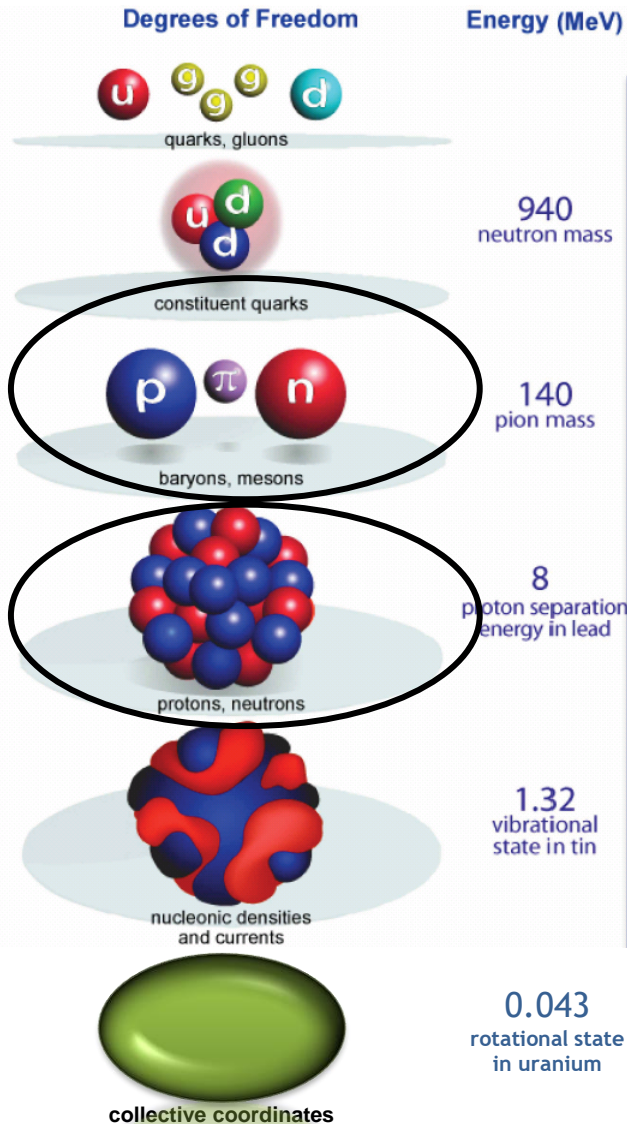
J^ν Hadronic component of the electroweak current



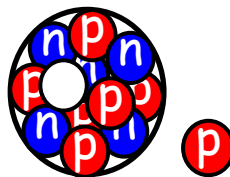
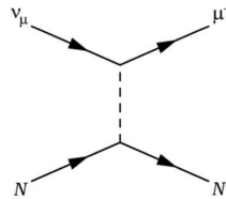
A general expression

- valid for different degrees of freedom (quark, nucleon, nucleon resonances, nucleus)
- valid for different currents (electromagnetic, weak; one-body, two-body,...)

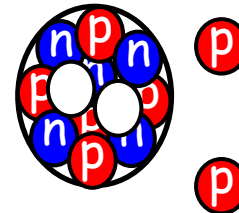
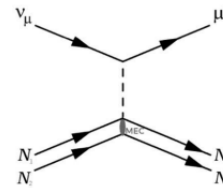
In the following:



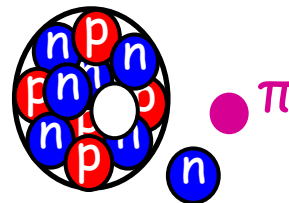
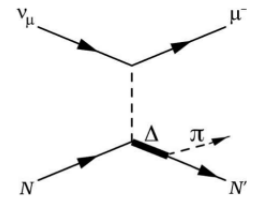
Quasielastic



2p-2h



RES π production



A simplified expressions particularly useful for illustration

- Final lepton mass contributions ignored ($m_l=0$)
- Obtained by keeping only the leading terms for the hadronic tensor in the development of the hadronic current in p/M_N

$$\frac{d^2\sigma}{d\cos\theta d\omega} = \frac{G_F^2 \cos^2\theta_c}{\pi} |k'| E_l' \cos^2\frac{\theta}{2} \left[\frac{(\mathbf{q}^2 - \omega^2)^2}{\mathbf{q}^4} G_E^2 R_T(\mathbf{q}, \omega) + \frac{\omega^2}{\mathbf{q}^2} G_A^2 R_{\sigma\tau(L)}(\mathbf{q}, \omega) \right] \\ + 2 \left(\tan^2\frac{\theta}{2} + \frac{\mathbf{q}^2 - \omega^2}{2\mathbf{q}^2} \right) \left(G_M^2 \frac{\mathbf{q}^2}{4M_N^2} + G_A^2 \right) R_{\sigma\tau(T)}(\mathbf{q}, \omega) \pm 2 \frac{E_\nu + E_l'}{M_N} \tan^2\frac{\theta}{2} G_A G_M R_{\sigma\tau(T)}(\mathbf{q}, \omega)$$

Explicitly appear:

1. The different **kinematic variables** (related to the leptonic tensor)
2. The nucleon Electric, Magnetic, and Axial **form factors** (\leftrightarrow nucleon properties)
3. The **nuclear response functions** (\leftrightarrow nuclear dynamics)

Nuclear response functions $R(\mathbf{q}, \omega)$:

$$R_\alpha^{PP'}(\mathbf{q}, \omega) = \sum_n \langle n | \sum_{j=1}^A O_\alpha^P(j) e^{i\mathbf{q}\cdot\mathbf{x}_j} | 0 \rangle \langle n | \sum_{k=1}^A O_\alpha^{P'}(k) e^{i\mathbf{q}\cdot\mathbf{x}_k} | 0 \rangle^* \delta(\omega - E_n + E_0),$$

Isovector R_τ

$$O_\alpha^N(j) = \tau_j^\pm$$

Isospin Spin-Longitudinal $R_{\sigma\tau(L)}$

$$(\boldsymbol{\sigma}_j \cdot \hat{\mathbf{q}}) \tau_j^\pm$$

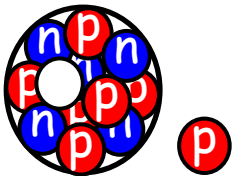
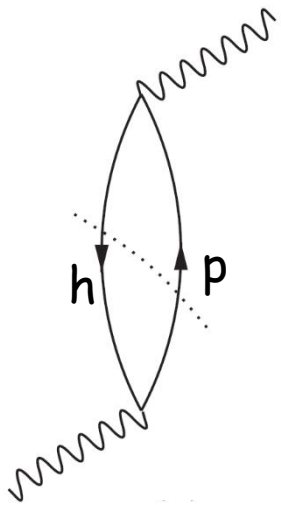
Isospin Spin-Transverse $R_{\sigma\tau(T)}$

$$(\boldsymbol{\sigma}_j \times \hat{\mathbf{q}})^i \tau_j^\pm$$

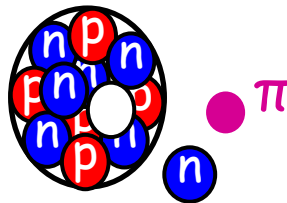
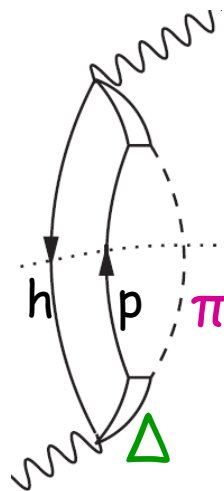
Nuclear Responses for different excitations

$$R_\alpha = \sum_{n \neq 0} |\langle n | \hat{O}_{(\alpha)} | 0 \rangle|^2 \delta[\omega - (E_n - E_0)]$$

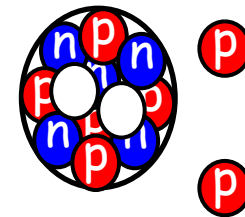
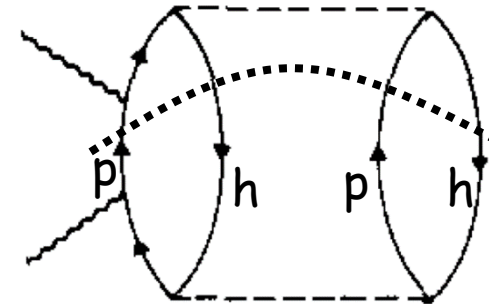
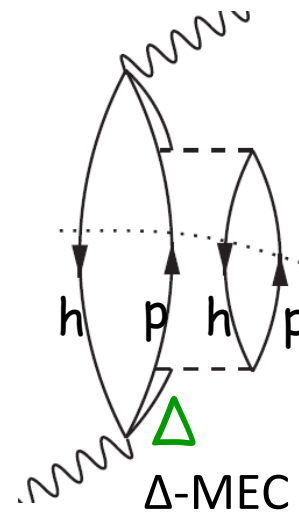
1p-1h
Quasielastic



1p-1h
($\Delta \rightarrow \pi N$) 1π production



2p-2h:
two examples



The single nucleon electroweak current

Electromagnetic current - Electron scattering

$$J_{s's}^\mu(\mathbf{p}', \mathbf{p}) = \bar{u}_{s'}(\mathbf{p}') \left[F_1(Q^2) \gamma^\mu + F_2(Q^2) i \sigma^{\mu\nu} \frac{q_\nu}{2m_N} \right] u_s(\mathbf{p})$$

$$Q^2 = -q^2 \quad \sigma^{\mu\nu} = \frac{i}{2} [\gamma^\mu, \gamma^\nu]$$

Weak current – CC neutrino scattering

$$J^\mu = V^\mu - A^\mu \quad \text{Vector – Axial}$$

Vector $V_{s's}^\mu(\mathbf{p}', \mathbf{p}) = \bar{u}_{s'}(\mathbf{p}') \left[2F_1^V \gamma^\mu + 2F_2^V i \sigma^{\mu\nu} \frac{q_\nu}{2m_N} \right] u_s(\mathbf{p})$

Conserved Vector Current (CVC) $q_\alpha V^\alpha = 0$ and isospin symmetry $\Rightarrow F_i^V = F_i^p - F_i^n$

Axial $A_{s's}^\mu(\mathbf{p}', \mathbf{p}) = \bar{u}_{s'}(\mathbf{p}') \left[G_A \gamma^\mu \gamma_5 + G_P \frac{q^\mu}{2m_N} \gamma_5 \right] u_s(\mathbf{p})$

Partially Conserved Axial Current (PCAC) and pion-pole dominance $\Rightarrow G_P = \frac{4m_N^2}{m_\pi^2 + Q^2} G_A$

$q_\alpha A^\alpha = i(m_u + m_d) \bar{q}_u \gamma_5 q_d \rightarrow 0$

The nucleon form factors

The form factors are corrections to “point-like coupling”

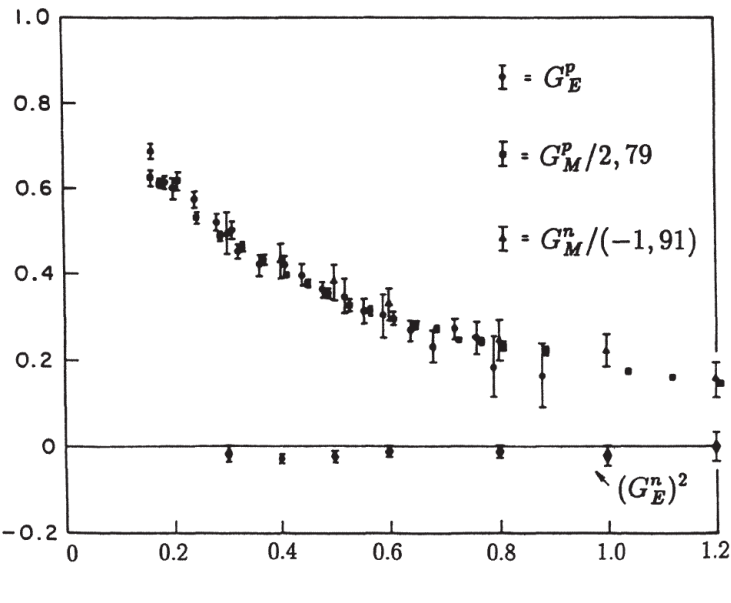
They reflect the fact that the nucleon has an internal structure and a finite size

F_1 and F_2 can be written as a combination of the Electric and Magnetic form factors G_E and G_M

$$F_1^{p,n} = \left[G_E^{p,n} + \frac{Q^2}{4m_N^2} G_M^{p,n} \right] \left[1 + \frac{Q^2}{4m_N^2} \right]^{-1} \quad F_2^{p,n} = [G_M^{p,n} - G_E^{p,n}] \left[1 + \frac{Q^2}{4m_N^2} \right]^{-1}$$

Electron-nucleon cross section

$$\left(\frac{d\sigma}{d\Omega} \right) = \left(\frac{d\sigma}{d\Omega} \right)_{\text{Mott}} \cdot \left[\frac{G_E^2(Q^2) + \tau G_M^2(Q^2)}{1 + \tau} + 2\tau G_M^2(Q^2) \tan^2 \frac{\theta}{2} \right]$$



Global dipole-like behavior

$$G_E^p(Q^2) = \frac{G_M^p(Q^2)}{2.79} = \frac{G_M^n(Q^2)}{-1.91} = G^{\text{dipole}}(Q^2)$$

$$G^{\text{dipole}}(Q^2) = \left(1 + \frac{Q^2}{0.71 (\text{GeV}/c)^2} \right)^{-2}$$

Several models to calculate the responses and the ν cross sections

- Local Fermi Gas + Random Phase Approximation

Lyon M. Martini, M. Ericson, G. Chanfray, J. Marteau, *Phys. Rev. C* 80 065501 (2009)

Valencia J. Nieves, I. Ruiz Simo, M.J. Vicente Vacas, *Phys. Rev. C* 83 045501 (2011)

- Hartree-Fock + (Continuum) Random Phase Approximation

Ghent V. Pandey, N. Jachowicz, T. Van Cuyck, J. Ryckebusch, M. Martini, *Phys. Rev. C* 92 024606 (2015)

Other groups focused on giant resonances and below Kolbe et al. ; Volpe et al.; Co' et al.; ...

- SuSAv2 superscaling/relativistic mean field

Granada, Madrid, MIT, Sevilla, Torino

G.D. Megias, J.E. Amaro, M.B. Barbaro, J.A. Caballero, T.W. Donnelly, I. Ruiz Simo, *PRD* 94 093004 (2016)

- Spectral function approach

Roma N. Rocco, C. Barbieri, O. Benhar, A. De Pace, A. Lovato, *Phys. Rev. C* 99 025502 (2019)

- Relativistic Green's function

Pavia A. Meucci, C. Giusti, F. D. Pacati, *Nucl.Phys.A* 739 277-290 (2004)

- Green's function Monte Carlo ("ab initio")

Argonne, Los Alamos A. Lovato, J. Carlson, S. Gandolfi, N. Rocco, R. Schiavilla, *PRX* 10 031068 (2020)

- GiBUU transport theory

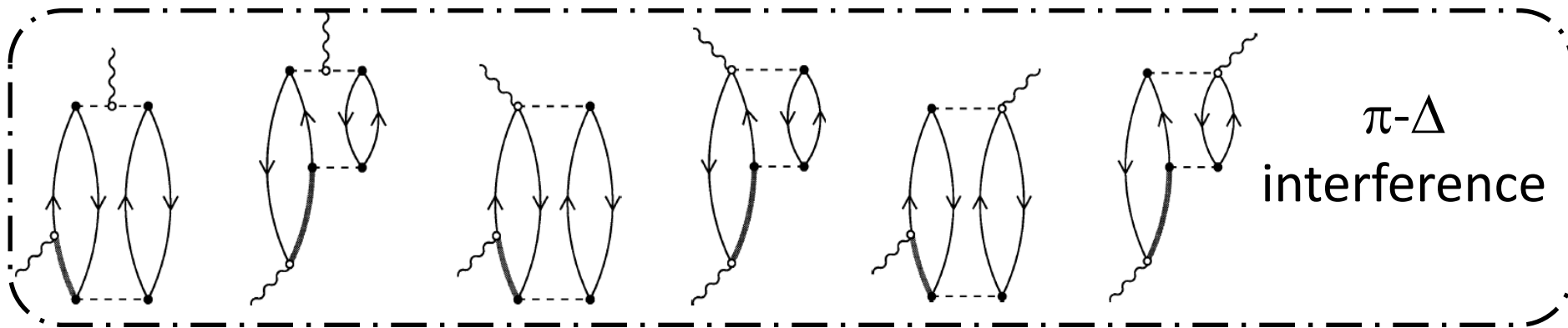
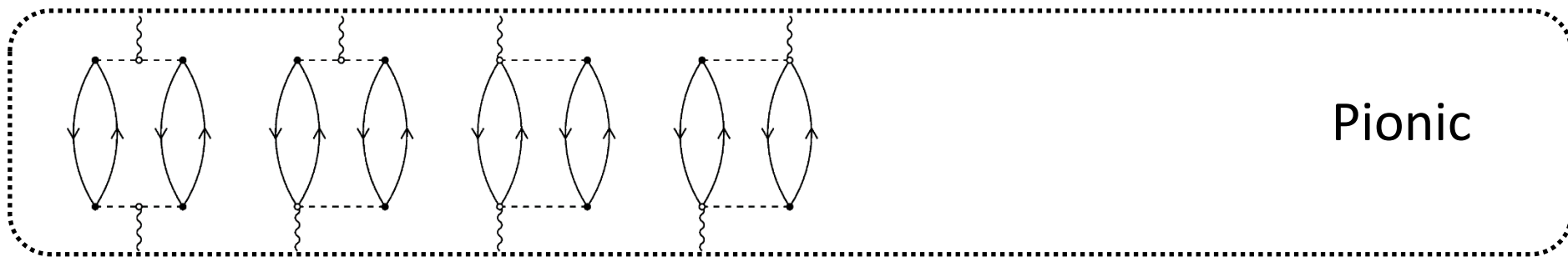
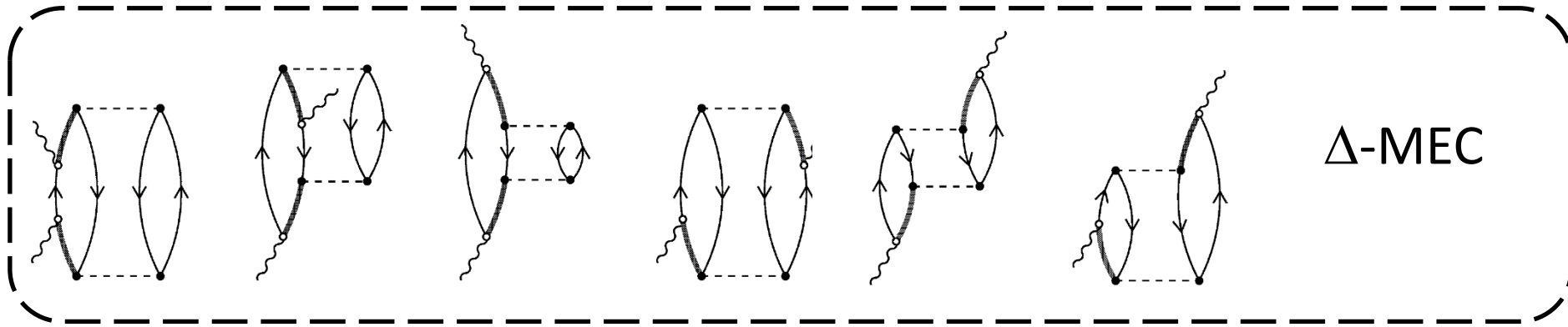
Giessen O. Buss, T. Gaitanos, K. Gallmeister, H. van Hees, M. Kaskulov, O. Lalakulich, A.B. Larionov, T. Leitner, J. Weil, U. Mosel, *Phys.Rept.* 512 1-124 (2012)

p.s. only one representative reference for each approach (not necessarily the founding paper)

For discussions and comparisons of different models see for example:

- G.T. Garvey, D.A. Harris, H.A. Tanaka, R. Tayloe, G.P. Zeller, *Phys.Rept.* 580 (2015) 1-45
- T. Katori, M. Martini, *J.Phys.G* 45 (2018) 1, 013001
- M. Sajjad Athar, A. Fatima, S. K. Singh *arxiv.* 2206.13792

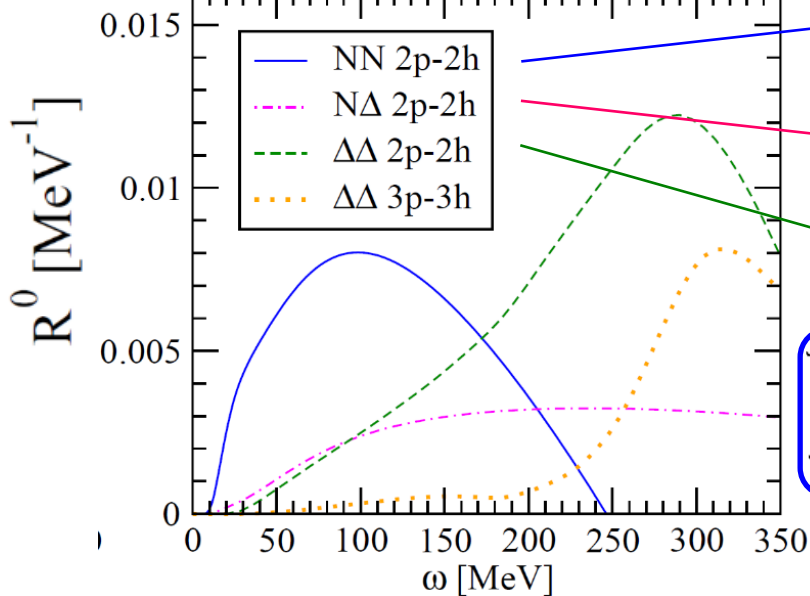
MEC contributions



De Pace, Nardi, Alberico, Donnelly, Molinari, NPA741 (2004)

Separation of np-nh contributions in the nuclear responses

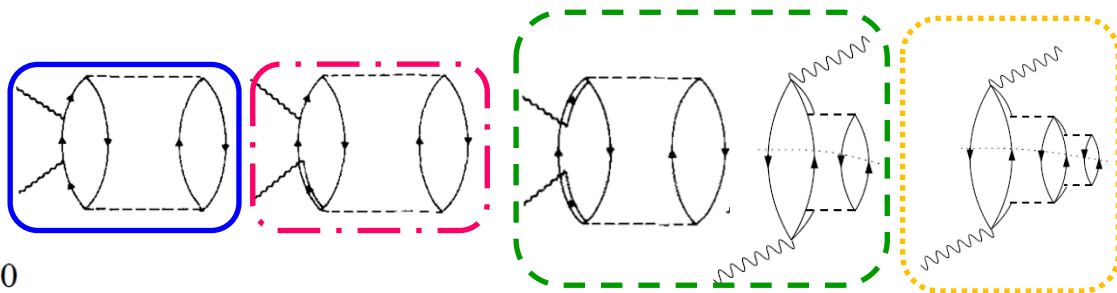
M. Martini, M. Ericson, G. Chanfray, J. Marteau, PRC 80 065501 (2009)



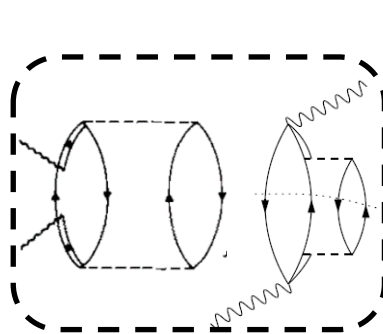
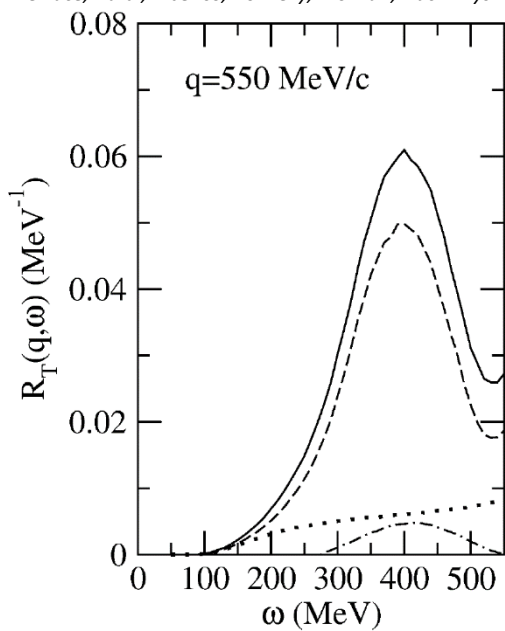
also called NN SRC; part of 1-body current contribution in correlated nuclear wave functions approaches, like SF or GFMC

$N\Delta$ interference, also called NN correlation- Δ MEC interference or 1-body—2-body interference

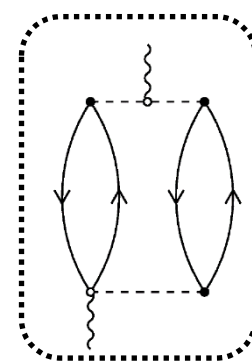
Δ mediated MEC



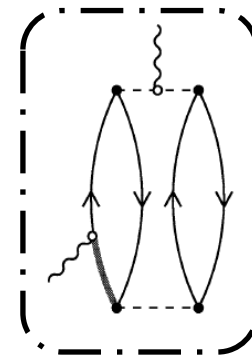
De Pace, Nardi, Alberico, Donnelly, Molinari, Nucl. Phys. A741, 249 (2004)



Δ



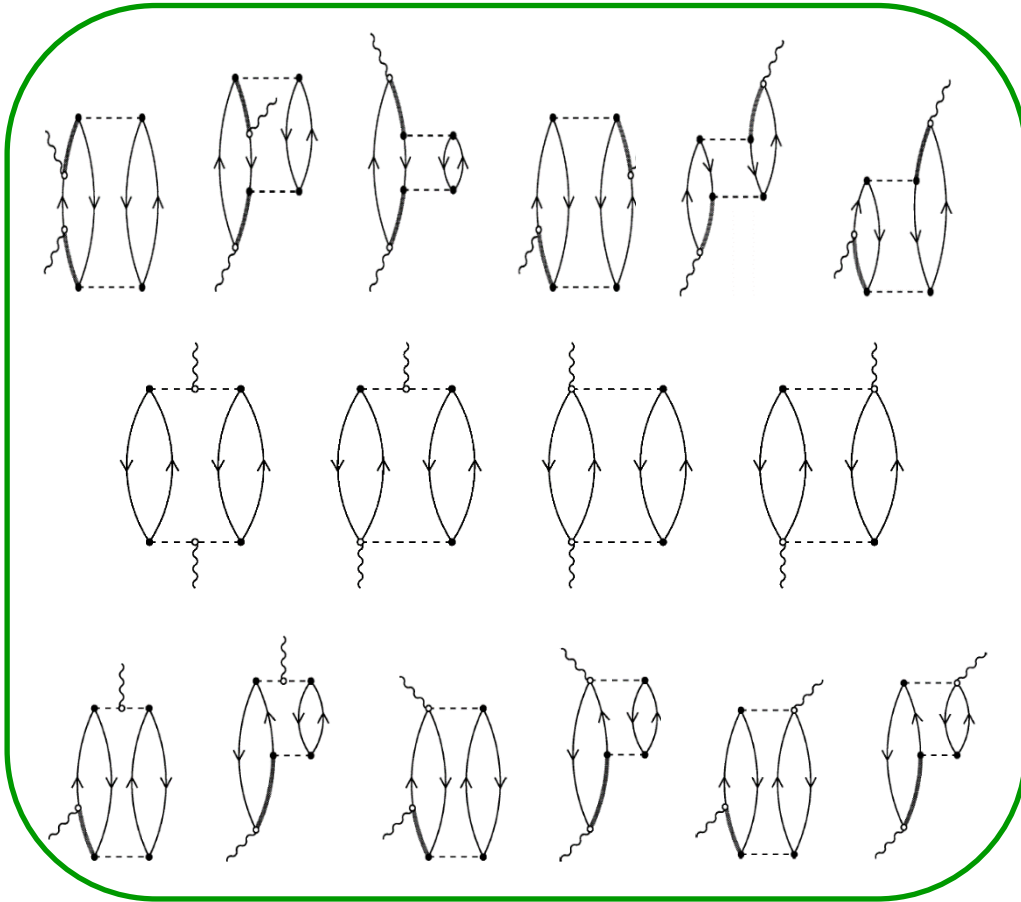
π



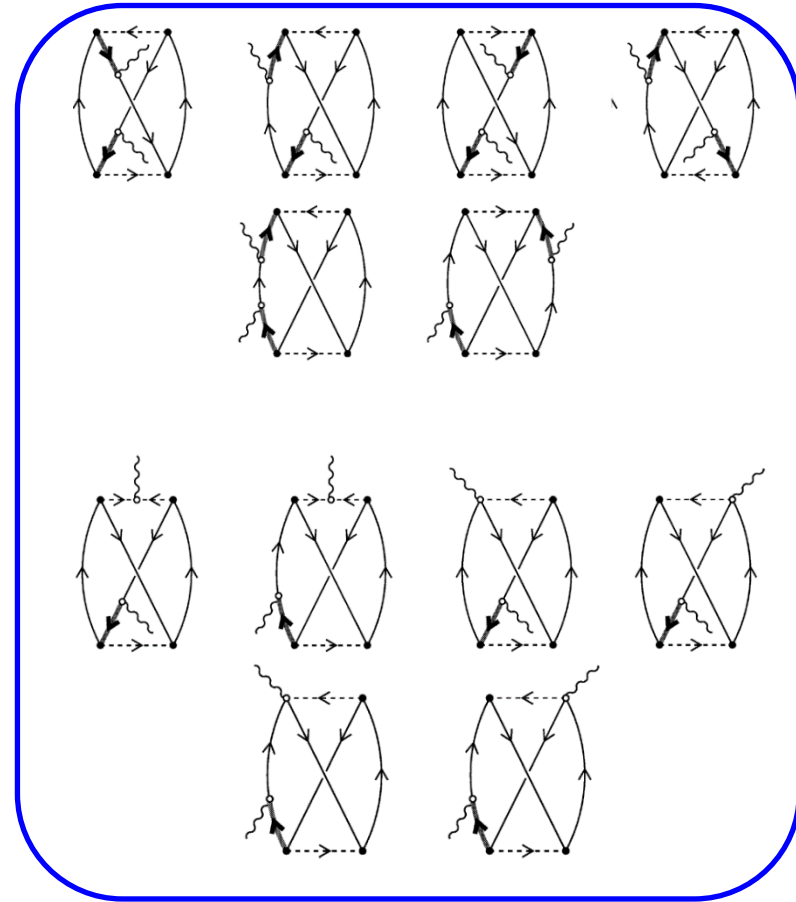
π - Δ intf.

Direct and exchange MEC contributions

Direct



Exchange



Fully relativistic calculation of *De Pace, Nardi, Alberico, Donnelly, Molinari, NPA741 (2004)*:

3000 direct terms

More than **100 000** exchange terms

Electromagnetic 2p-2h MEC response

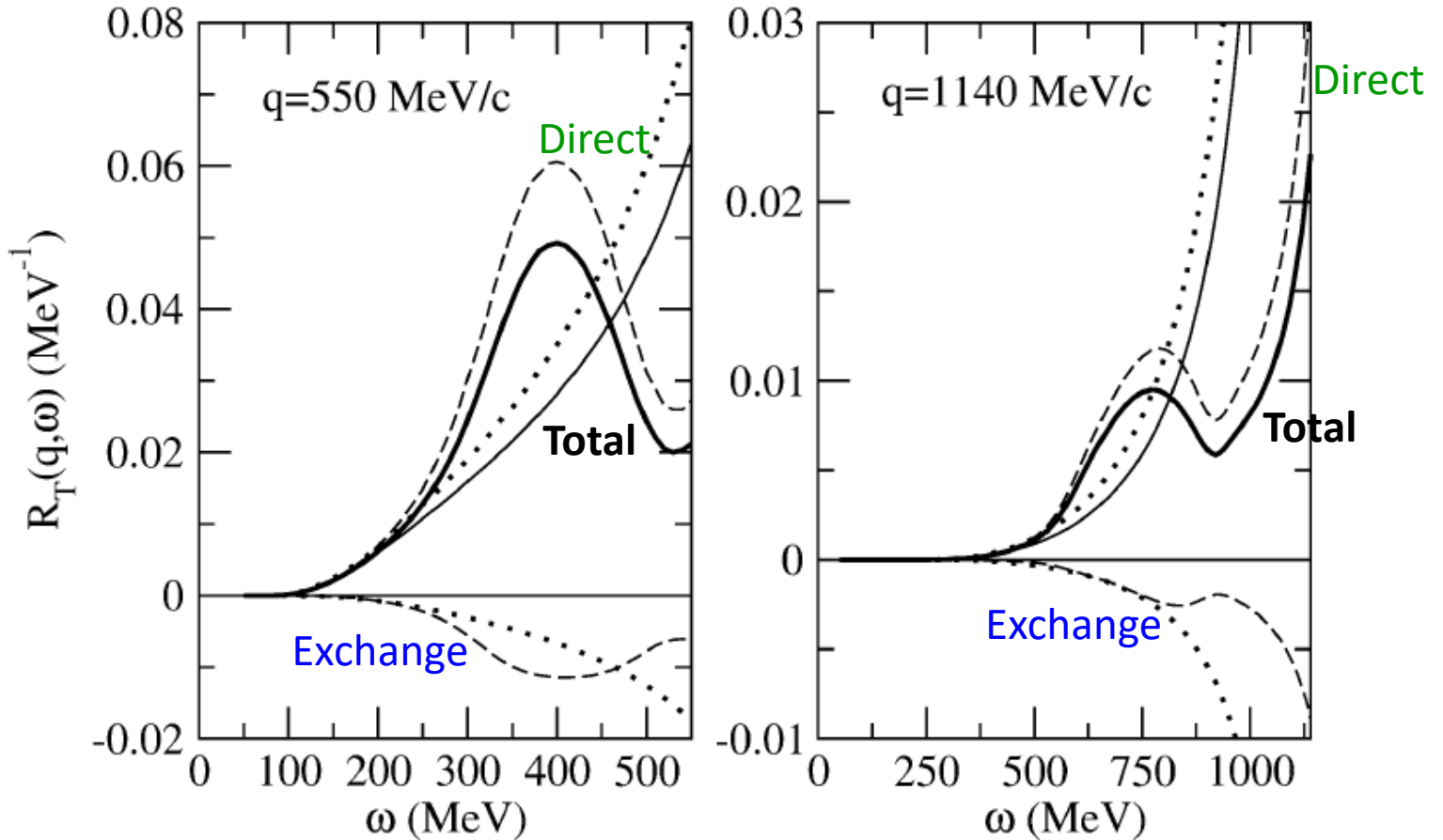
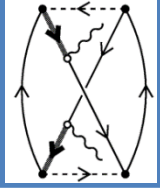
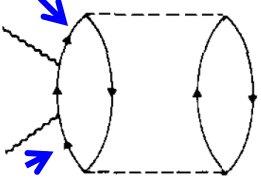


Fig. 12. The transverse response function $R_T(q, \omega)$ at $q = 550 \text{ MeV}/c$ and $q = 1140 \text{ MeV}/c$ including the exchange contributions: non-relativistic direct (positive dotted), non-relativistic exchange (negative dotted), non-relativistic total (light solid), relativistic direct (positive dashed), relativistic exchange (negative dashed) and relativistic total (heavy solid). In all instances $\bar{\epsilon}_2 = 70 \text{ MeV}$ and $k_F = 1.3 \text{ fm}^{-1}$.

De Pace, Nardi, Alberico, Donnelly, Molinari, Nucl. Phys. A741, 249 (2004)

Different approximations for the 2p-2h calculations

Approach	Vector	Axial	NN correlations	MEC	NN-MEC interference	Relativistic	
RPA Lyon Martini et al.	Yes	Yes	$ \pi, g' $	Yes (Only Δ MEC)	Yes	Some ingredients	No
RPA Valencia Nieves et al.	Yes	Yes	$ \pi, \rho, g' $	Yes	Yes	Approximations in the WNN π vertex	No
SuSAv2	Yes	Yes	Already in Superscaling function (1p-1h part)	Yes	No	Fully Relativistic	Yes



$$(p_0 - E_{\mathbf{p}} + i\epsilon)^{-2}$$

• Divergences in NN correlations, prescriptions:

- nucleon propagator only off the mass shell (*Alberico et al. Ann. Phys. 1984*)
- kinematical constraints + nucleon self energy in the medium (*Nieves et al PRC 83*)
- regularization parameter taking into account the finite size of the nucleus to be fitted to data (*Amaro et al. PRC 82 044601 2010*)

T. Katori, M. Martini, J.Phys.G 45 (2018) 1, 013001

2p-2h phase space integral

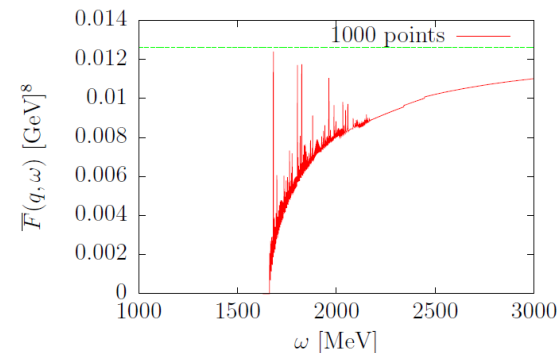
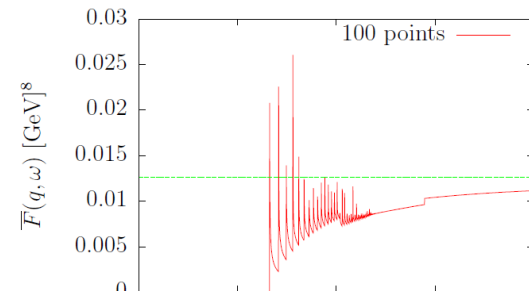
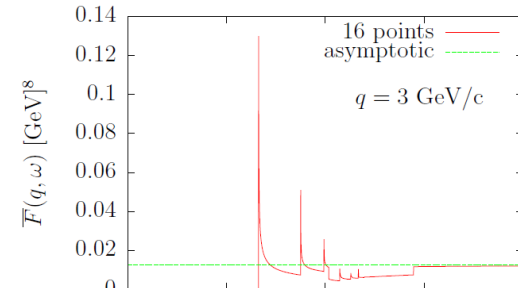
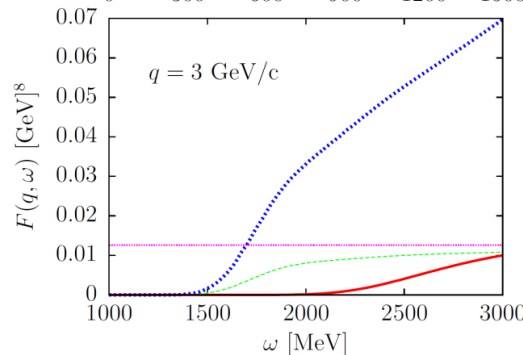
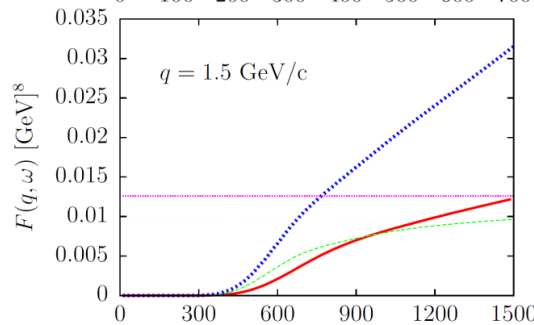
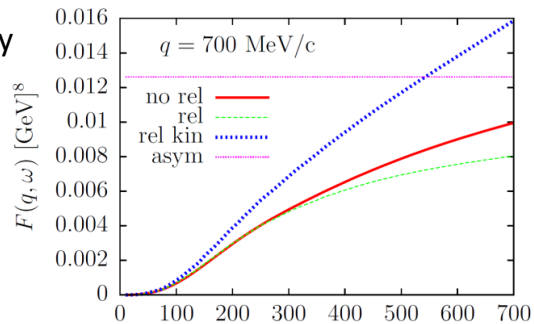
$$F(\omega, q) \equiv \int d^3 h_1 d^3 h_2 d^3 p'_1 \frac{m_N^4}{E_1 E_2 E'_1 E'_2} \Theta(p'_1, p'_2, h_1, h_2) \delta(E'_1 + E'_2 - E_1 - E_2 - \omega)$$

$$\bar{F}(\omega, q) = \left(\frac{4}{3} \pi k_F^3 \right)^2 \int d^3 p'_1 \delta(E'_1 + E'_2 - \omega - 2m_N) \Theta(p'_1, p'_2, 0, 0) \frac{m_N^2}{E'_1 E'_2}$$

Ruiz Simo, Albertus, Amaro, Barbaro, Caballero, Donnelly

Phys. Rev. D 90 033012 (2014)

Phys. Rev. D 90 053010 (2014)



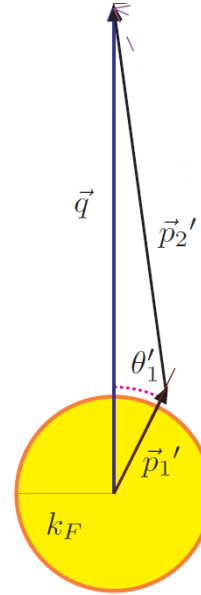
Angular distribution of ejected nucleons

$$\bar{F}(\omega, q) = \left(\frac{4}{3} \pi k_F^3 \right)^2 2\pi \int_0^\pi d\theta'_1 \Phi(\theta'_1)$$

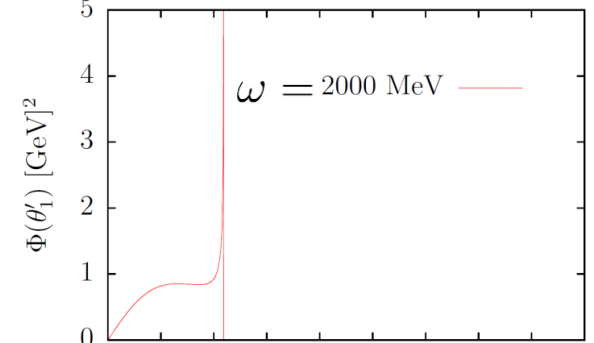
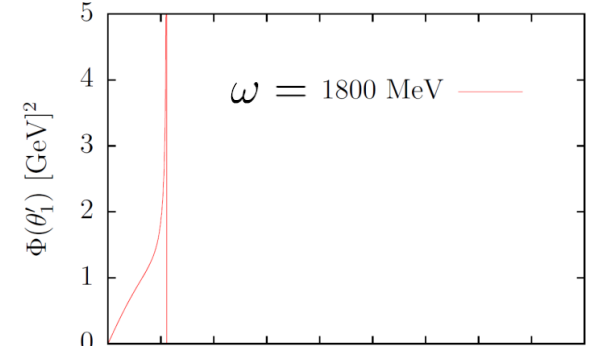
$$\Phi(\theta'_1) = \sin \theta'_1 \int p_1'^2 dp_1' \delta(E_1 + E_2 + \omega - E_1' - E_2')$$

$$\times \Theta(p_1', p_2', h_1, h_2) \frac{m_N^4}{E_1 E_2 E_1' E_2'}$$

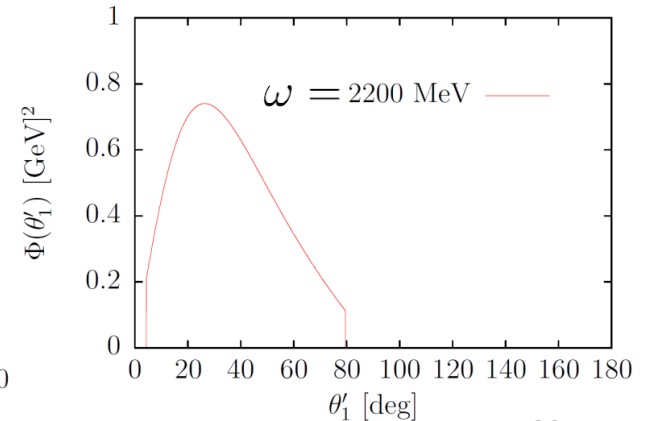
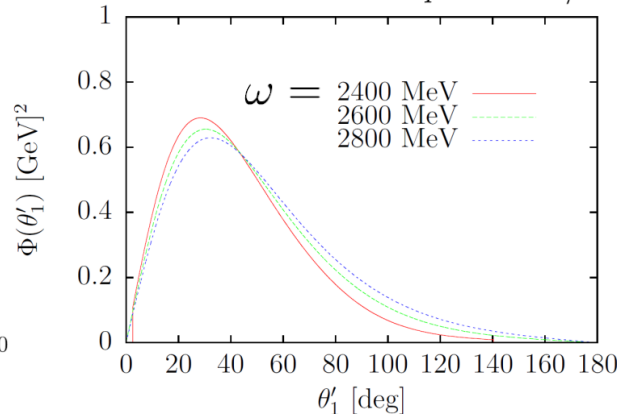
$$= \sum_{\alpha=\pm} \frac{m_N^4 \sin \theta'_1 p_1'^2 \Theta(p_1', p_2', h_1, h_2)}{E_1 E_2 E_1' E_2' \left| \frac{p_1'}{E_1} - \frac{p_2'}{E_2} \right|} \Bigg|_{p_1'=p_1'^{(\alpha)}}$$



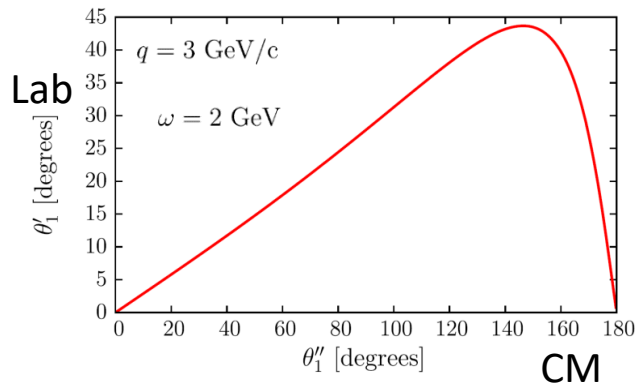
$q = 3 \text{ GeV}/c$



$q = 3 \text{ GeV}/c$



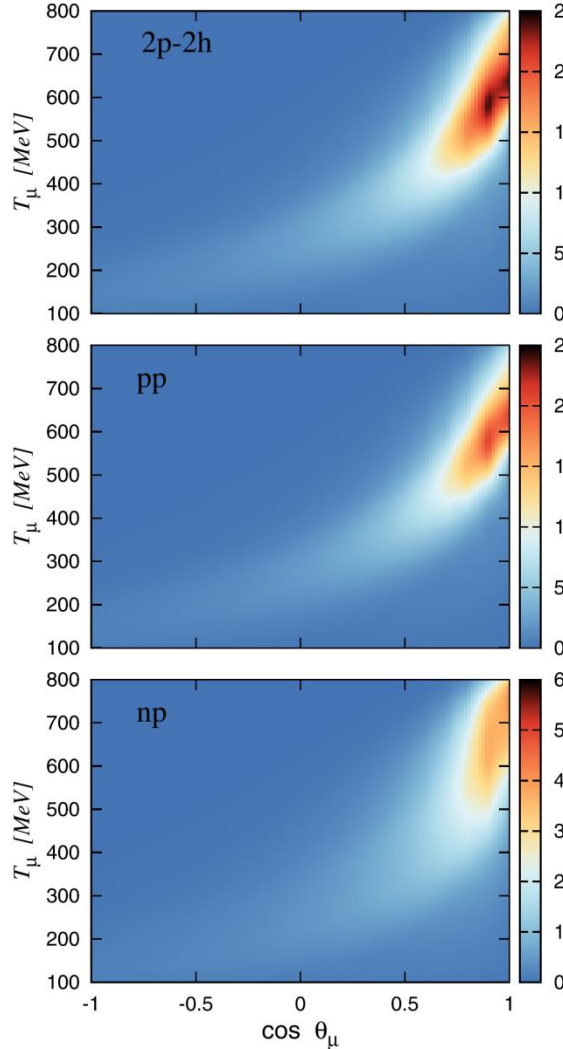
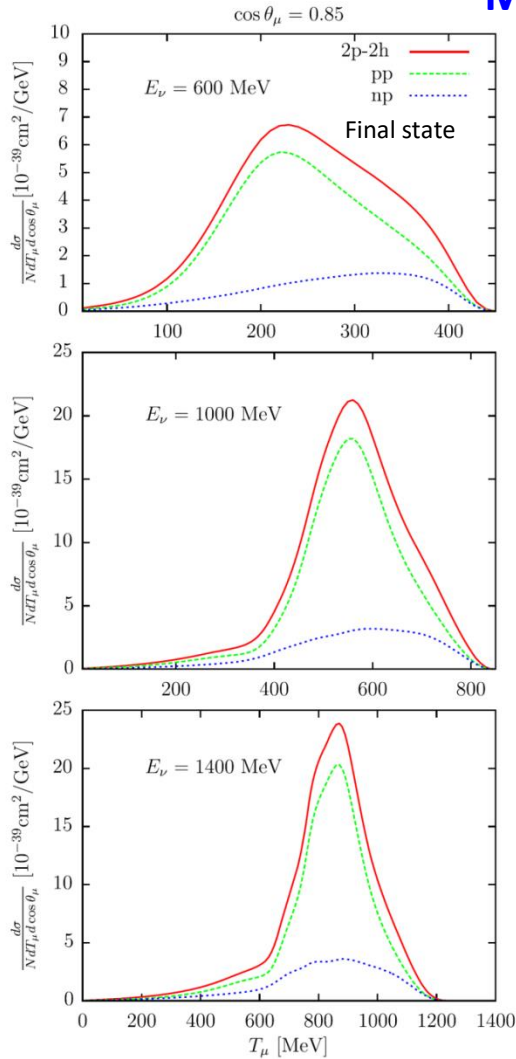
Ruiz Simo, Albertus, Amaro, Barbaro, Caballero, Donnelly
 Phys. Rev. D 90 033012 (2014)
 Phys. Rev. D 90 053010 (2014)



Theoretical studies on hadron information – Isospin content

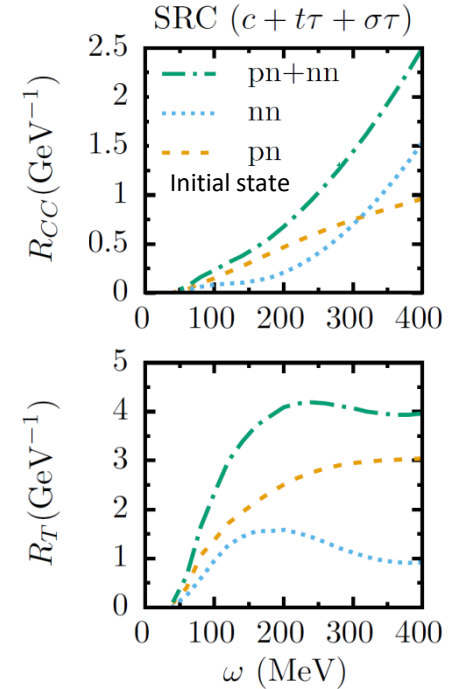
I. Ruiz Simo et al. Phys. Lett.B762, 124 (2016)

MEC



T. Van Cuyck et al. PRC 94, 024611(2016)

NN SRC

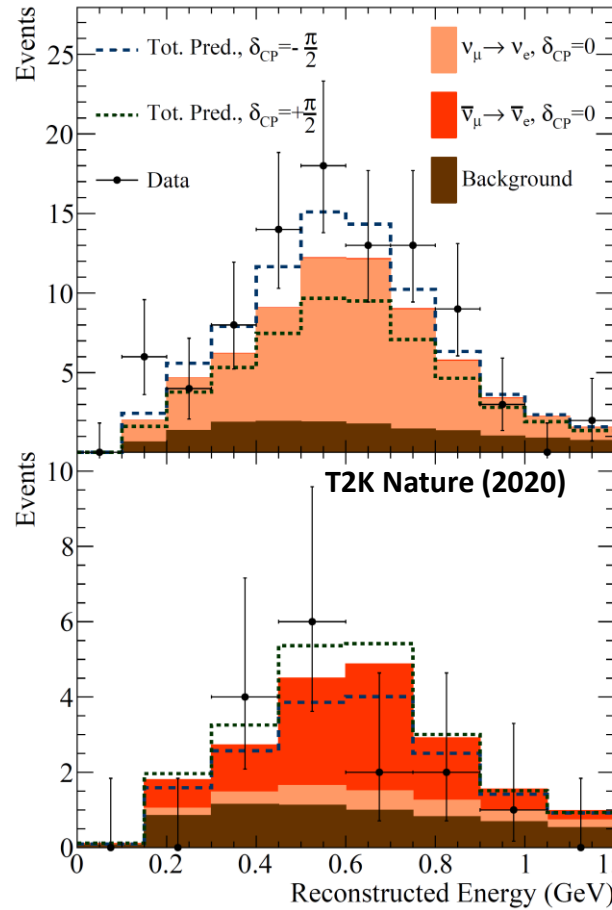
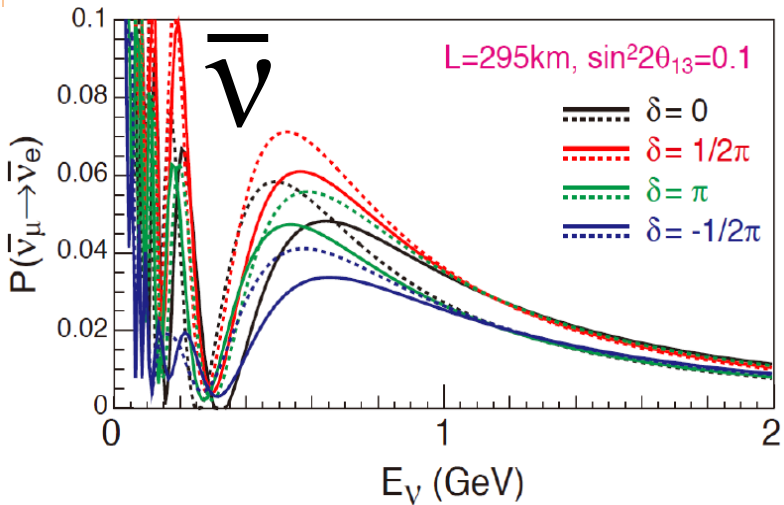
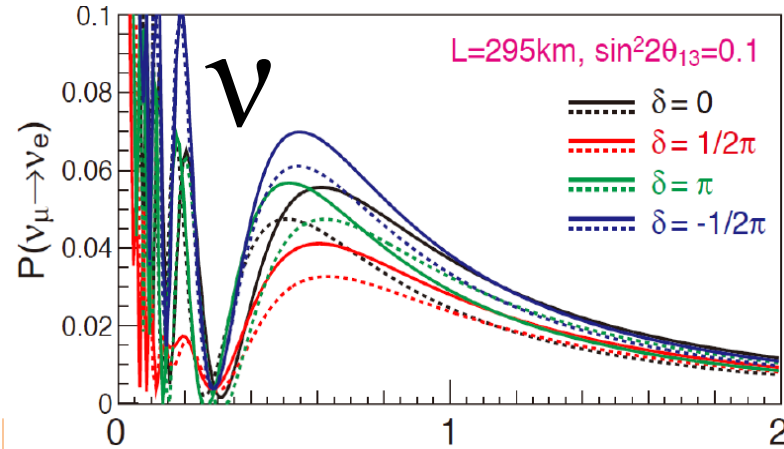


- The **pp** channel final state (**np** in the initial state) dominates in MEC and SRC
- The **pp/np** ratio depends on the kinematics

ν .vs. $\bar{\nu}$ and ν_{μ} .vs. ν_e

ν oscillation and CP violation

$$P(\nu_\mu \rightarrow \nu_e) \stackrel{?}{\neq} P(\bar{\nu}_\mu \rightarrow \bar{\nu}_e) \iff \delta_{\text{CP}}$$



$\nu_\mu \rightarrow \nu_e$

$\bar{\nu}_\mu \rightarrow \bar{\nu}_e$

A precise and simultaneous knowledge of the four cross sections is important in connection to the oscillation experiments aiming at the search for CP violation in the lepton sector.

Neutrino vs Antineutrino interactions

The ν and anti ν cross sections differ by the sign of the V-A interference term

$$\frac{d^2\sigma}{d\cos\theta d\omega} = \frac{G_F^2 \cos^2\theta_c |\mathbf{k}'| E_l' \cos^2\frac{\theta}{2}}{\pi} \left[\frac{(\mathbf{q}^2 - \omega^2)^2}{\mathbf{q}^4} G_E^2 R_\tau(\mathbf{q}, \omega) + \frac{\omega^2}{\mathbf{q}^2} G_A^2 R_{\sigma\tau(L)}(\mathbf{q}, \omega) \right. \\ \left. + 2 \left(\tan^2\frac{\theta}{2} + \frac{\mathbf{q}^2 - \omega^2}{2\mathbf{q}^2} \right) \left(G_M^2 \frac{\mathbf{q}^2}{4M_N^2} + G_A^2 \right) R_{\sigma\tau(T)}(\mathbf{q}, \omega) \pm 2 \frac{E_\nu + E_l'}{M_N} \tan^2\frac{\theta}{2} G_A G_M R_{\sigma\tau(T)}(\mathbf{q}, \omega) \right]$$

Vector-Axial interference

$$\begin{cases} + & (\nu) \\ - & (\bar{\nu}) \end{cases}$$

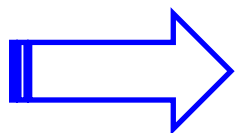
Vector-Axial interference:

basic asymmetry from weak interaction theory

different sign in the Leptonic tensor

$$L_{\mu\nu} = k_\mu k'_\nu + k_\nu k'_\mu - g_{\mu\nu} k \cdot k' \mp i\varepsilon_{\mu\nu\alpha\beta} k^\alpha k'^\beta$$

ν
 $\bar{\nu}$

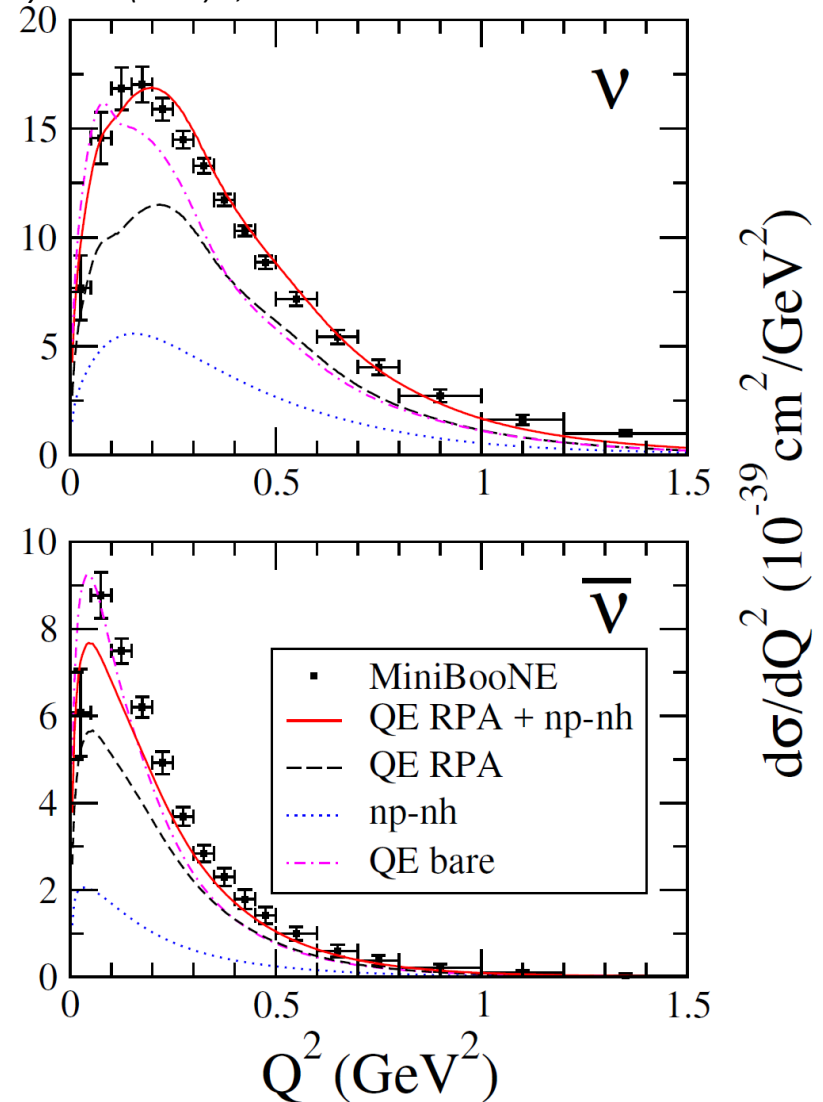
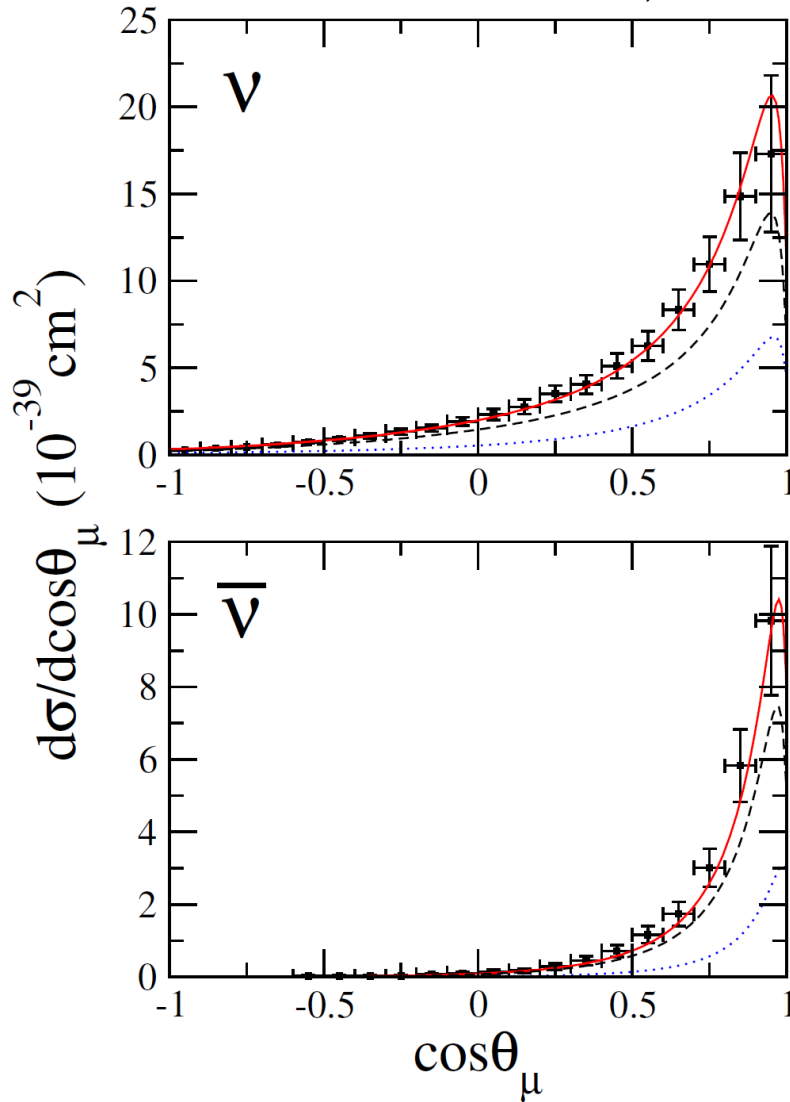


Even neglecting nuclear effects, the absolute value and the kinematic behavior of neutrino and antineutrino cross sections are different

$d\sigma/d\cos\theta$

Q^2 distribution

T. Katori, M. Martini, *J.Phys.G* 45 (2018) 1, 013001



- Antineutrino cross section falls more rapidly than the neutrino one
- Antineutrino Q^2 distribution peaks at smaller Q^2 values than the neutrino one

Neutrino vs Antineutrino interactions and nuclear effects

$$\frac{d^2\sigma}{d\cos\theta d\omega} = \frac{G_F^2 \cos^2\theta_c}{\pi} |\mathbf{k}'| E_l' \cos^2\frac{\theta}{2} \left[\frac{(\mathbf{q}^2 - \omega^2)^2}{\mathbf{q}^4} G_E^2 R_\tau(\mathbf{q}, \omega) + \frac{\omega^2}{\mathbf{q}^2} G_A^2 R_{\sigma\tau(L)}(\mathbf{q}, \omega) \right]$$

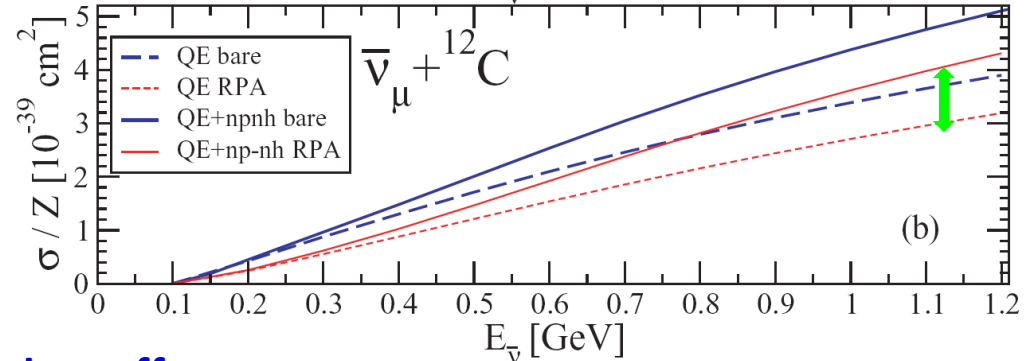
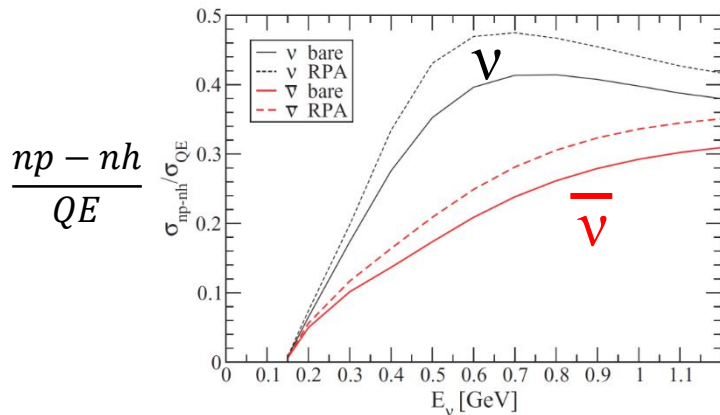
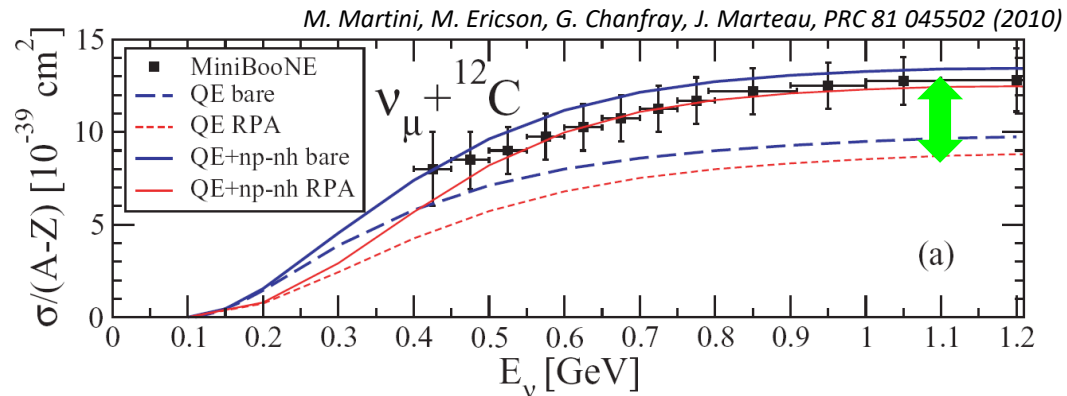
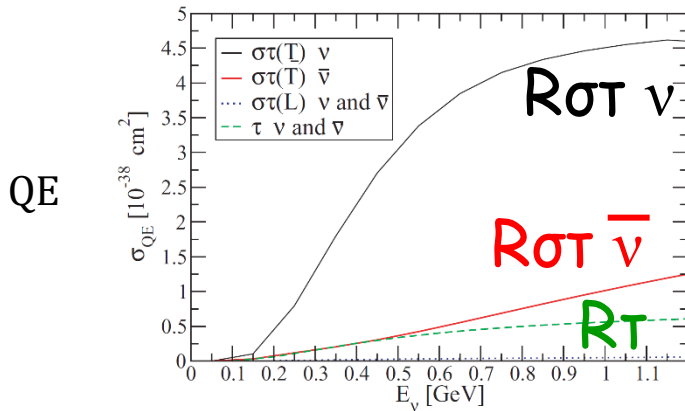
$$+ 2 \left(\tan^2\frac{\theta}{2} + \frac{\mathbf{q}^2 - \omega^2}{2\mathbf{q}^2} \right) \left(G_M^2 \frac{\mathbf{q}^2}{4M_N^2} + G_A^2 \right) R_{\sigma\tau(T)}(\mathbf{q}, \omega) \pm 2 \frac{E_\nu + E_l'}{M_N} \tan^2\frac{\theta}{2} G_A G_M R_{\sigma\tau(T)}(\mathbf{q}, \omega)$$

Vector-Axial interference

The ν and anti ν interactions differ by the sign of the V-A interference term

→ the relative weight of the different nuclear responses is different for neutrinos and antineutrinos

→ the relative role of np-nh contributions is different for neutrinos and antineutrinos



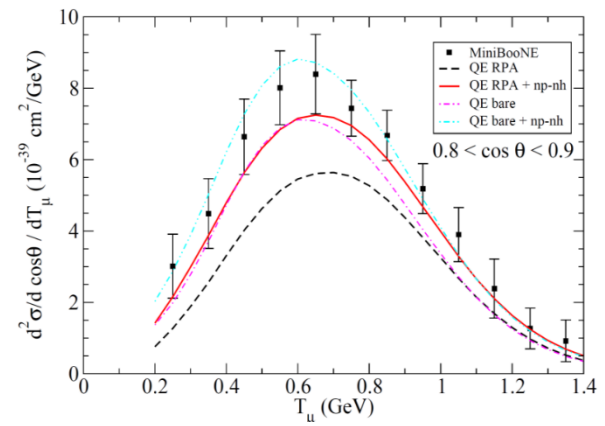
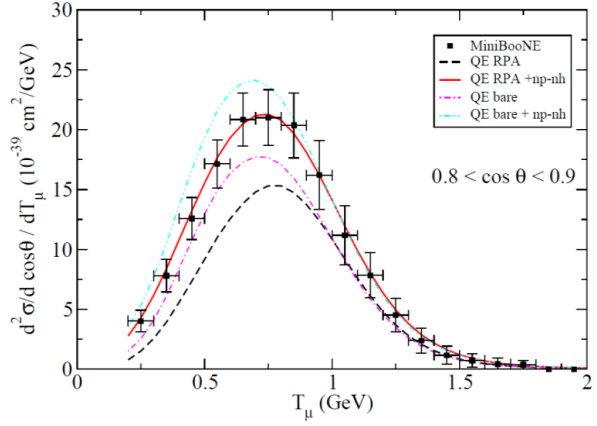
Nuclear effects generate an asymmetry unrelated to CP violation

The relative role of np-nh for neutrinos and antineutrinos is different in different approaches



Lyon RPA
Martini et al.

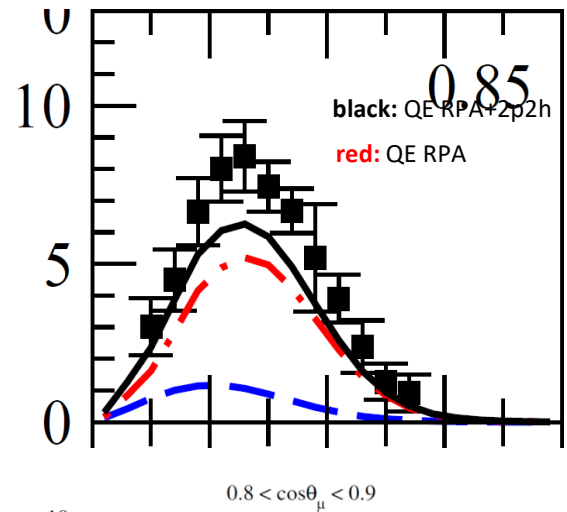
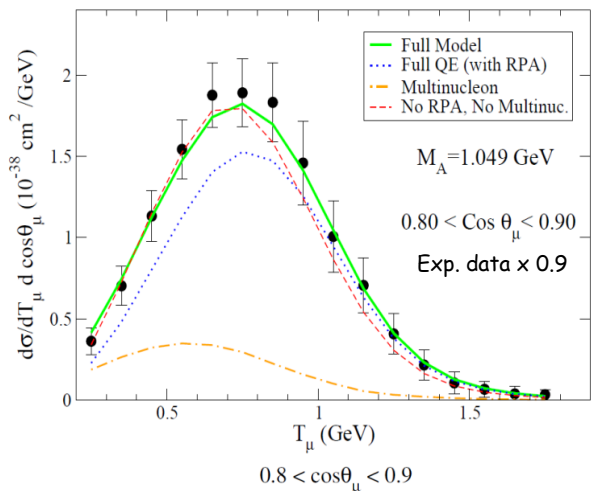
PRC 84 (2011)



PRC 87 (2013)

Valencia RPA
Nieves et al.

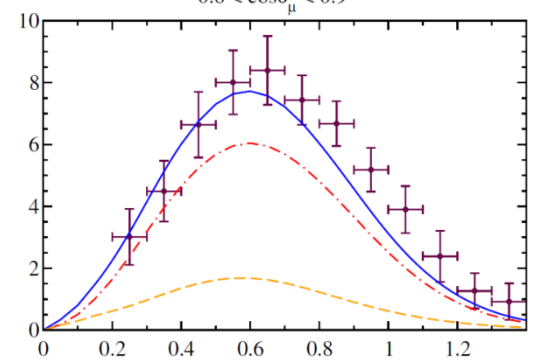
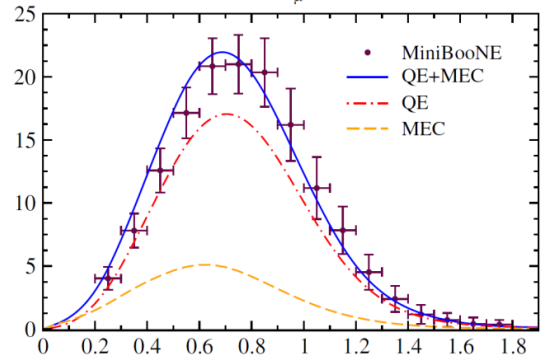
PLB 707 (2012)



PLB 721 (2013)

SuSAv2

PRD 94 (2016)



PRD 94 (2016)

Difference of ν and $\bar{\nu}$ cross sections and the VA interference term

$$d\sigma \sim d\sigma_L + d\sigma_T \pm d\sigma_{VA}$$

$$d\sigma_\nu - d\sigma_{\bar{\nu}} \overset{?}{\leftrightarrow} 2d\sigma_{VA}$$

Difference gives only the VA term for identical ν and $\bar{\nu}$ flux

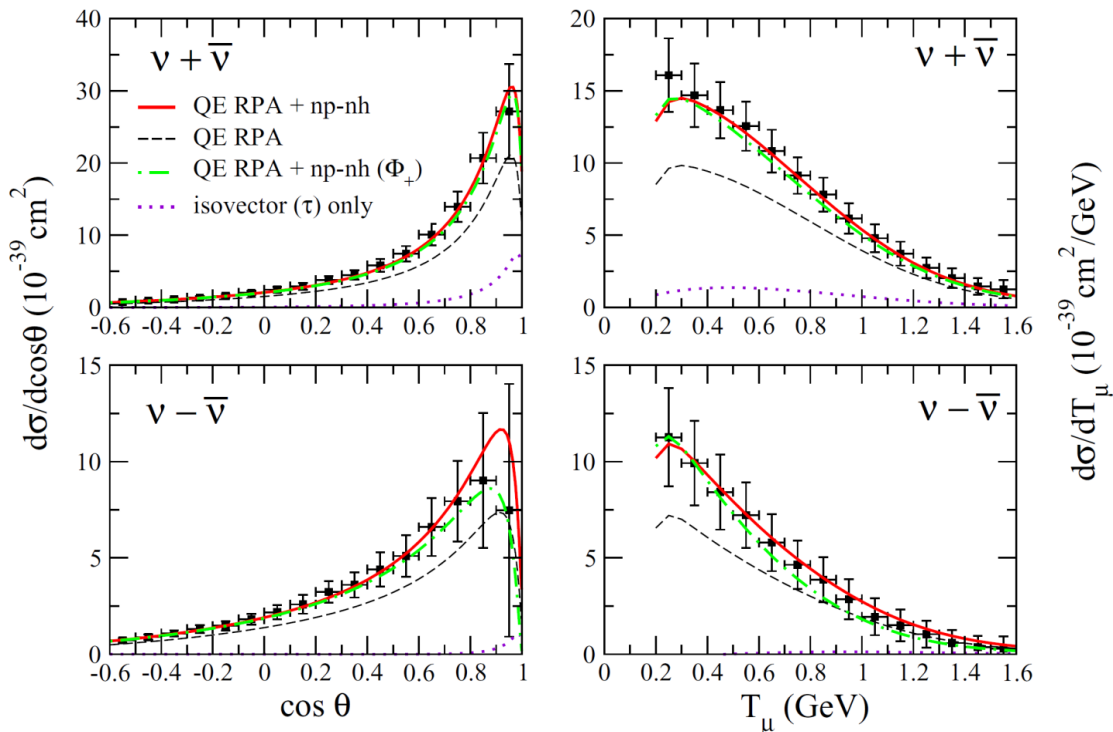
Problem: flux dependence of $d\sigma$ $\frac{d^2\sigma}{dE_\mu d\cos\theta} = \int dE_\nu \left[\frac{d^2\sigma}{d\omega d\cos\theta} \right]_{\omega=E_\nu-E_\mu} \Phi(E_\nu)$

We introduce the **mean flux**

$$\Phi_+ = 1/2[\Phi_\nu + \Phi_{\bar{\nu}}]$$

We calculate the sum and the difference using **real** and **mean** MiniBooNE fluxes results

M. Ericson, M. Martini *Phys. Rev. C* 91 035501 (2015)



The mean flux contribution is dominant



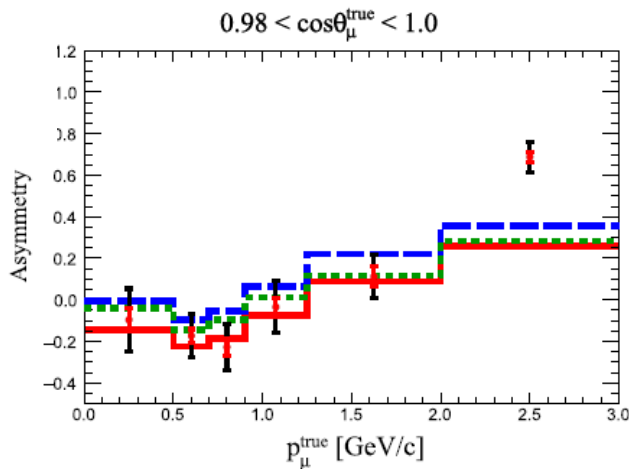
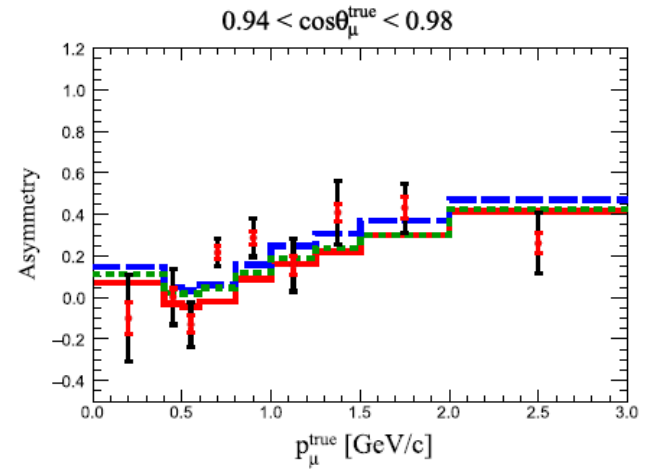
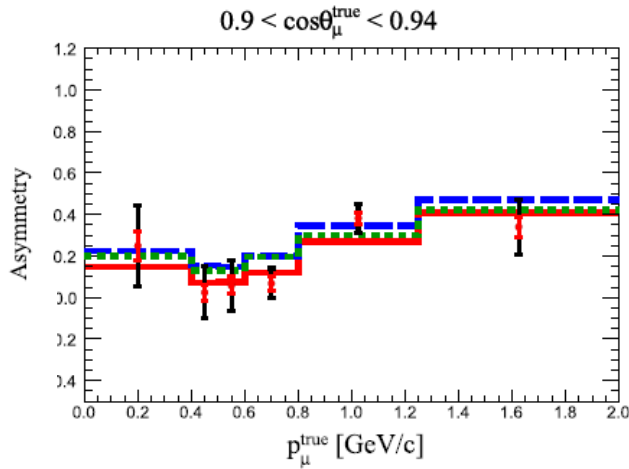
The VA interference term is experimentally accessible in MBdata








Need for the multinucleon component in the VA interference

First combined measurement of the muon neutrino and antineutrino charged-current cross section without pions in the final state at T2K

$$\frac{\nu - \bar{\nu}}{\nu + \bar{\nu}}$$

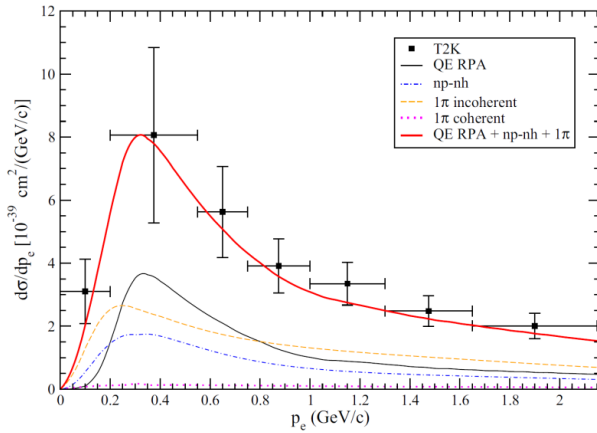


-  Total Uncertainty (stat+syst)
-  Systematic Uncertainty
-  NEUT LFG+2p2h $\chi^2 = 150.5(147.8)/58$
-  Martini et al. $\chi^2 = 93.9(131.2)/48$
-  SuSAv2 $\chi^2 = 152.6(146.3)/58$

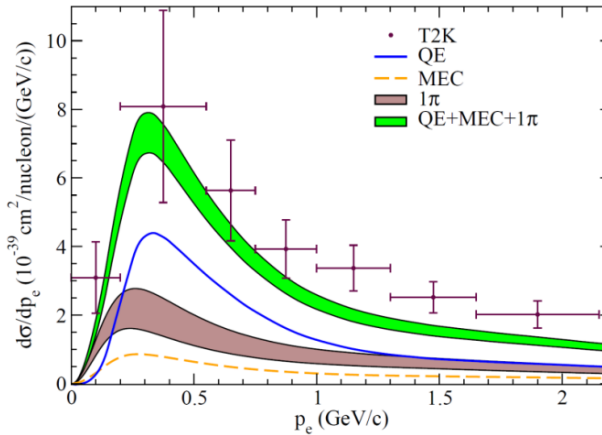
ν_e cross sections

- There are few published results on ν_e cross sections. This is essentially due the relatively small component of ν_e fluxes with respect to the ν_μ ones hence to small statistics.
- The ν_e experimental published results essentially concern inclusive cross sections
T2K flux-integrated ν_e CC inclusive differential cross sections on carbon

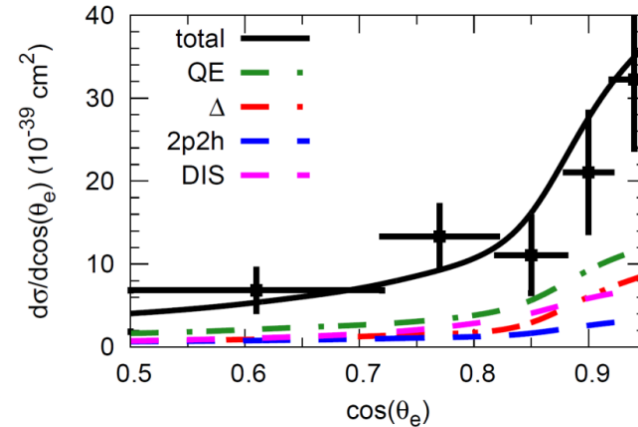
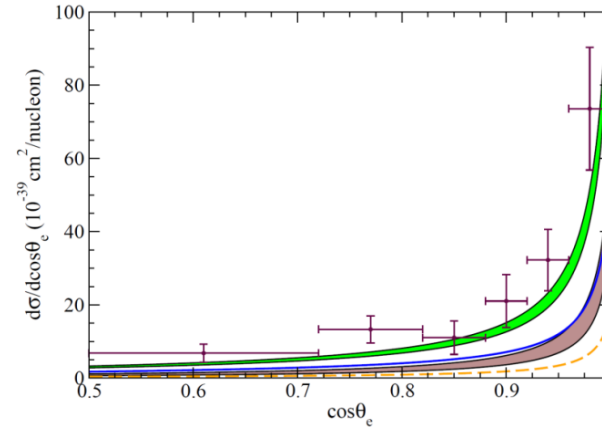
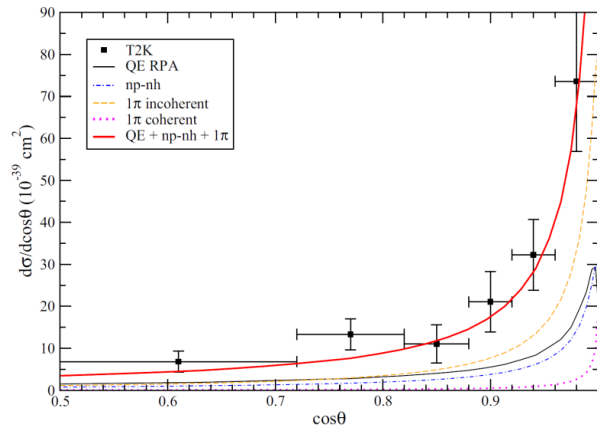
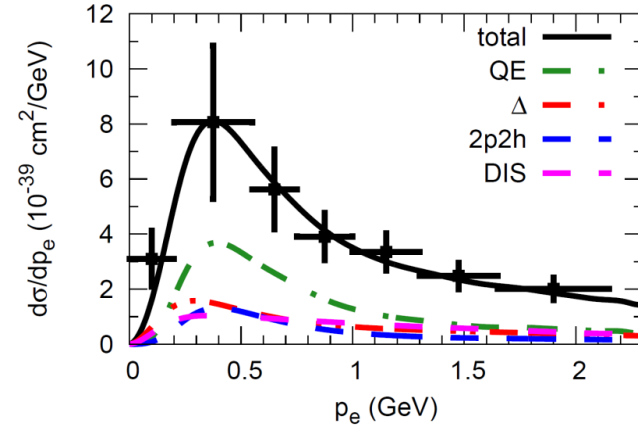
Martini et al., PRC 94 (2016)



Megias et al., PRD 94 (2016)

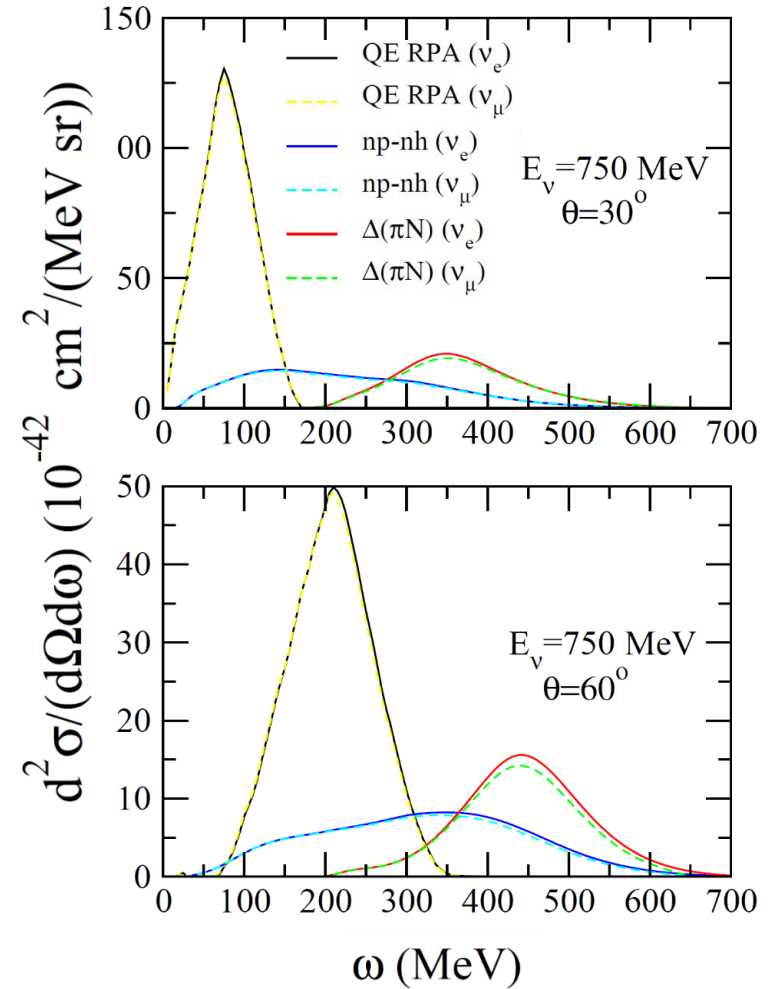
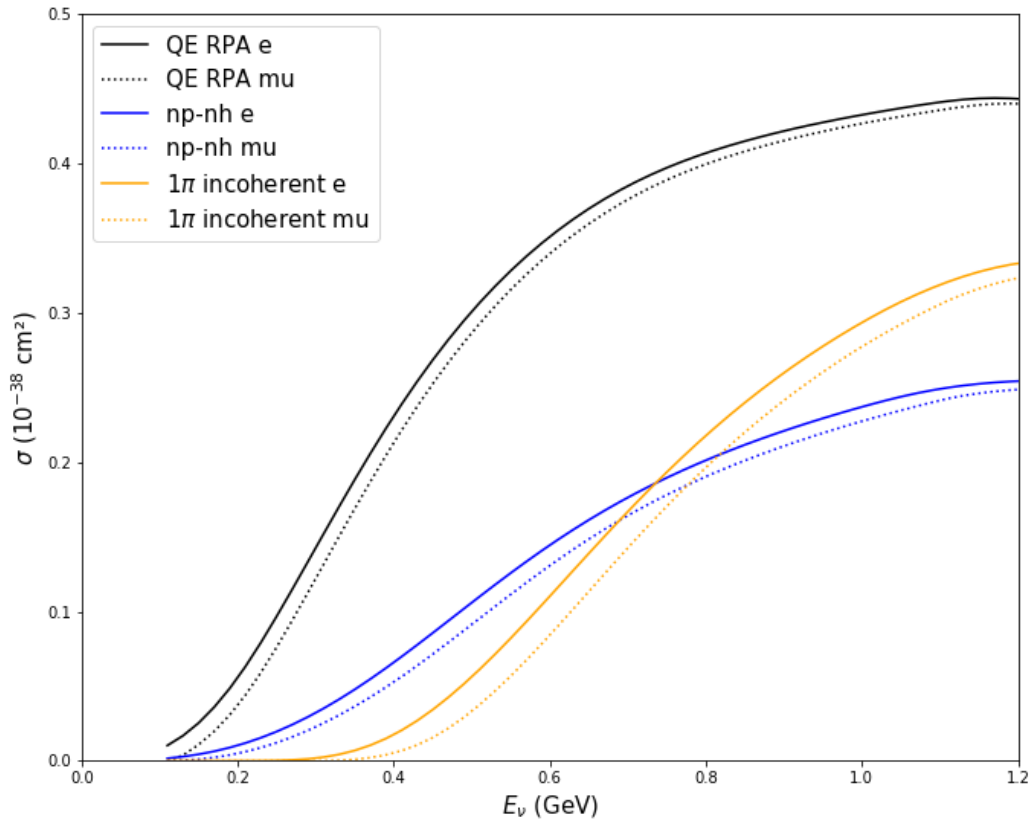


Gallmeister et al. PRC 94(2016)



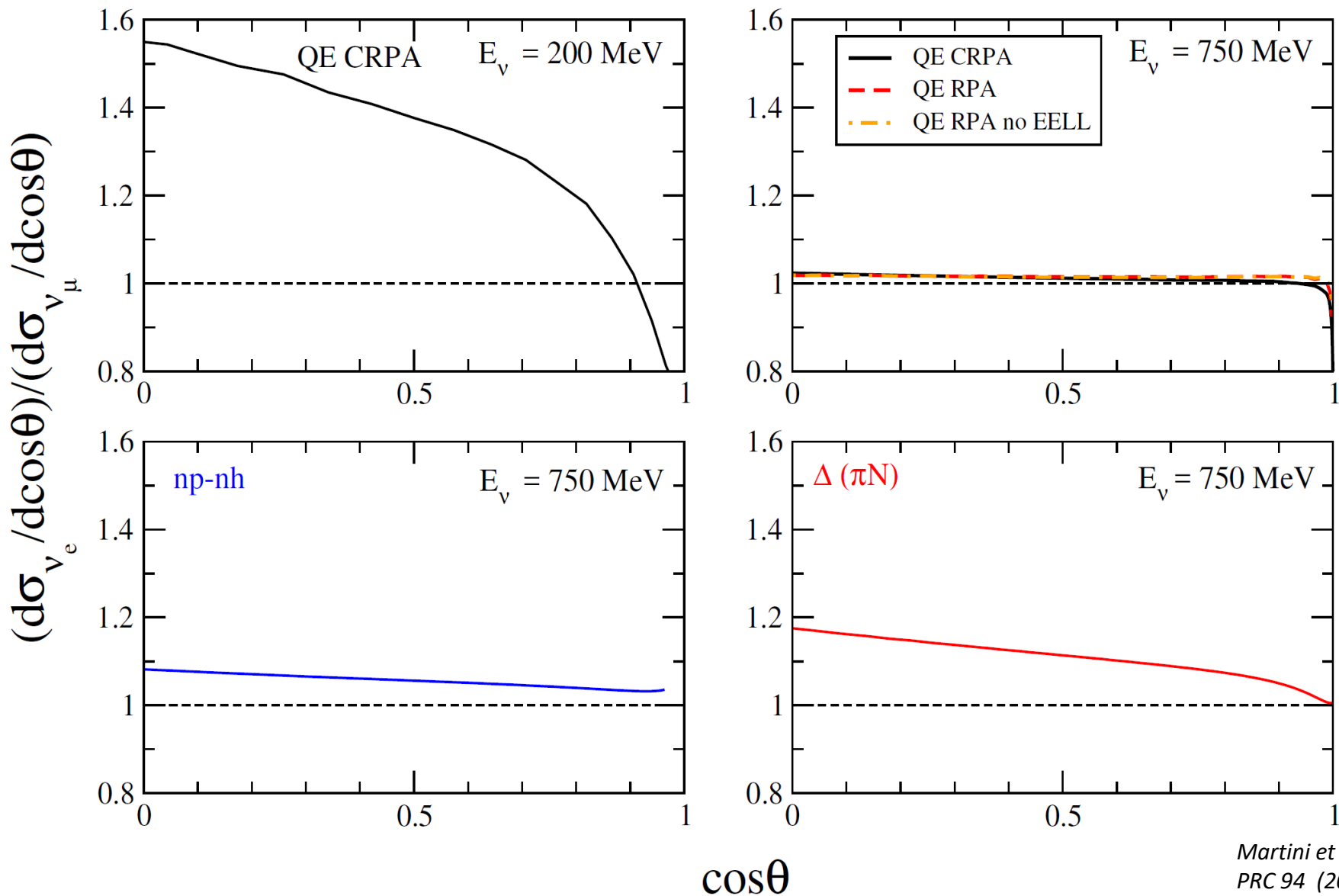
- Theoretical results agree with data
- Similarity of the theoretical results for the inclusive $d\sigma$

ν_e and ν_μ total and double differential cross sections



Due to the different kinematic limits, the ν_e cross sections are expected to be larger than the ν_μ ones

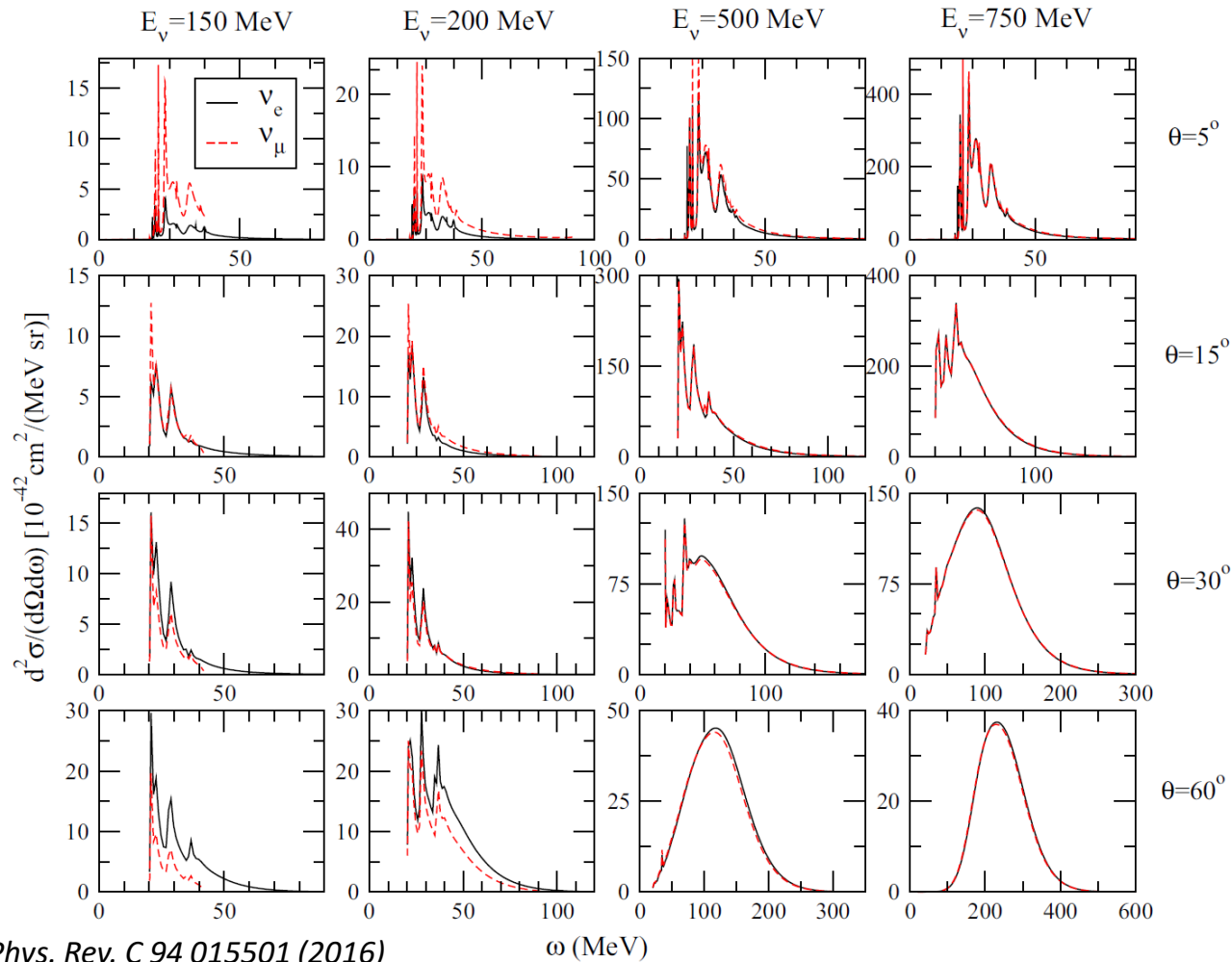
Ratio v_e/v_μ for $d\sigma/d\cos\theta$ in different channels



Martini et al.,
PRC 94 (2016)

Due to the different kinematic limits, the ν_e cross sections are expected to be larger than the ν_μ ones. However for forward scattering angles this hierarchy is opposite in the QE channel.

A theoretical study (HF+CRPA Ghent) of the ν_μ and ν_e $d^2\sigma$



M. Martini et al., Phys. Rev. C 94 015501 (2016)

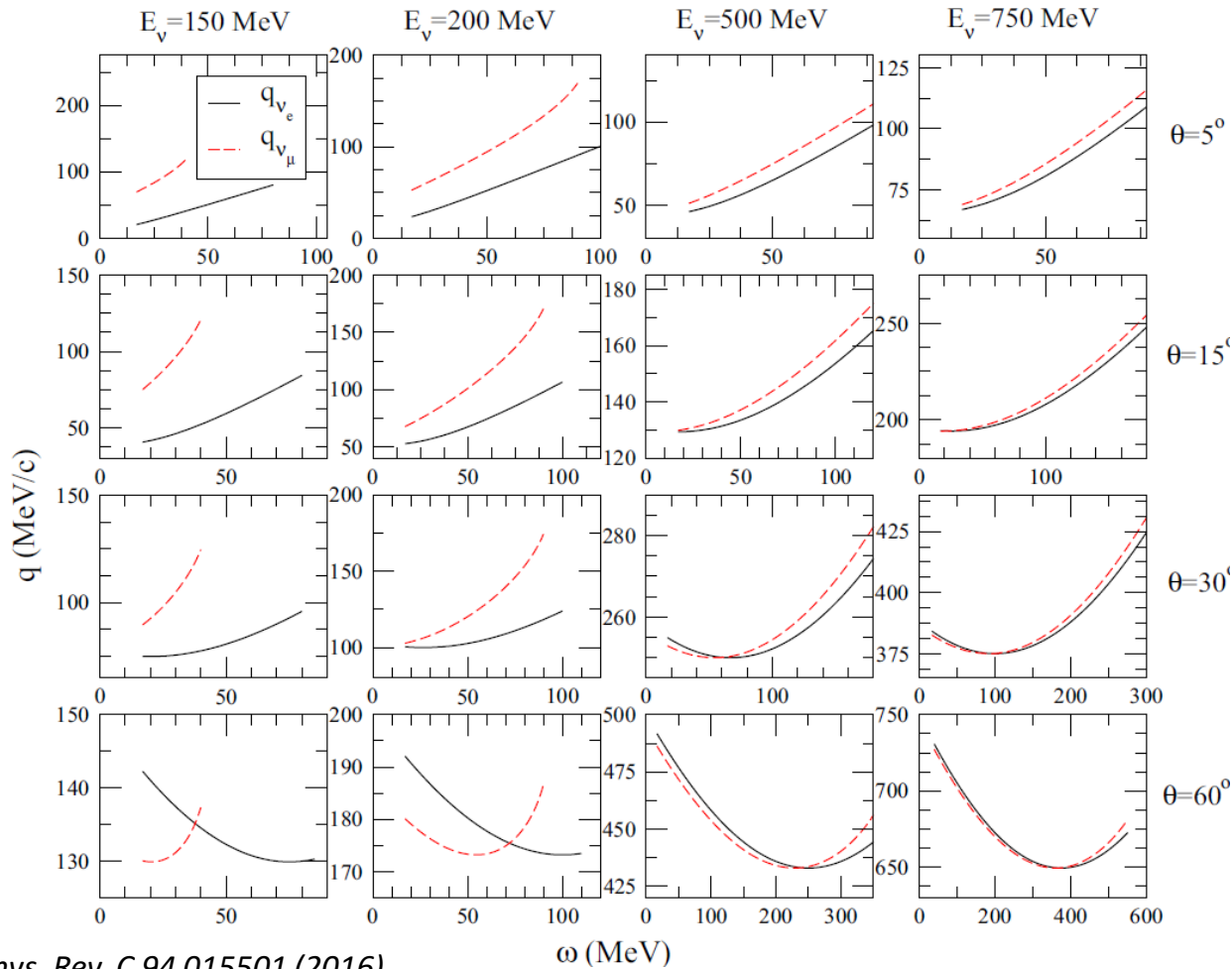
Due to the different kinematic limits, the ν_e cross sections are expected to be larger than the ν_μ ones. However for forward scattering angles this hierarchy is opposite.

The only difference between ν_μ and ν_e cross sections is the mass of the outgoing lepton.

But the mass affects the three momentum transfer which enters into the kinematics as well as the dynamics of the nuclear model

Momentum transfer q versus transferred energy ω for ν_μ and ν_e $d^2\sigma$

Kinematical conditions of the previous slide



M. Martini et al., Phys. Rev. C 94 015501 (2016)

$$q^2 = E_\nu^2 + p_l^2 - 2E_\nu p_l \cos \theta$$

$$p_l^2 = E_l^2 - m_l^2 = (E_\nu - \omega)^2 - m_l^2$$

The only difference between ν_μ and ν_e cross sections is the mass of the outgoing lepton. But the mass affects the three-momentum transfer which enters into the kinematics as well as the dynamics of the nuclear model

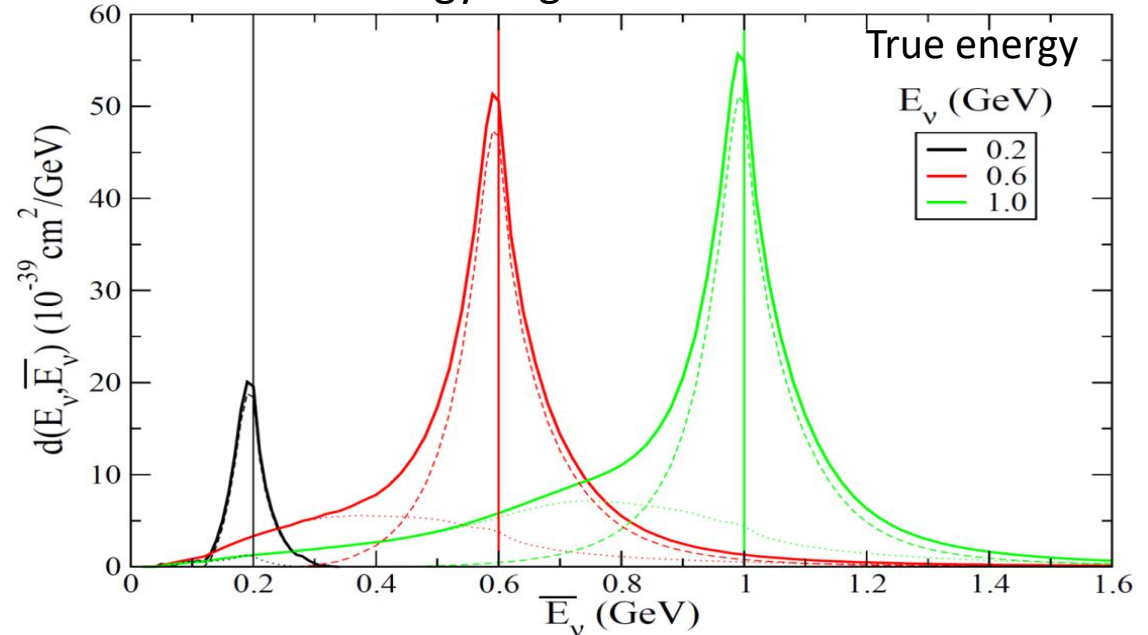
From true neutrino energy to reconstructed neutrino energy

$$D_{rec}(\bar{E}_\nu) = \int dE_\nu \Phi(E_\nu) \int_{E_l^{min}}^{E_l^{max}} dE_l \frac{ME_l - m_l^2/2}{\bar{E}_\nu^2 P_l} \left[\frac{d^2\sigma}{d\omega d\cos\theta} \right]_{\omega=E_\nu-E_l, \cos\theta=\cos\theta(E_l, \bar{E}_\nu)}$$

v energy migration matrix

The quantity $D_{rec}(\bar{E}_\nu)$ corresponds to the product $\sigma(E_\nu)\Phi(E_\nu)$ but in terms of reconstructed neutrino energy

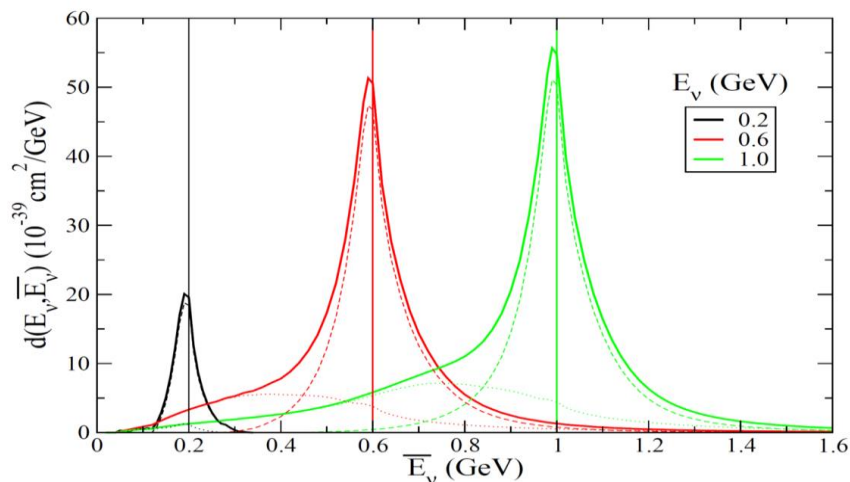
M. Martini, M. Ericson, G. Chanfray
 - *Phys. Rev. D* 85 093012 (2012)
 - *Phys. Rev. D* 87 013009 (2013)



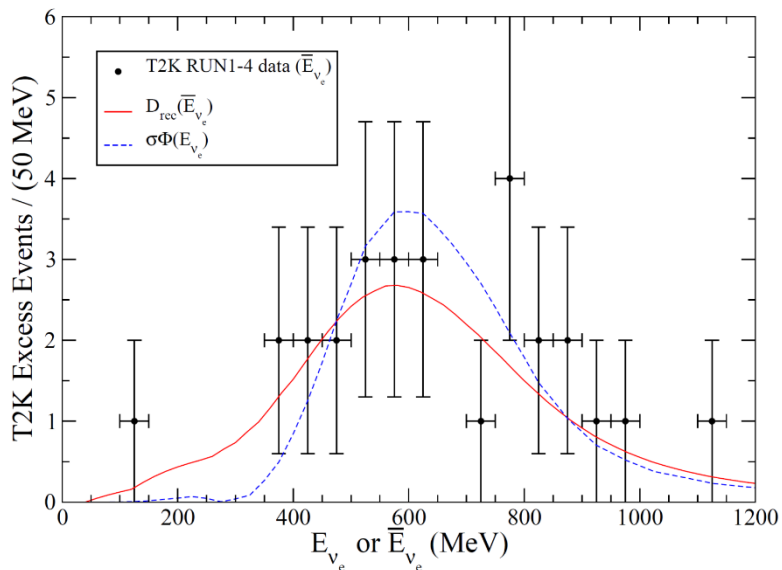
- Distributions not symmetrical around E_ν
- Crucial role of np-nh: low energy tail

QE-based neutrino energy reconstruction and neutrino oscillations

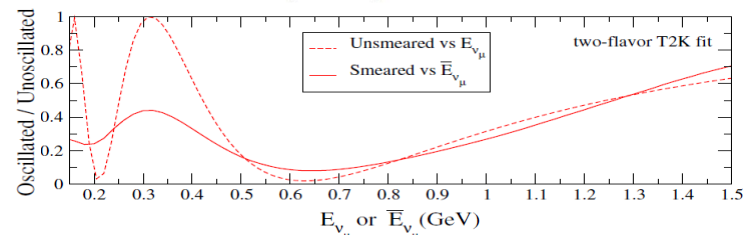
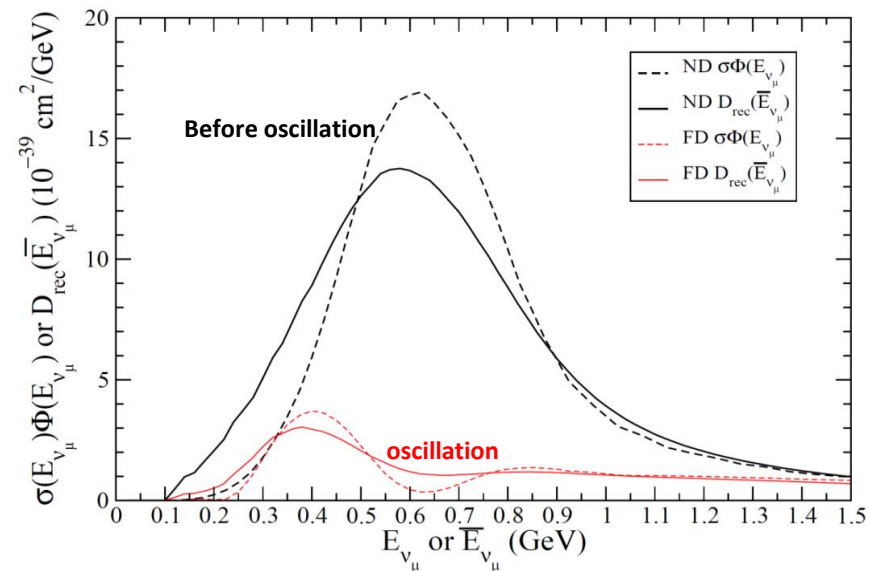
ν_e energy migration matrix



ν_e appearance T2K



ν_{μ} disappearance T2K



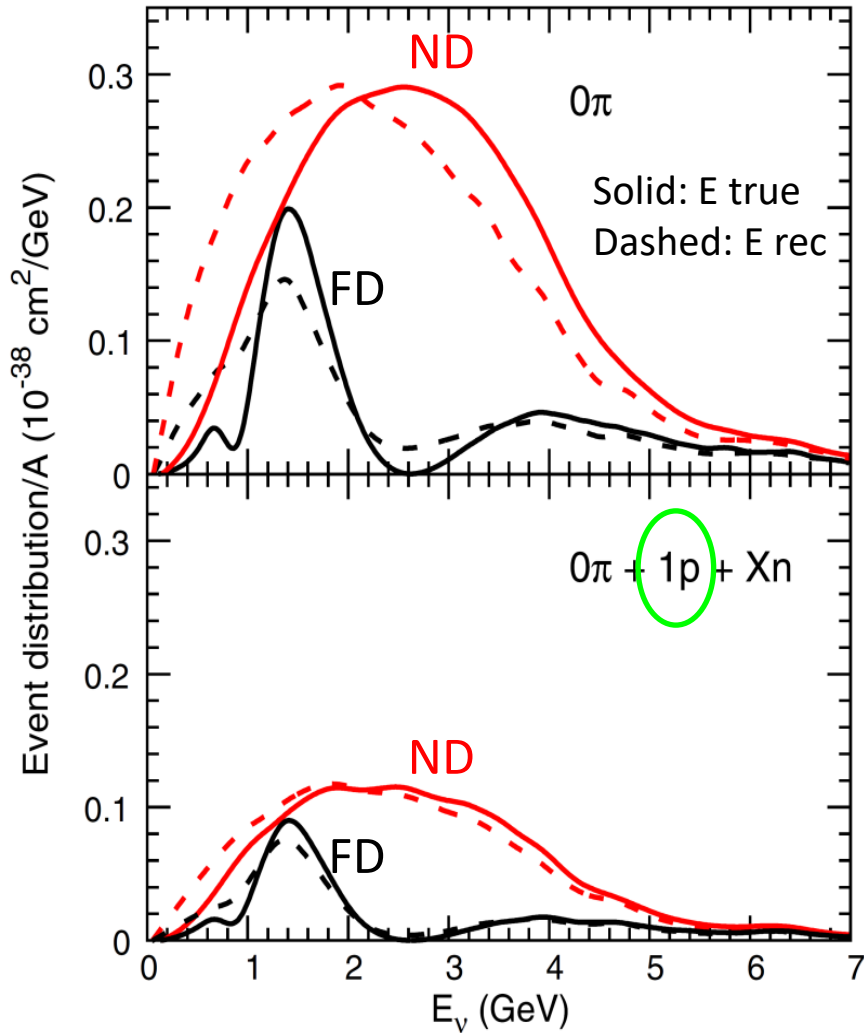
M. Martini, M. Ericson, G. Chanfray
Phys. Rev. D 85 093012 (2012); Phys. Rev. D 87 013009 (2013)

Similar results in:
Nieves et al. PRD 85 113008 (2012);
Lalakulich et al. PRC 86 054606 (2012)

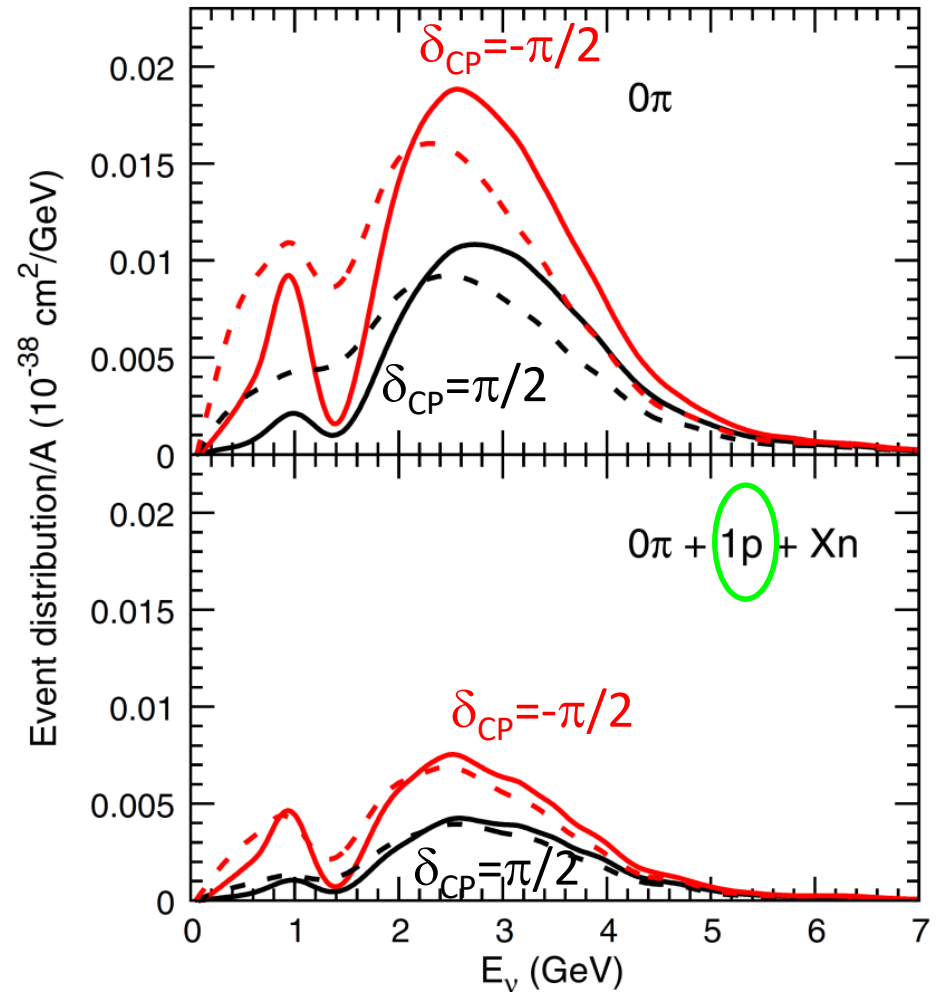
Neutrino energy reconstruction and neutrino oscillation analysis are affected by np-nh

QE-based E_ν reconstruction using proton information

ν_μ disappearance in DUNE



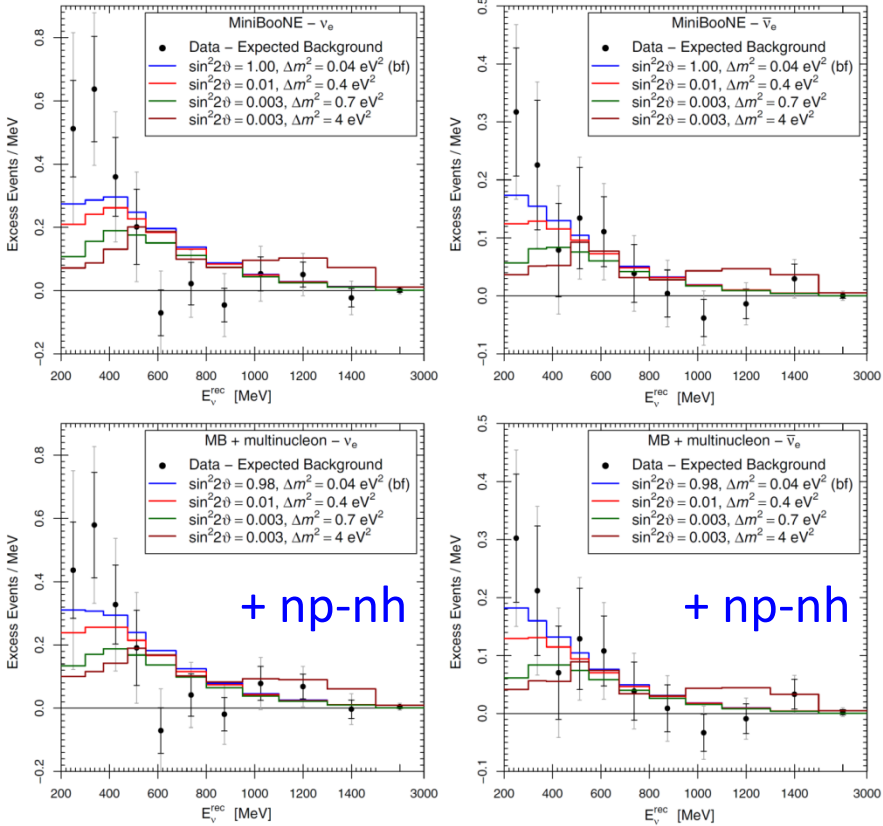
ν_e appearance in DUNE



Major improvement in $0\pi + 1p + Xn$ sample, events down by only factor 3

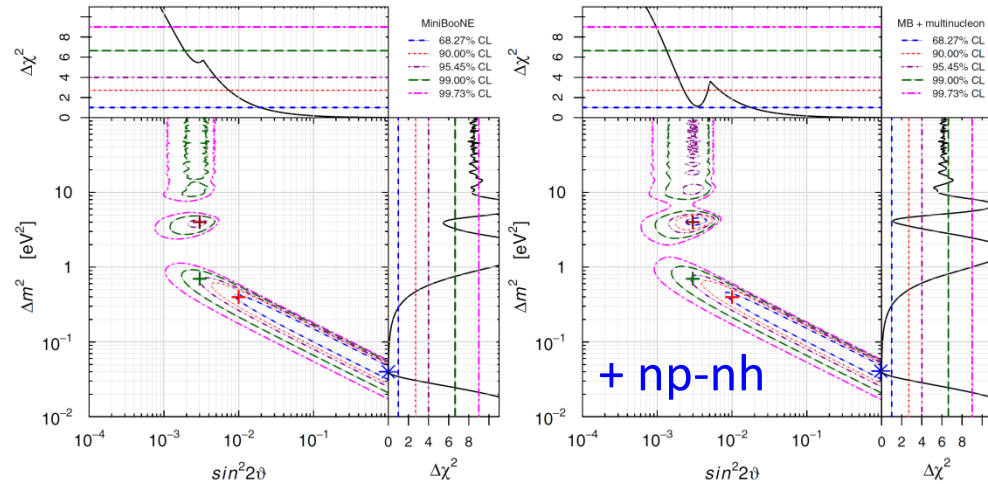
The role of np-nh in the $\nu_\mu \rightarrow \nu_e$ MiniBooNE low-energy anomaly

Quantitative analysis

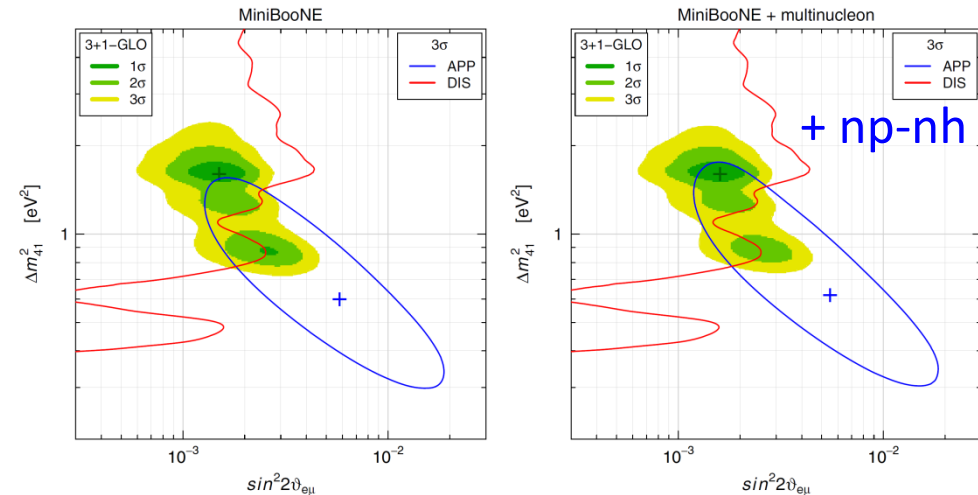


Taking into account np-nh allows a slightly better fit of the MiniBooNE low-energy excess

M.Ericson, M.V.Garzelli, C.Giunti, M.Martini, Phys. Rev. D 93, 073008 (2016)

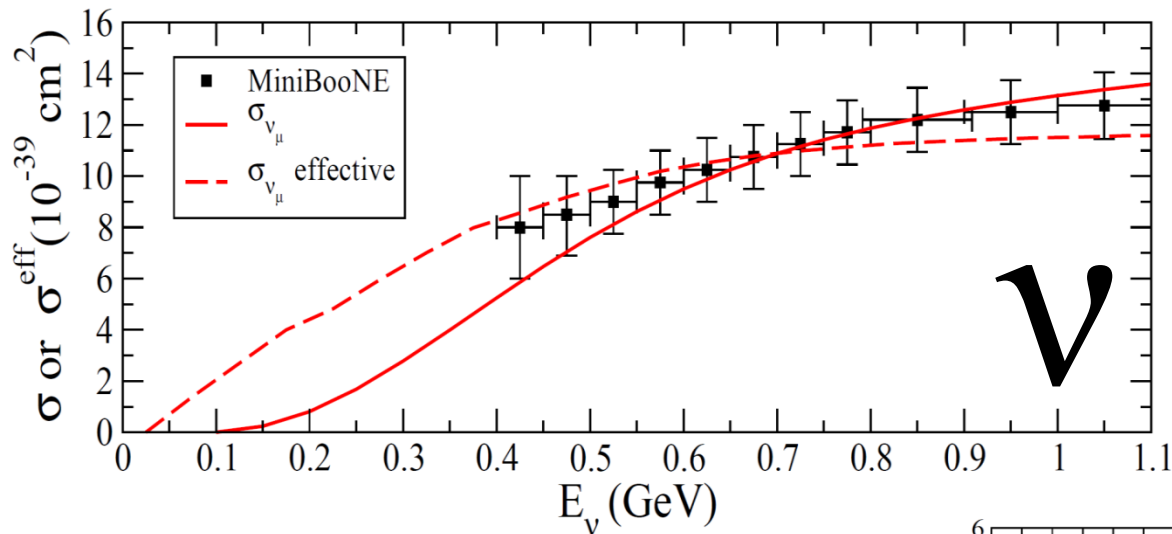


Taking into account np-nh induces a shift of the allowed region towards smaller values of $\sin^2 2\theta$ and larger values of Δm^2 in the framework of 2ν oscillations

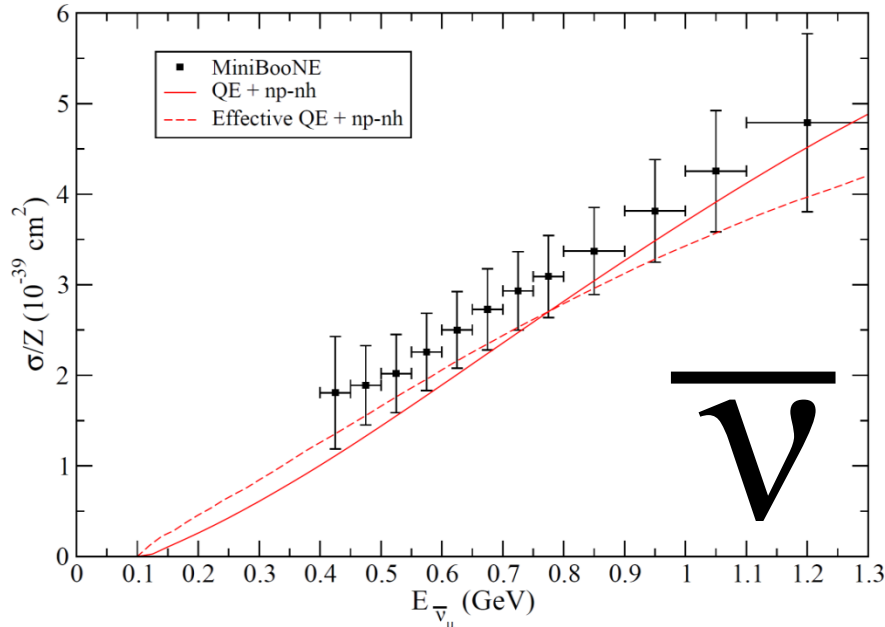


Taking into account np-nh leads to a decrease of the appearance-disappearance tension but not enough to solve the problem in the global fit of short-baseline ν oscillation data

CCQE-like cross sections as a function of real (continuous line) and reconstructed (dashed line) neutrino energy

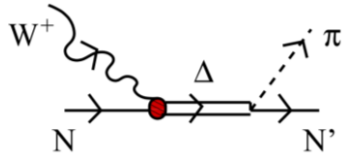


M. Martini, M. Ericson, G. Chanfray, *Phys. Rev. D* 87 013009 (2013)

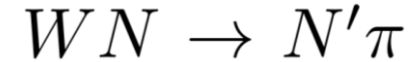


Martini, Ericson, *Phys. Rev. C* 87 065501 (2013)

The 1π production via $\Delta(1232)$ resonance excitation and decay



At energies of our interest, it is the dominant mechanism of the reaction



E. Hernandez et al. Phys. Rev. D 76, 033005 (2007)

$$W^+ n \rightarrow \Delta^+ \quad \text{Hadron matrix element} \quad \langle \Delta^+; p_\Delta = p + q | j_{cc+}^\mu(0) | n; p \rangle = \bar{u}_\alpha(\vec{p}_\Delta) \Gamma^{\alpha\mu}(p, q) u(\vec{p}) \cos \theta_C$$

Electroweak vertex

$$\Gamma^{\alpha\mu}(p, q) = \left[\frac{C_3^V}{M} (g^{\alpha\mu} \not{q} - q^\alpha \gamma^\mu) + \frac{C_4^V}{M^2} (g^{\alpha\mu} q \cdot p_\Delta - q^\alpha p_\Delta^\mu) + \frac{C_5^V}{M^2} (g^{\alpha\mu} q \cdot p - q^\alpha p^\mu) + C_6^V g^{\mu\alpha} \right] \gamma_5$$

$$+ \left[\frac{C_3^A}{M} (g^{\alpha\mu} \not{q} - q^\alpha \gamma^\mu) + \frac{C_4^A}{M^2} (g^{\alpha\mu} q \cdot p_\Delta - q^\alpha p_\Delta^\mu) + C_5^A g^{\alpha\mu} + \frac{C_6^A}{M^2} q^\mu q^\alpha \right], \quad p_\Delta = p + q$$

Vector form factors $C_{3,4,5,6}^V$ can be extracted from single-pion electro-production data

Axial form factors $C_{3,4,5,6}^A$ $C_5^A(Q^2) = \frac{C_5^A(0)}{(1 + Q^2/M_{A\Delta}^2)^2}$ $C_6^A = M^2/(m_\pi^2 + Q^2) \cdot C_5^A$ PCAC $C_4^A = -1/4 \cdot C_5^A$ Adler C_3^A Small, usually neglected

Δ propagator

$$G^{\mu\nu}(p_\Delta) = \frac{P^{\mu\nu}(p_\Delta)}{p_\Delta^2 - M_\Delta^2 + iM_\Delta\Gamma_\Delta}$$

Spin 3/2 projection operator

$$P^{\mu\nu}(p_\Delta) = -(\not{p}_\Delta + M_\Delta) \left[g^{\mu\nu} - \frac{1}{3} \gamma^\mu \gamma^\nu - \frac{2}{3} \frac{p_\Delta^\mu p_\Delta^\nu}{M_\Delta^2} + \frac{1}{3} \frac{p_\Delta^\mu \gamma^\nu - p_\Delta^\nu \gamma^\mu}{M_\Delta} \right]$$

$N\Delta\pi$ coupling

$$\mathcal{L}_{\pi N \Delta} = \frac{f^*}{m_\pi} \bar{\Psi}_\mu \vec{T}^\dagger (\partial^\mu \vec{\phi}) \Psi + \text{h.c.}$$

Pion puzzle – Tension 2016 Workshop

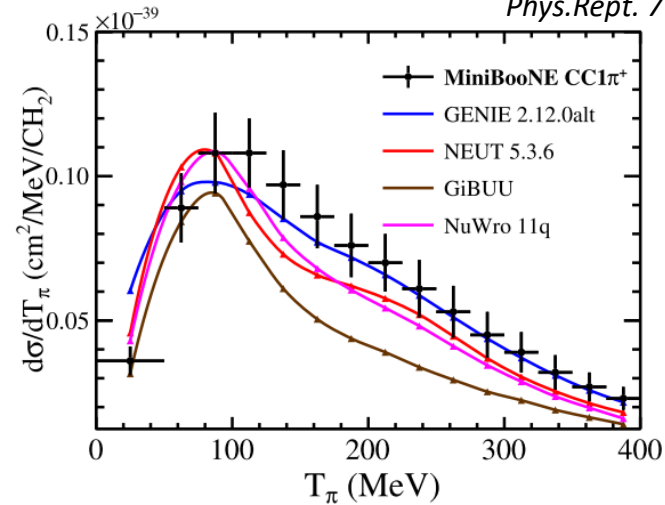
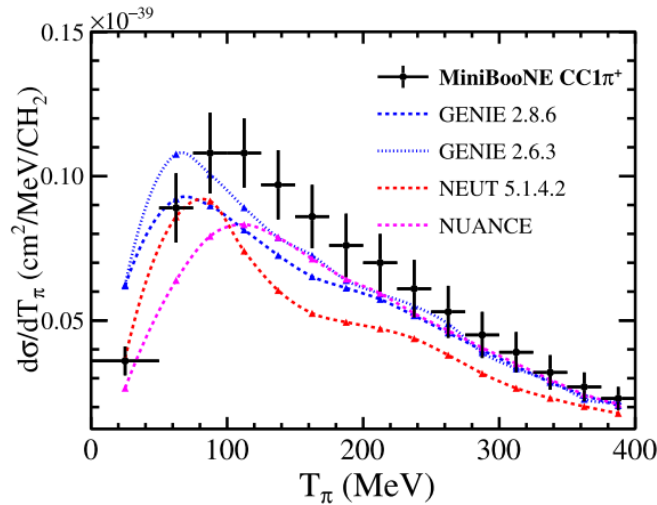
Old

New (after Tension)

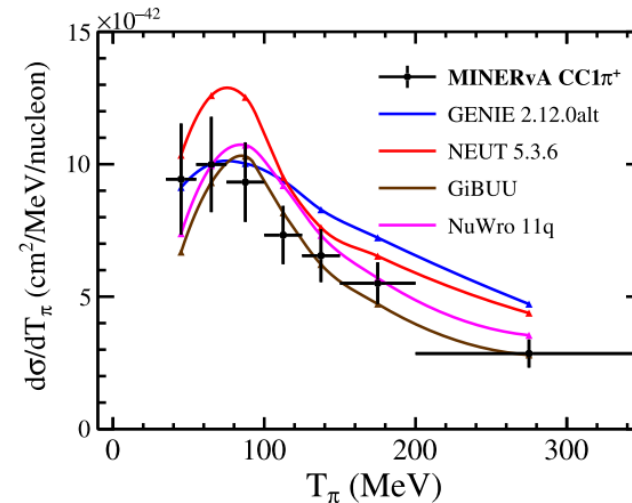
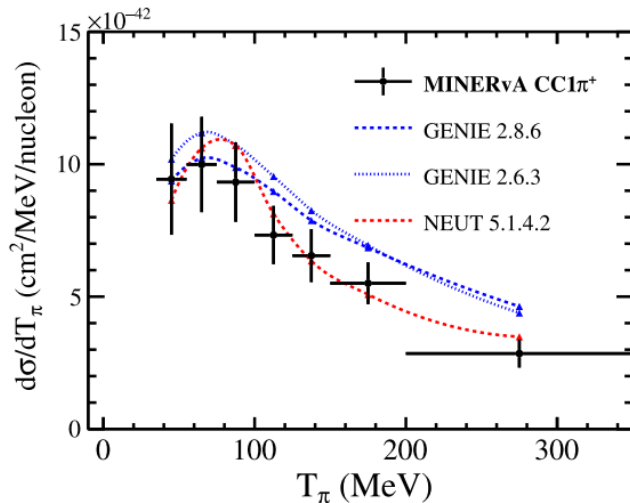
M. Betancourt et al.

Phys.Rept. 773-774 (2018) 1-28

MiniBooNE



MINERVA



- Same models, correct signal definition, proper flux averaging
- Updated flux prediction from MINERVA

Better normalization agreement but shape discrepancies remain

Pion puzzle – Tuning GENIE with MINERvA data (2019)

P. Stowell et al. PRD 100 (2019) 7, 072005

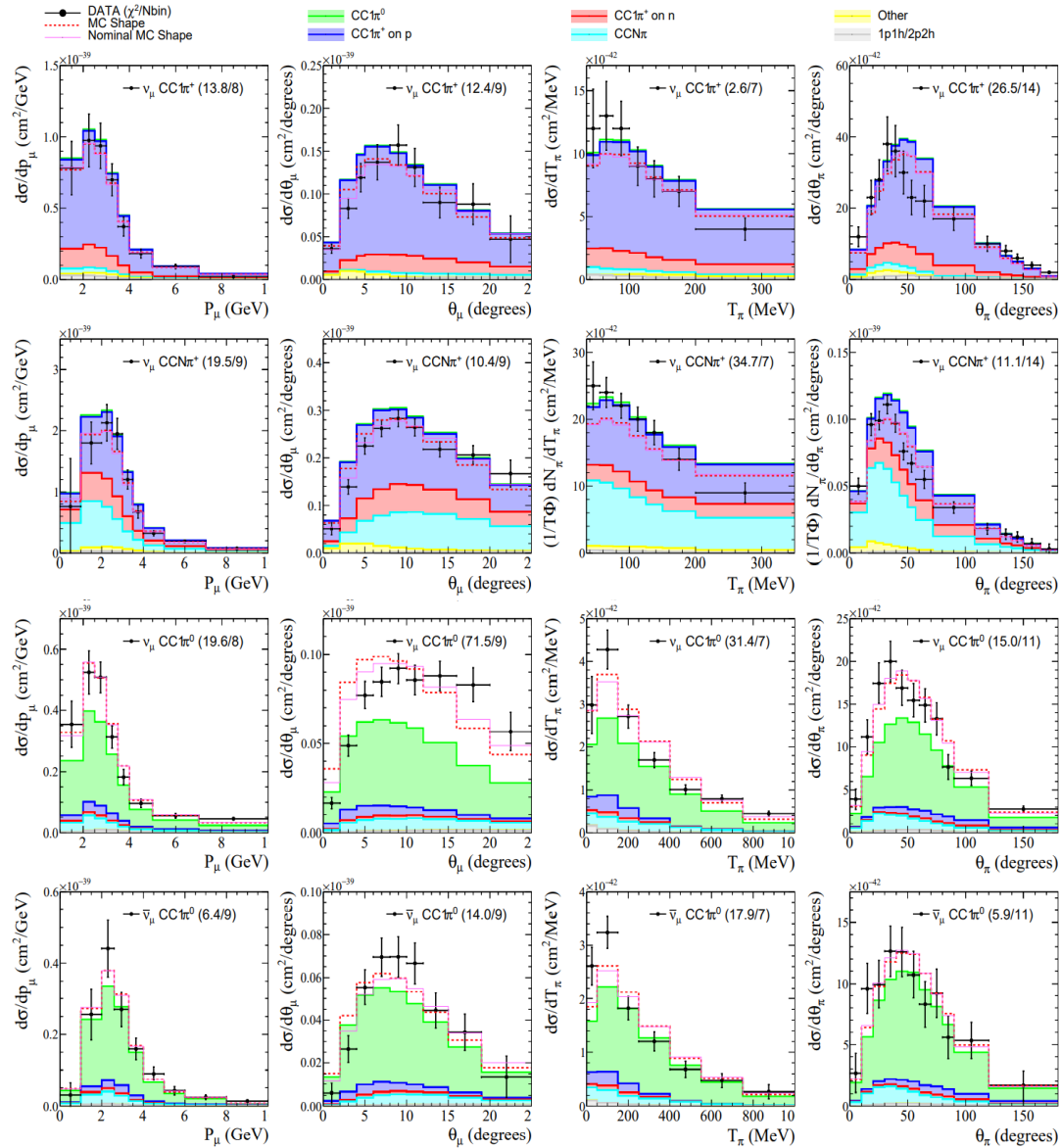
Tune Monte Carlo to simultaneously fit 4 datasets

$$\nu_{\mu} CC1\pi^{+}$$

$$\nu_{\mu} CCN\pi^{+}$$

$$\nu_{\mu} CC1\pi^{0}$$

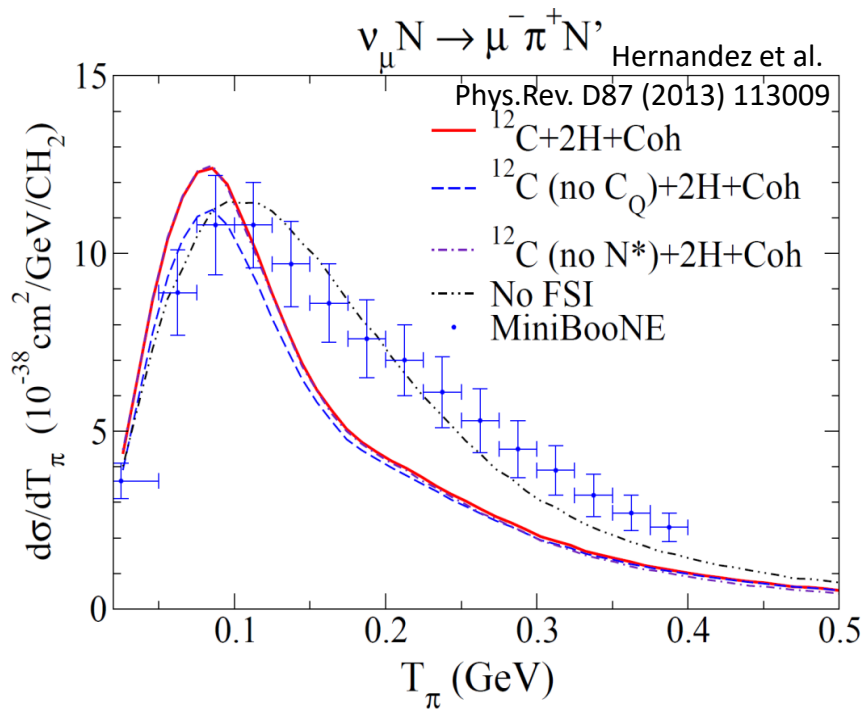
$$\bar{\nu}_{\mu} CC1\pi^{0}$$



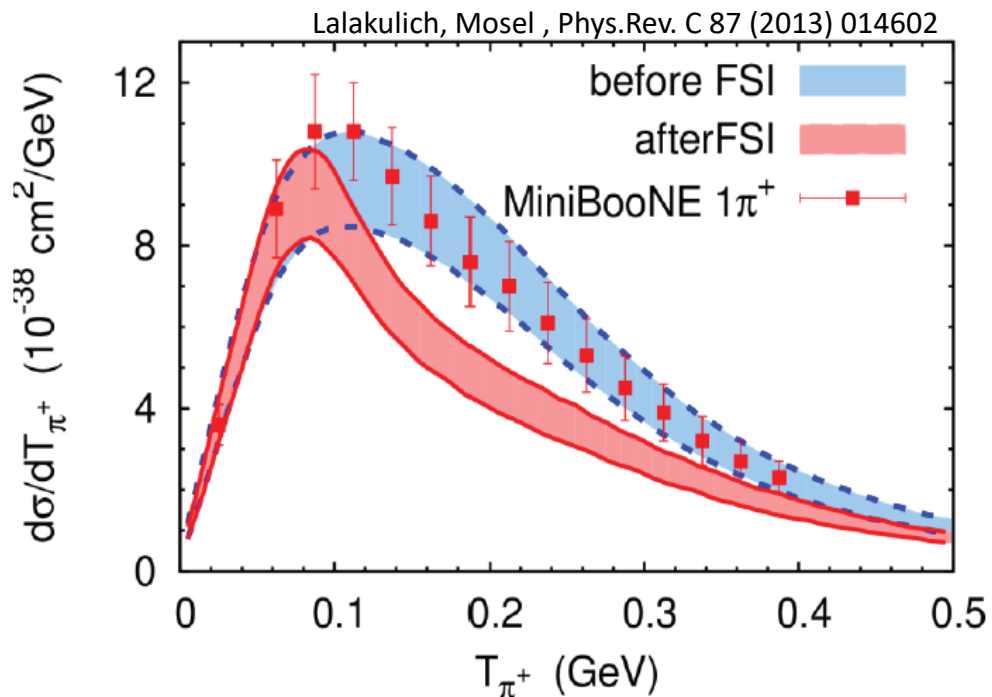
The tuning improves the model, but tensions remain

1 Pion production controversy

Best theories (with Δ medium effects and pion rescattering) do not agree with pion KE spectrum



Valencia



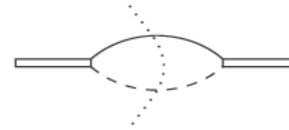
GiBUU

Data prefer calculations with no Final State Interaction for the pion

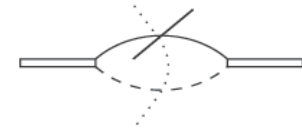
Delta in the nuclear medium

Mass

$$\tilde{M}_\Delta = M_\Delta + 40(\text{MeV}) \frac{\rho}{\rho_0}$$



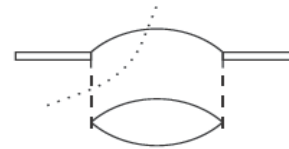
$\Delta \rightarrow \pi N$



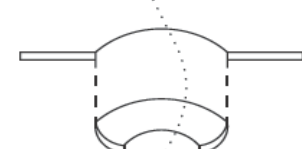
Pauli correction (F_P)

Width

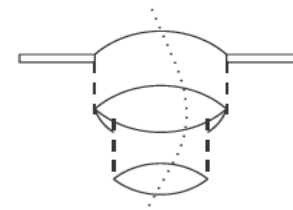
$$\tilde{\Gamma}_\Delta = \Gamma_\Delta F_P - 2\text{Im}(\Sigma_\Delta)$$



Pion distortion (C_Q)



2p-2h



3p-3h

Self energy

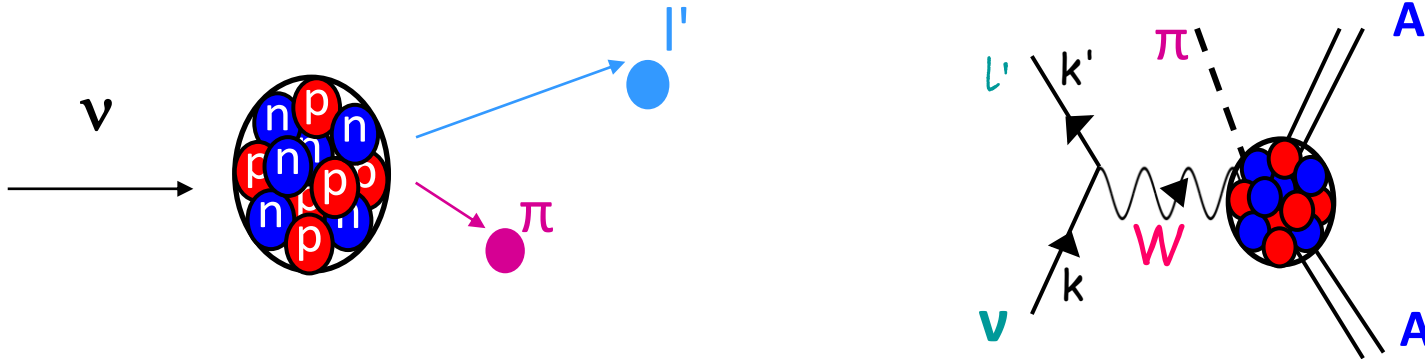
$$\text{Im}(\Sigma_\Delta(\omega)) = - \left[C_Q \left(\frac{\rho}{\rho_0} \right)^\alpha + C_{2p2h} \left(\frac{\rho}{\rho_0} \right)^\beta + C_{3p3h} \left(\frac{\rho}{\rho_0} \right)^\gamma \right]$$

E. Oset and L. L. Salcedo, Nucl. Phys. A 468, 631 (1987)

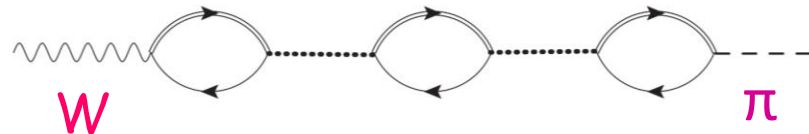
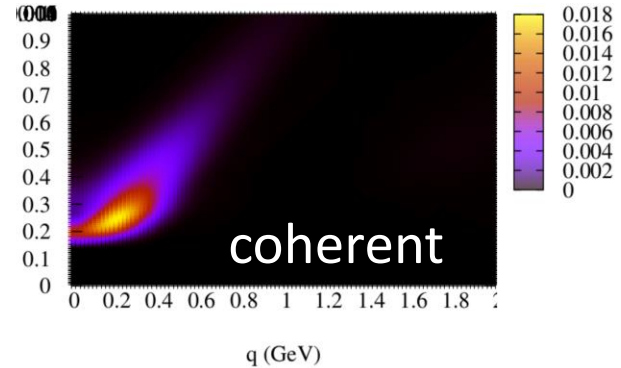
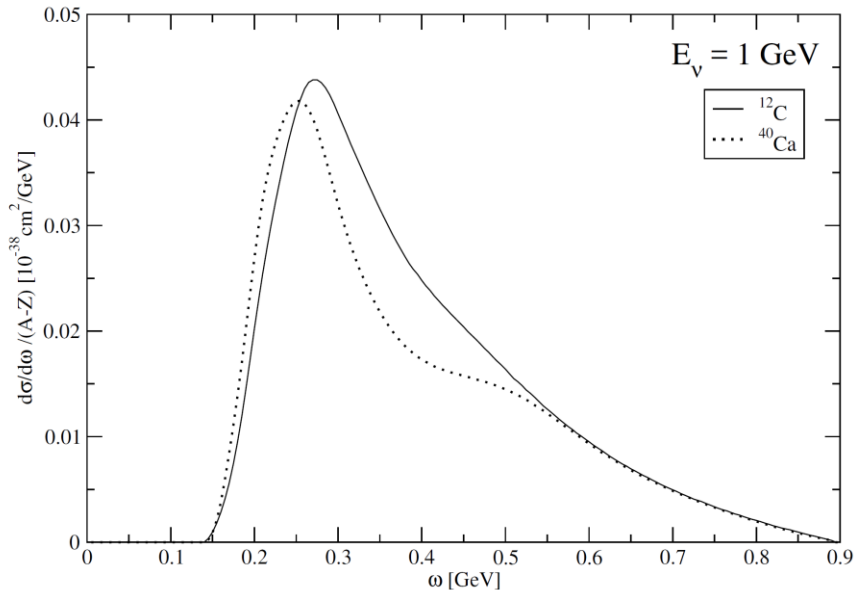
The coherent 1π production

Production of 1 pion with the nucleus remaining in its ground state

Relatively rare interaction channel, but can mimic oscillation signals



M. Martini, M. Ericson, G. Chanfray, J. Marteau, PRC 80 065501 (2009)



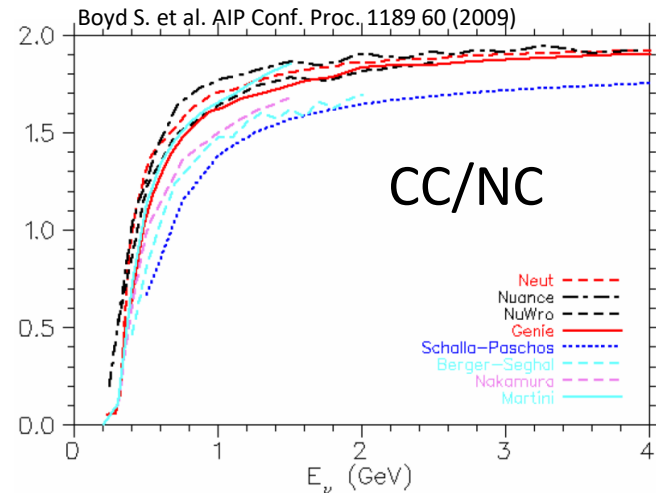
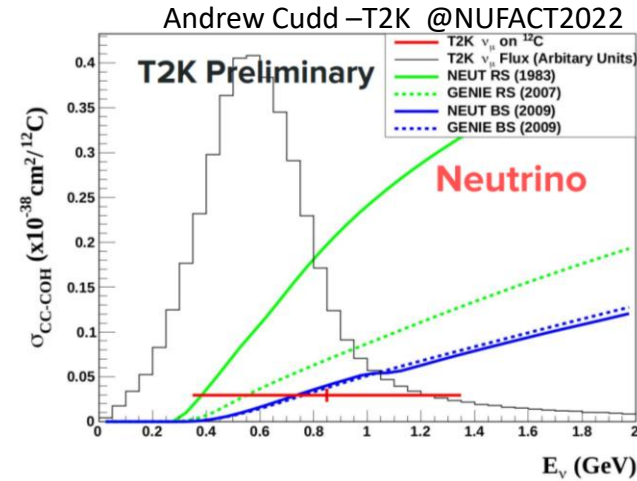
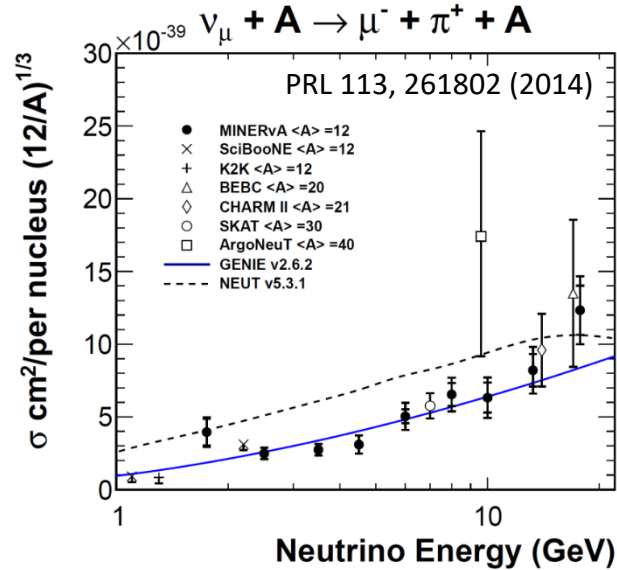
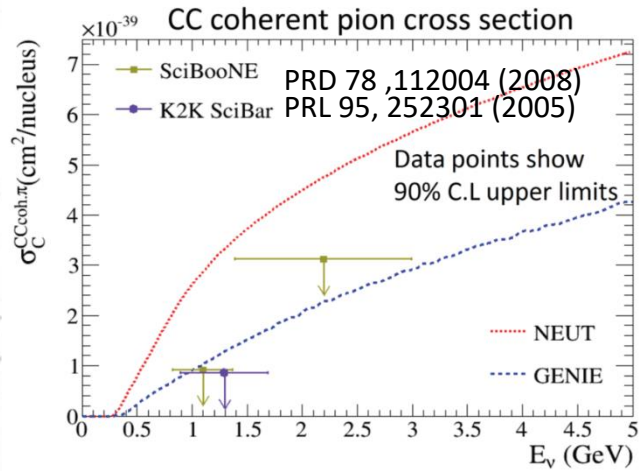
Cross sections reshaped by nuclear collective effects

Coherent 1π production experimental results

K2K and SciBooNE did not observe coherent π^+ production at neutrino energies $\sim 1\text{GeV}$

MINERvA and ArgoNeut see evidence for CC coherent pion production

Preliminary T2K cross section measurement: coherent π^+ production at neutrino energies $\sim 1\text{GeV}$



Coherent puzzle at $E_\nu \sim 1\text{ GeV}$

Theoretical models:

$$\frac{\pi^+ \text{ coh. CC}}{\pi^0 \text{ coh. NC}} = 1.5 \sim 2$$

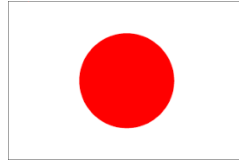
SciBooNE:

$$\frac{\pi^+ \text{ coh. CC}}{\pi^0 \text{ coh. NC}} = 0.14^{+0.30}_{-0.28}$$

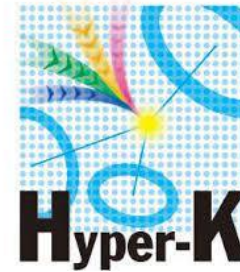
Kurimoto et al, PRD 81 (2010)

Nuclear targets of present and future LBL oscillation experiments

Present



Future



Carbon: T2K(ND) and NOvA

Oxygen (water): T2K (SuperK) and Hyper-K

Argon: DUNE

In the last 15 years many cross sections measurements and theoretical studies have been performed for Carbon (^{12}C). Less for Oxygen (^{16}O) and Argon (^{40}Ar)

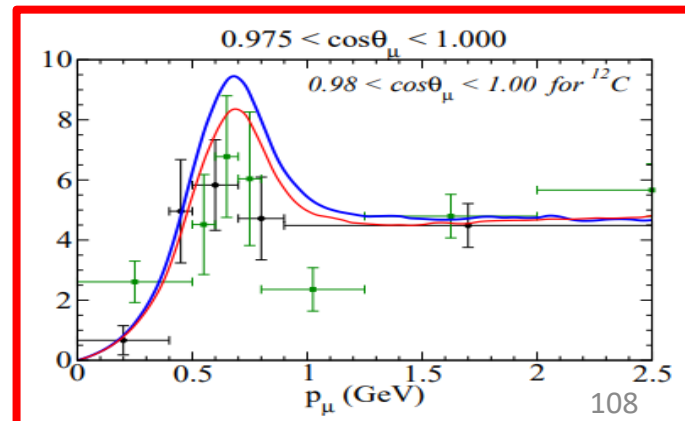
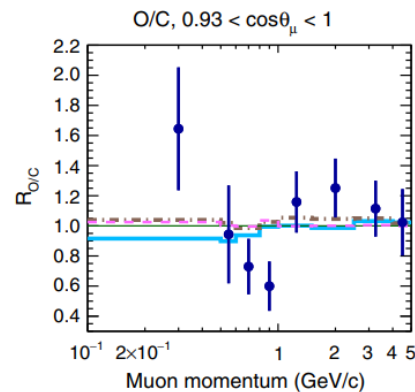
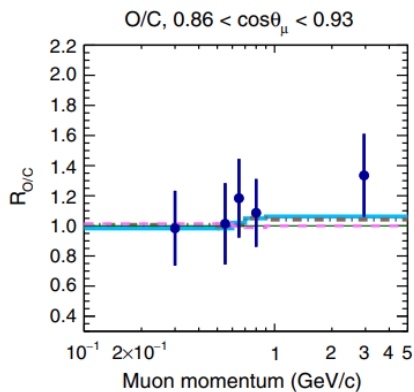
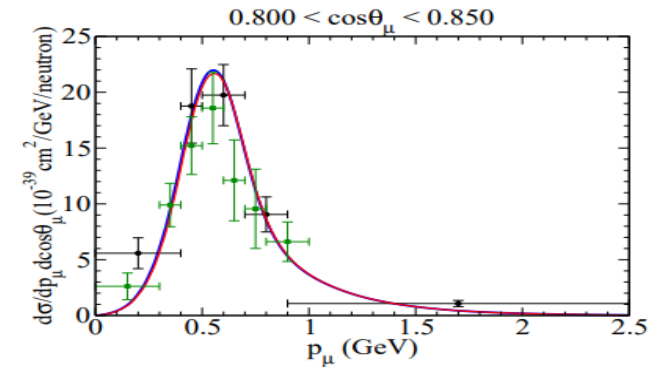
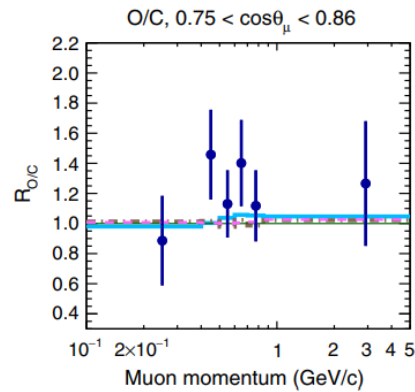
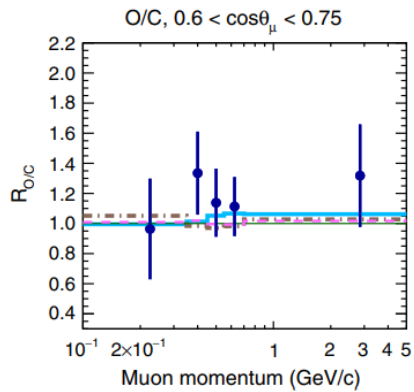
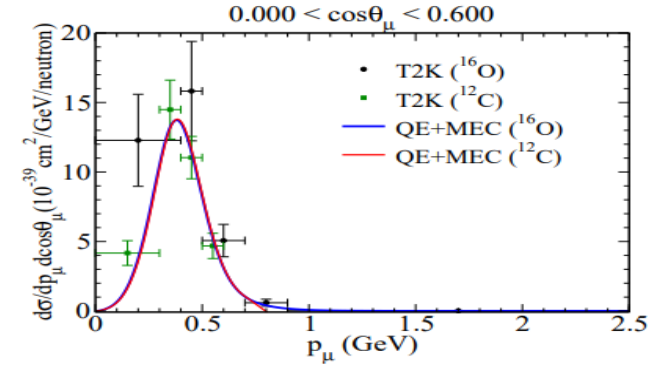
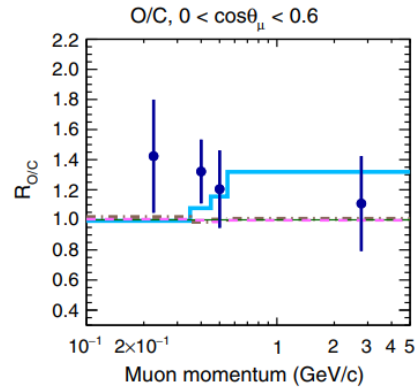
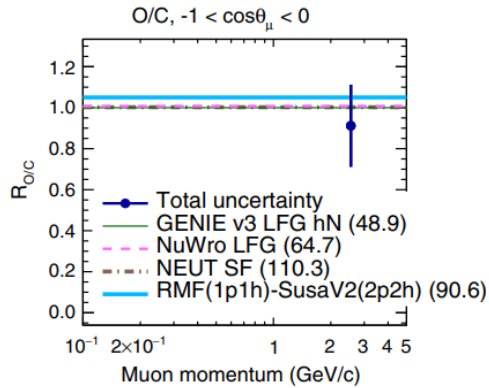
T2K CC0 π d² σ cross sections on oxygen and carbon

Ratio $^{16}\text{O}/^{12}\text{C}$ per nucleon

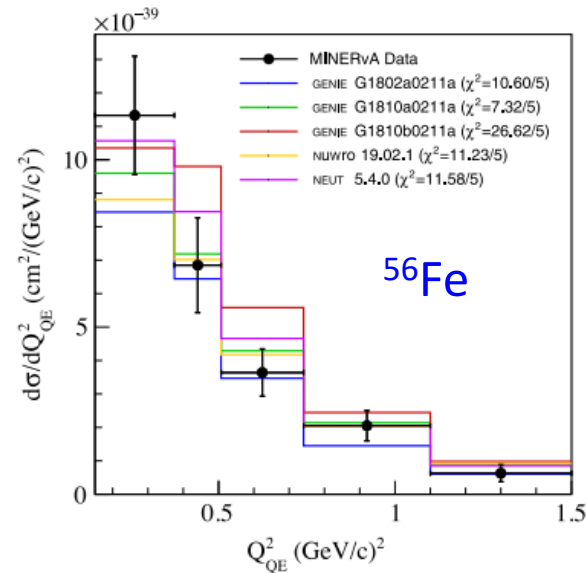
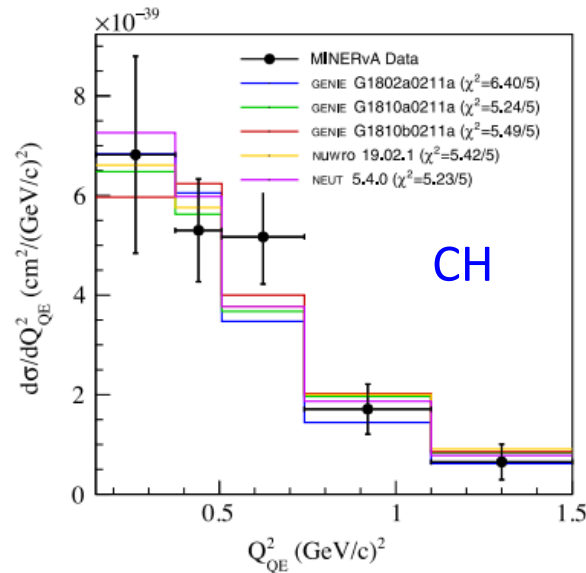
T2K PRD 101 (2020)

SuSAv2+MEC

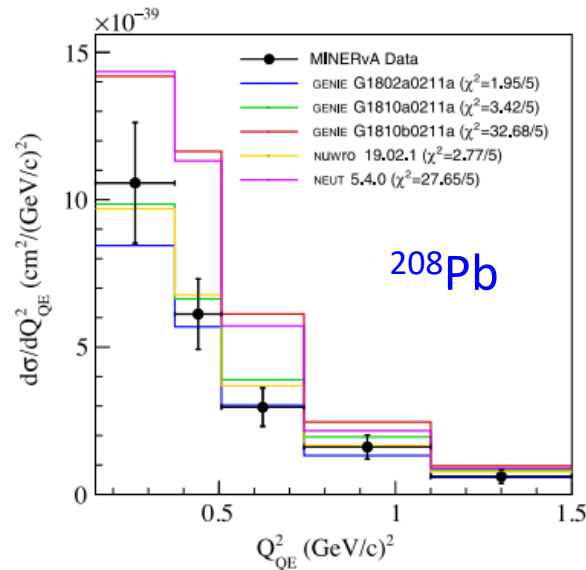
Megias et al., JPG46 (2019)



MINERvA CC0 π 1p(at least) Q²distributions for carbon, iron, lead



M. Buizza Avanzini et al. PRD 105, 092004 (2022)

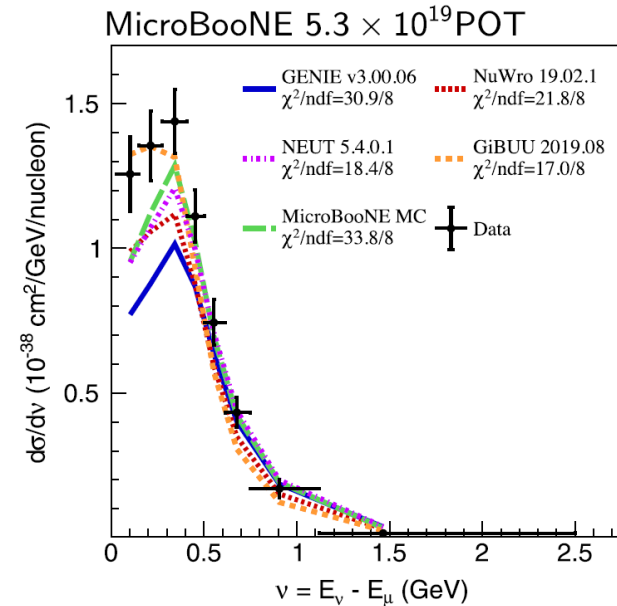
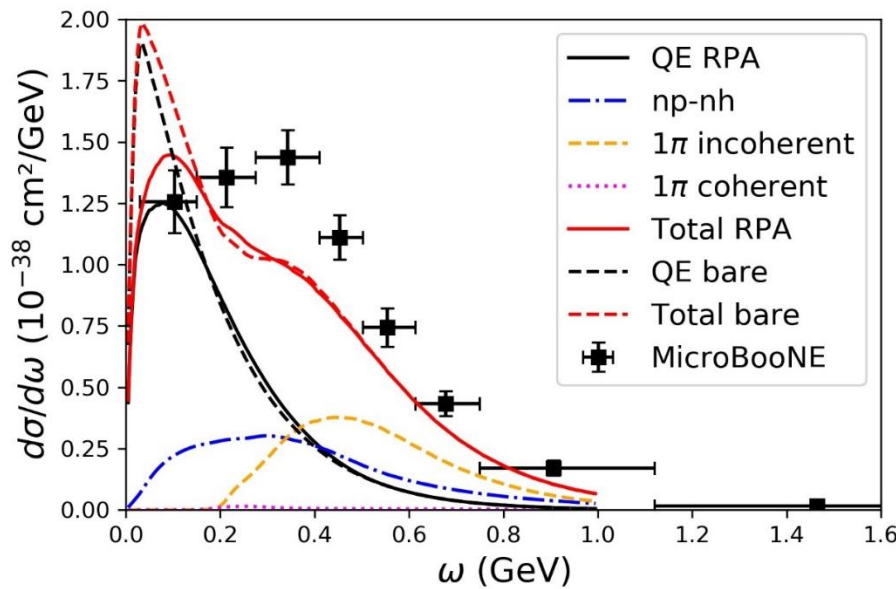
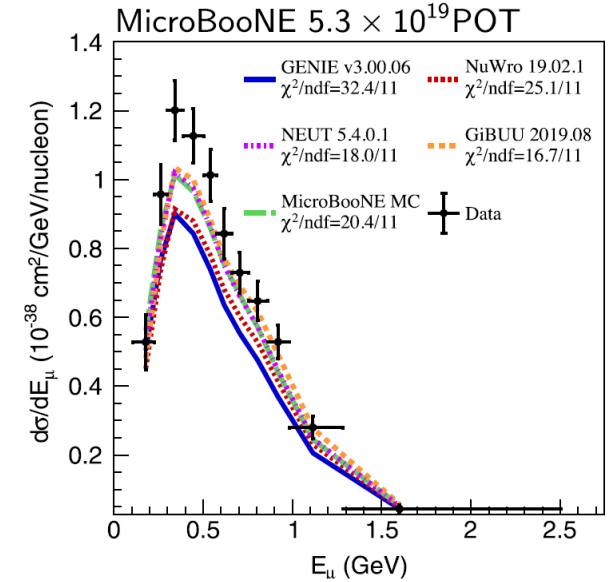
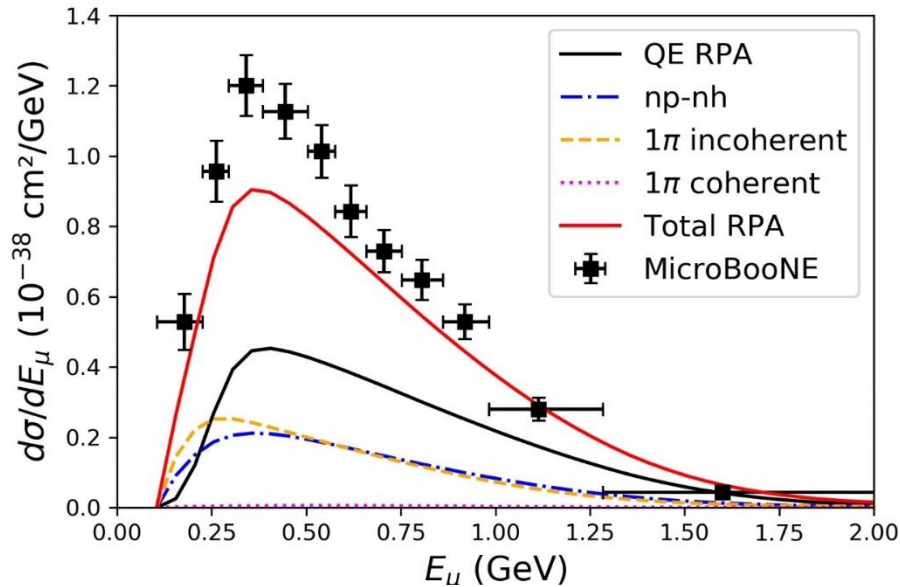


- The spread of distributions predicted by generators increases from carbon to lead
- Most significant deviations are at low Q² where nuclear effects are more important

MicroBooNE flux-averaged inclusive $d\sigma/dE_\mu$ and $d\sigma/d\omega$ on argon

M. Martini, M. Ericson, G. Chanfray, Phys. Rev. C 106, 015503 (2022)

PRL 128, 151801 (2022)

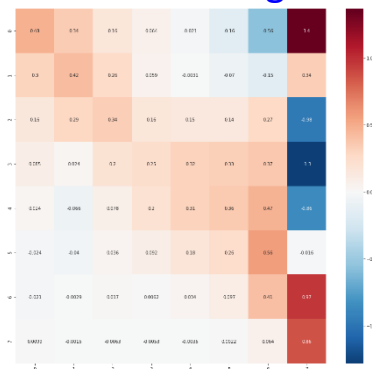


$d\sigma/d\omega$ allows a better separation of the different channels

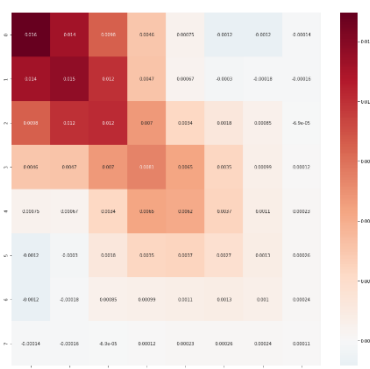
Quantitative analysis of MicroBooNE inclusive $d\sigma/d\omega$ on argon

MicroBooNE shared additional smearing and covariant matrices for quantitative analysis

Additional Smearing Matrix



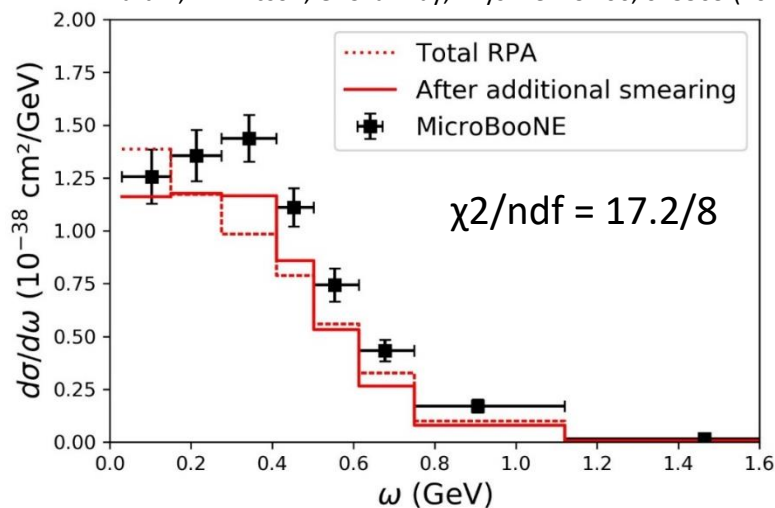
Covariant Matrix



$$\sigma_{smearred} = M_{add_smr} \times \sigma_{model}$$

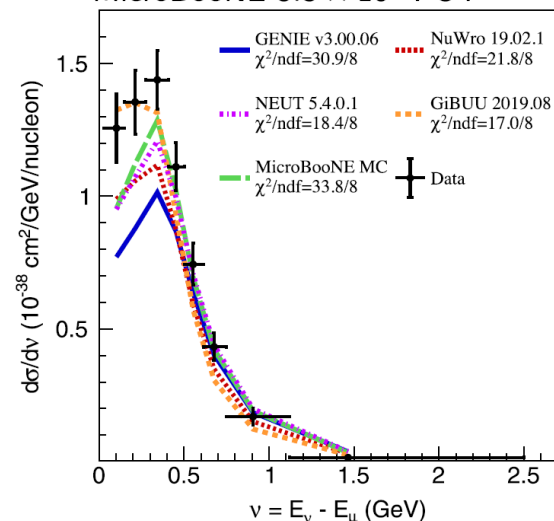
$$\chi^2 = (M - P)^T \times Cov_{full}^{-1}(M, P) \times (M - P)$$

M. Martini, M. Ericson, G. Chanfray, Phys. Rev. C 106, 015503 (2022)



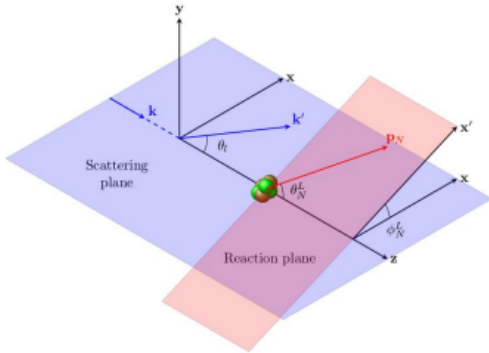
PRL 128, 151801 (2022)

MicroBooNE 5.3×10^{19} POT



- RPA $\chi^2/ndf=17.2/8$. Comparable with the one of GiBUU and better than all the Monte Carlo predictions
- A possible reason is that GENIEv3, MicroBooNE MC, NEUT and NuWro implement np-nh contribution deduced by Nieves et al. model. This contribution is smaller than the one of other evaluations (GiBUU, Martini et al,...)

Semi-inclusive neutrino-nucleus formalism in the IA



$$\left\langle \frac{d^6\sigma}{dk_l d\Omega_l dp_N d\Omega_N} \right\rangle = \int dk \Phi(k) \times K \times L_{\mu\nu} H^{\mu\nu}$$

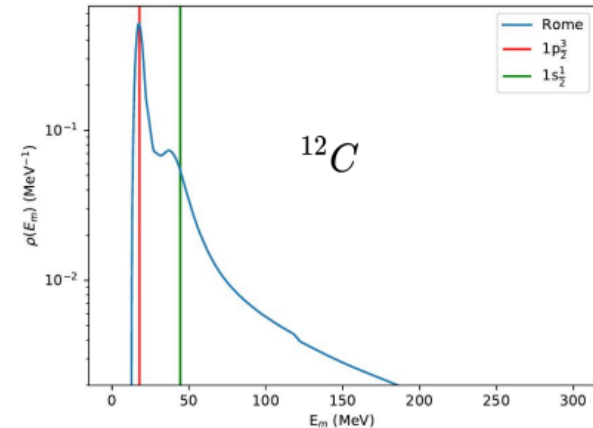
$$H_{\kappa}^{\mu\nu} = \rho_{\kappa}(E_m) \times \sum_{m_j, s_N} [J_{\kappa, m_j, s_N}(Q, P_N)]^* J_{\kappa, m_j, s_N}(Q, P_N) \Rightarrow \text{Factorization NOT assumed!!}$$

$$J_{\kappa, m_j, s_N}^{\mu} = \int d\mathbf{r} e^{i\mathbf{r}\cdot\mathbf{q}} \left[\bar{\Psi}_{s_N}(\mathbf{p}_N, \mathbf{r}) \left(F_1 \gamma^{\mu} + \frac{iF_2}{2m_N} \sigma^{\mu\nu} Q_{\nu} + G_A \gamma^{\mu} \gamma^5 + \frac{G_P}{2m_N} Q^{\mu} \gamma^5 \right) \Psi_{\kappa}^{m_j}(\mathbf{r}) \right]$$

• W.F. scattered nucleon
• CC2 operator
• W.F. bound nucleon

Description of the initial state:

- Pure shell model (first approximation): energy density is given by a Dirac delta per shell
- Realistic model (i.e. Rome spectral function used in electron exclusive processes): short- and long-range correlations included

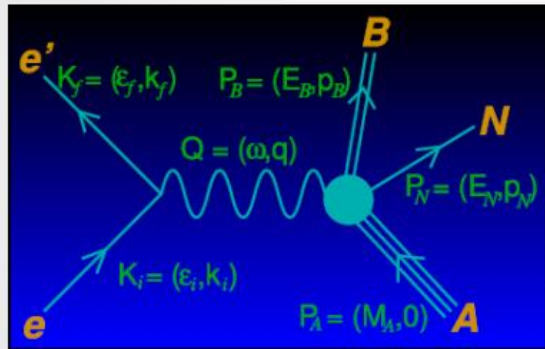


Relativistic scattering: notations and formalism

Four-vectors $A^\mu = (A_0, \vec{A})$

Bjorken&Drell conventions $g^{00} = 1, g^{kk} = -1 (k = 1, 2, 3)$

First Born approximation: one virtual boson exchange



$Q^2 = \omega^2 - q^2 < 0$ space-like virtual boson

$Q^\mu = K^\mu - K'^\mu = P_f^\mu - P_i^\mu$ 4-momentum conservation

$P^2 = M^2$ on-shell condition

$\not{\partial} \equiv \gamma_\mu \partial^\mu$ $\{\gamma^\mu, \gamma^\nu\} = \gamma^\mu \gamma^\nu + \gamma^\nu \gamma^\mu = 2g^{\mu\nu} \mathbb{1}$

$\gamma_5 \equiv i\gamma^0 \gamma^1 \gamma^2 \gamma^3$ $\sigma_{\mu\nu} = \frac{i}{2} [\gamma_\mu, \gamma_\nu]$

Dirac equation and Dirac spinors:

$(i \not{\partial} - M) \Psi = 0$ free particles

$(i \not{\partial} - e \not{A} - M) \Psi = 0$ in presence of e.m. field

$(\not{P} - M) u(\mathbf{p}, s) = 0$

$(\not{P} + M) v(\mathbf{p}, s) = 0$

$\Psi_{\mathbf{p}}^{(+)}(\mathbf{x}, t) = \sqrt{\frac{M}{EV}} u(\mathbf{p}, s) e^{-iP_\mu X^\mu}$ positive energy

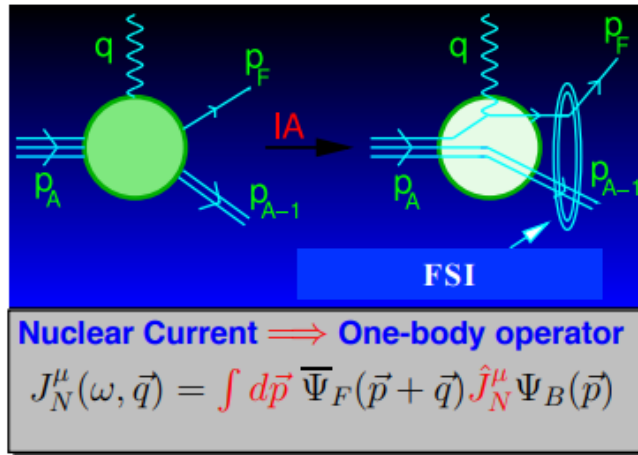
$\Psi_{\mathbf{p}}^{(-)}(\mathbf{x}, t) = \sqrt{\frac{M}{EV}} v(\mathbf{p}, s) e^{iP_\mu X^\mu}$ negative energy

$$u(\mathbf{p}, s) = \sqrt{\frac{E+M}{2M}} \begin{pmatrix} \chi_s \\ \frac{\boldsymbol{\sigma} \cdot \mathbf{p}}{E+M} \chi_s \end{pmatrix}, \quad v(\mathbf{p}, s) = \sqrt{\frac{E+M}{2M}} \begin{pmatrix} \frac{\boldsymbol{\sigma} \cdot \mathbf{p}}{E+M} \xi_s \\ \xi_s \end{pmatrix}$$

Relativistic Mean Field Model

The RMF model is based on the **impulse approximation (IA)**:

scattering off a nucleus = incoherent sum of single nucleon scattering processes.



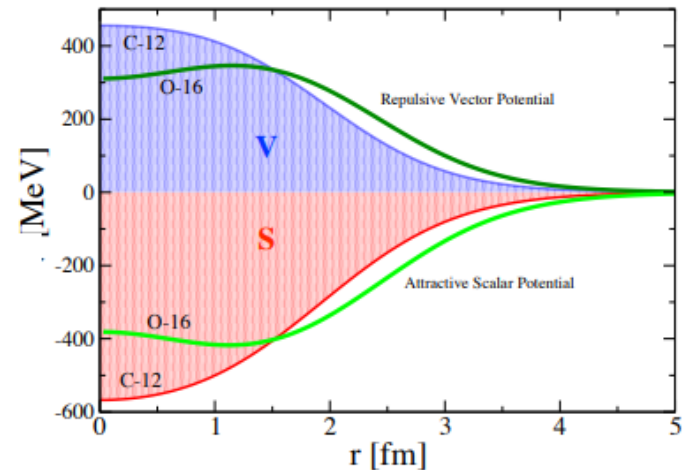
Bound wave function

$$\Psi_B = \begin{pmatrix} \phi^{up} \\ \phi^{down} \end{pmatrix} = \begin{pmatrix} \phi^{up} \\ \frac{\sigma \cdot \mathbf{p}}{E + M + S - V} \phi^{up} \end{pmatrix} = \alpha u + \beta v$$

Scattered wave function

The nucleon wave functions are finite nucleus solutions of the Dirac equation with phenomenological **relativistic scalar and vector potentials** obtained from a Walecka-type Lagrangian fitted to properties of nuclear radii and masses:

$$(i\gamma^\mu \partial_\mu - M - S + V) \psi(\vec{r}, t) = 0$$



The ejected nucleon wave function is distorted by **Final State Interactions (FSI)** with the residual nucleus. In the RMF model it is a scattering solution of the same Dirac equation used to describe the bound state. **Orthogonality is preserved:** the initial and final nucleon wave functions are eigenstates of the same Hamiltonian.

Semi-inclusive cross section: impact of different initial state modeling

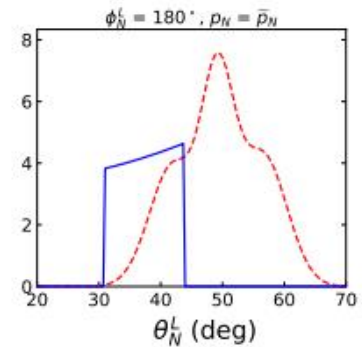
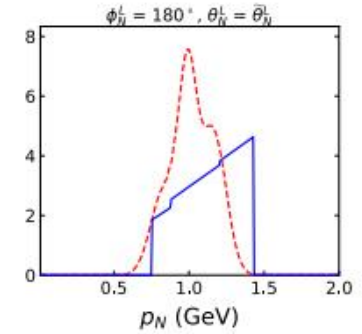
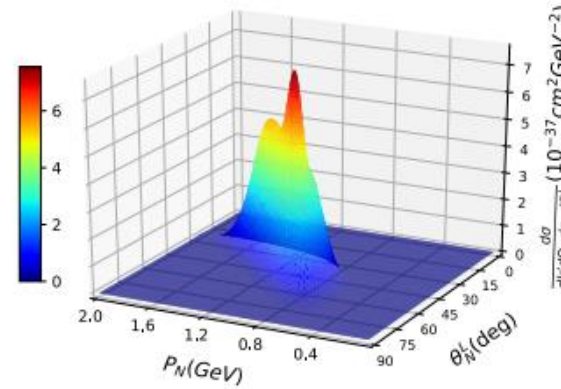
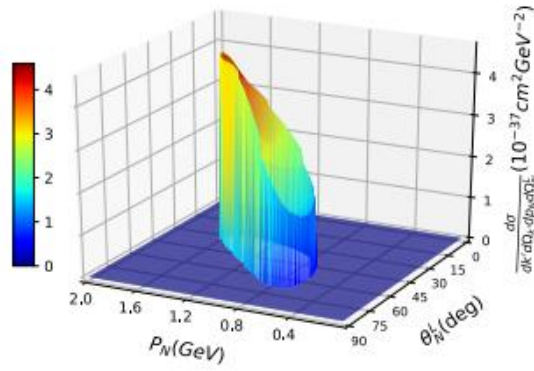
M. Barbaro
talk @IPSA
2022

6-differential semi-inclusive cross section ($\nu_\mu, \mu p$) nucleon knock-out

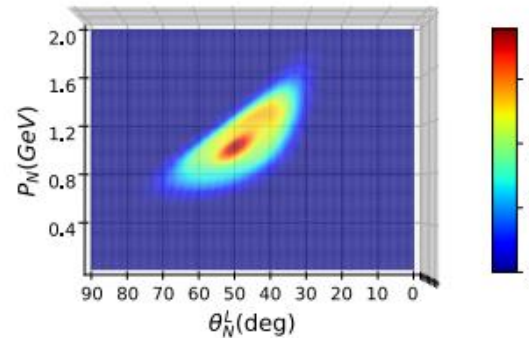
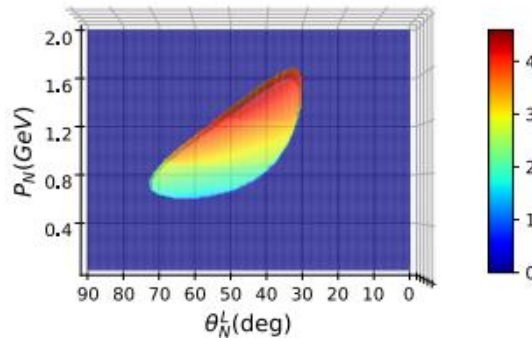
$${}^{40}\text{Ar}(\nu_\mu, \mu^- p){}^{39}\text{Cl} \quad \text{DUNE flux} \quad k' = 1.5 \text{ GeV}, \theta_\mu = 30^\circ, \phi_N^L = \pi$$

Relativistic Fermi Gas

Independent Particle Shell Model



--- IPSM
— RFG



J.M. Franco-Patiño *et al.*, PRC 102, 064626 (2020)

Relativistic Plane Wave Impulse Approximation (no FSI included)

Striking differences in the cross section due to initial state physics described by different spectral functions.
The precise knowledge of the SF is crucial for a reliable modelling of semi-inclusive reactions.

Scattered Nucleon Description

Regarding the scattered nucleon, we can consider several situations:

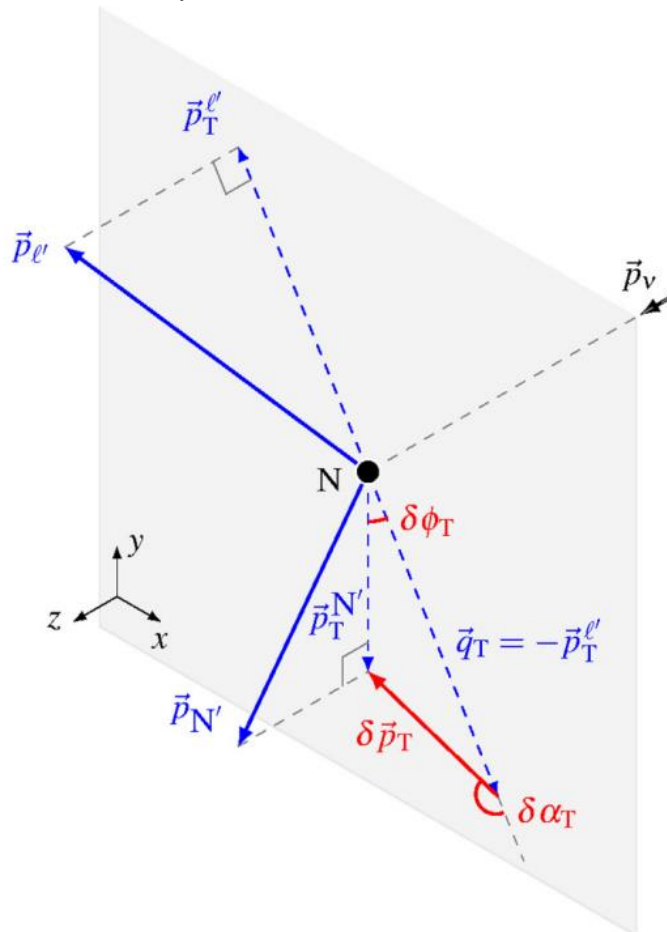
- **Relativistic Plane-Wave Impulse Approximation (RPWIA)**: the ejected nucleon is considered a plane-wave (i.e, there are not final state interactions)
- **Energy-Dependent Relativistic Mean Field (ED-RMF)**: W.F. solution of the Dirac equation in the continuum using the same RMF potential that describes the initial state times a phenomenological function that weakens the potentials at high energies
- **Relativistic Optical Potential (ROP)**: The scattered nucleon travels under the influence of a phenomenological relativistic optical potential fitted to reproduce elastic proton scattering data. Keeping only the real part of the OP (**rROP**) is an effective way to take into account all the channels (elastic and inelastic)

$$\Psi_{s_N}(\mathbf{r}, \mathbf{p}_N) = 4\pi \sqrt{\frac{E_N + m_N}{2E_N}} \sum_{\kappa, m_l, m_j} e^{-i\delta_\kappa^*} i^l \langle l m_l 1/2 s_N | j m_j \rangle Y_{l m_l}^*(\Omega_N) \psi_\kappa^{m_j}(\mathbf{r})$$

$$\psi_\kappa^{m_j}(\mathbf{r}) = \begin{pmatrix} g_\kappa(r) \phi_\kappa^{m_j}(\Omega_r) \\ i f_\kappa(r) \phi_{-\kappa}^{m_j}(\Omega_r) \end{pmatrix} \quad \begin{aligned} \frac{dg_\kappa}{dr} &= -\frac{\kappa}{r} g_\kappa + [E_N + S(r, E_N) - V(r, E_N)] f_\kappa \\ \frac{df_\kappa}{dr} &= -\frac{\kappa}{r} f_\kappa + [E_N - S(r, E_N) - V(r, E_N)] g_\kappa \end{aligned}$$

Measurement of nuclear effects in neutrino interactions with minimal dependence on neutrino energy

X.-G. Lu,^{1,*} L. Pickering,² S. Dolan,¹ G. Barr,¹ D. Coplowe,¹ Y. Uchida,² D. Wark,^{1,3} M. O. Wascko,² A. Weber,^{1,3} and T. Yuan⁴



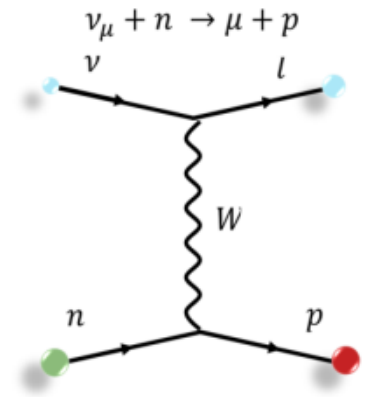
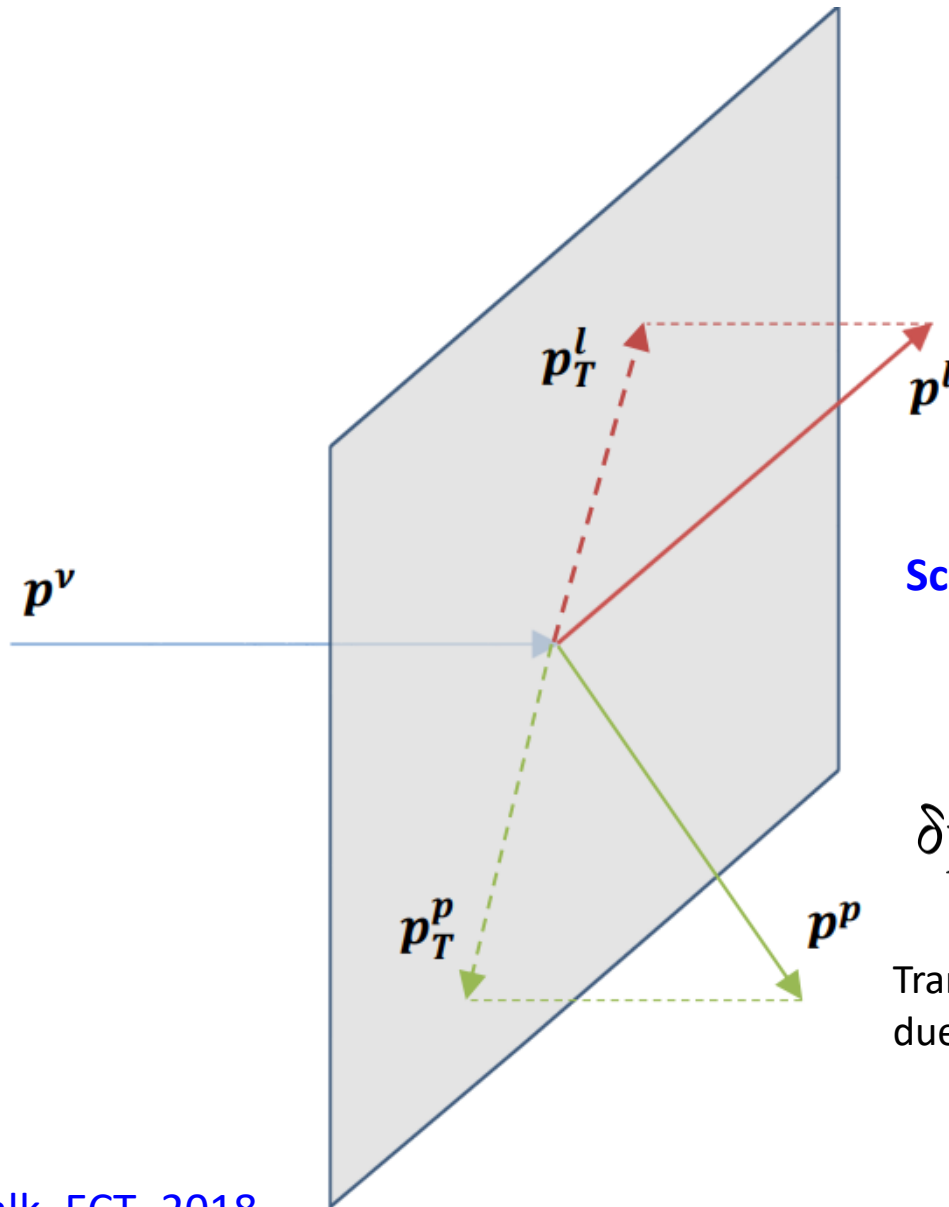
Single Transverse Variables (STV)

$$\delta \vec{p}_T \equiv \vec{p}_T^{\ell'} + \vec{p}_T^{N'}$$

$$\delta \alpha_T \equiv \arccos \frac{-\vec{p}_T^{\ell'} \cdot \delta \vec{p}_T}{p_T^{\ell'} \delta p_T}$$

$$\delta \phi_T \equiv \arccos \frac{-\vec{p}_T^{\ell'} \cdot \vec{p}_T^{N'}}{p_T^{\ell'} p_T^{N'}}$$

Single Transverse Kinematic Variables



No nuclear Effects

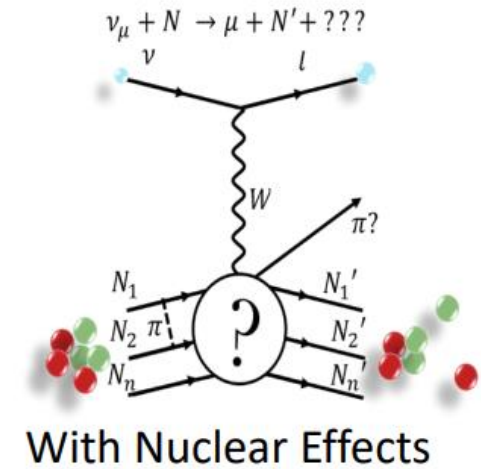
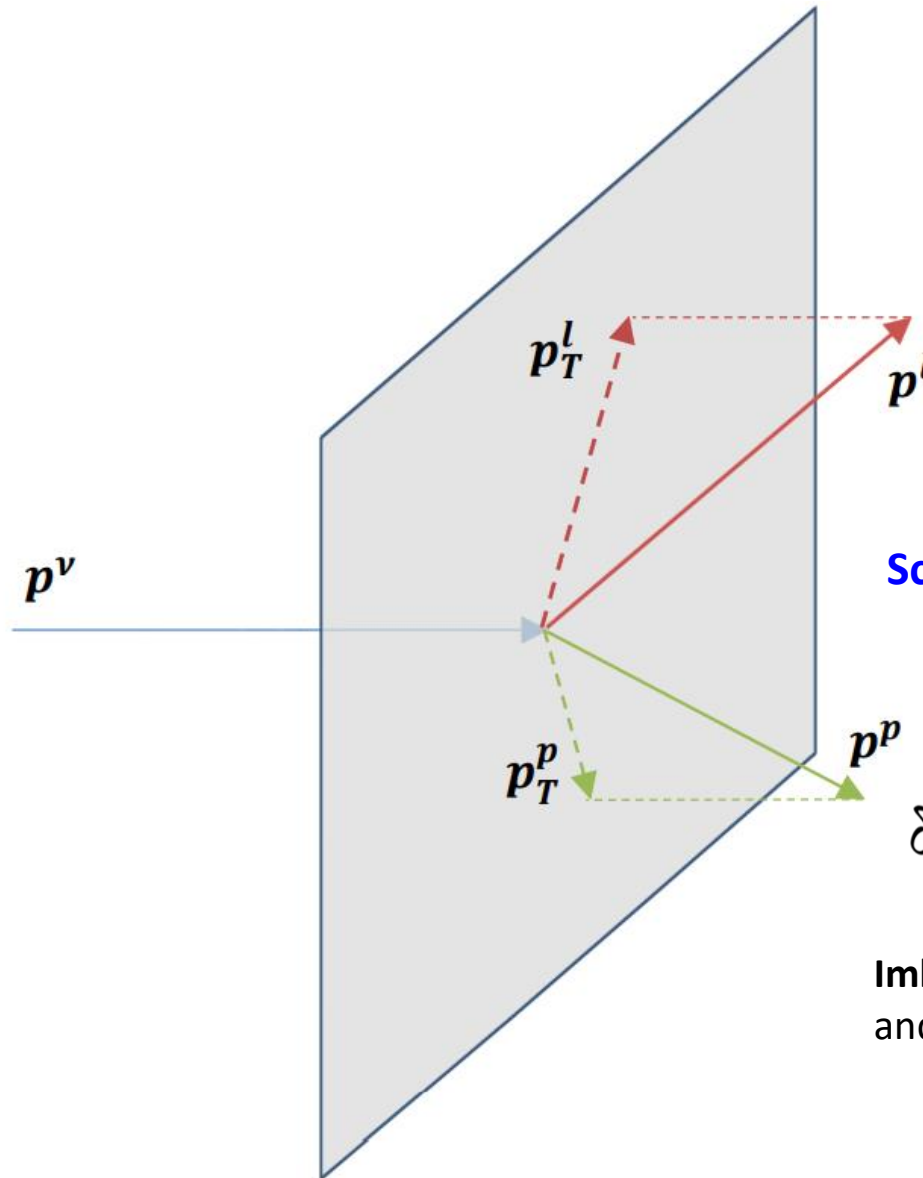
Scattering on a free nucleon at rest

$$\mathbf{p}_T^l = -\mathbf{p}_T^p$$

$$\delta p_T = |\mathbf{p}_T^\mu + \mathbf{p}_T^p| = 0$$

Transverse projections equal and opposite due to momentum conservation

Single Transverse Kinematic imbalance (STKI)



Scattering on nucleus

$$\mathbf{p}_T^l \neq -\mathbf{p}_T^p$$

$$\delta p_T = |\mathbf{p}_T^l + \mathbf{p}_T^p| > 0$$

Imbalance due to initial nucleon motion and other nuclear effects

Unfolded $CC\ 2p0\pi$ Cross Section and Model comparison

